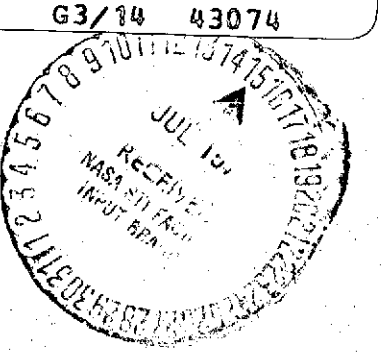

PERKIN-ELMER

PERKIN-ELMER
ELECTRO-OPTICAL DIVISION
NORWALK, CONNECTICUT

REPORT NO. 11923

LST SECONDARY MIRROR ARTICULATION MECHANISM

FINAL REPORT

PREPARED FOR

NATIONAL AERONAUTICS AND SPACE ADMINISTRATION

GEORGE C. MARSHALL SPACE FLIGHT CENTER

HUNTSVILLE, ALABAMA

CONTRACT NAS 8-29723

DATE: MAY 1974

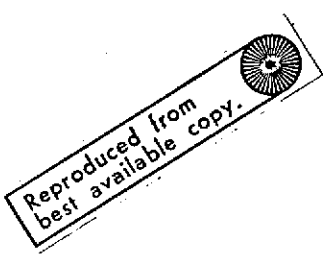

REF:

TABLE OF CONTENTS

TABLE OF CONTENTS (Continued)

LIST OF ILLUSTRATIONS

1.0 SUMMARY

This report describes the work performed by Perkin-Elmer under Contract NAS 8-29723 for the National Aeronautics and Space Administration, George C. Marshall Space Flight Center, Huntsville, Alabama.

The period of performance covered by this report is from September 15, 1973 through March 29, 1974.

1.1 CONTRACT REQUIREMENTS

This contract required the analysis, design, manufacture, test, and delivery of one secondary mirror articulation mechanism for the Large Space Telescope (LST). The mechanism provides angular freedom about two axes that are perpendicular to the optical axis of the secondary mirror. Motion in each axis is controlled from two sources; one source provides alignment, the other source provides stabilization.

Two articulation mechanism configurations were evaluated. In one configuration the stabilization system was assembled with piezoelectric actuators. In the second configuration the stabilization system utilized flexure torque motor actuators. The alignment system was the same for both configurations.

Contract Modification 1 (effective October, 1973) provided for system size coordination with LST optical design performed at Perkin-Elmer and added two position transducers in each axis for a total of four position transducers.

1.2 Performance Summary

System testing confirmed performance that met or exceeded all operational requirements. The two types of stabilization actuators had different performance characteristics. Both types demonstrated position resolution and frequency response better than specified limits.

2.0 SYSTEM DESCRIPTION

2.1 SUMMARY OF PERFORMANCE REQUIREMENTS

The mirror articulation mechanism provides angular freedom about two axes that are perpendicular to the optical axis of the LST secondary mirror. Motion in each axis (azimuth and elevation) is controlled from two sources. One source performs an alignment function. The other source performs an image stabilization function.

The performance requirements for each source are as follows:

a. Alignment (in both axes)

(1) Total angular range ±5 arc seconds
(2) Threshold: 0.1 arc-second
(3) Response: 10 arc-seconds in 1 minute
(4) Environment: Laboratory ambient or hard vacuum, with 20 to 120°F temperature and ±2g vibration from 20 to 2000 Hz.

b. Stabilization (in both axes)

(1) Total Angular range: ± 3 arc-seconds
(2) Frequency Response: Attenuation less than 3db at 4Hz for a sine wave input.
(3) Threshold: ±0.005 arc-second
(4) Environment: Same as for alignment.

2.2 DESCRIPTION OF MIRROR SUSPENSION SYSTEM

The motions specified for the secondary mirror require a mirror suspension system that is capable of responding to commands of 1 part in 600 over a very small range of motion. Resolution to this degree of precision makes the use of flexure mechanisms in the mirror suspension and articulation system mandatory. Elements that are critically dependent on manufacturing tolerance, operating clearances, finish of interfacing elements (such as rolling element bearings, screws, or cams) are not suited to this application.

Principal performance goals for the mirror suspension system can be summarized as follows:

- Must be able to accommodate maximum range of motion (±8 arc-seconds tilt) with limited lost motion compatible with actuator resolution requirements.
- Provide minimum mirror motion response to external lateral or rotational vibration (rigid body mirror motion).
- Minimize mirror figure degradation due to mechanical or thermal disturbances (mirror figure change)
- Survive launch loads with minimum resonant amplification without need for launch caging devices.

2.2.1 Universal Flexure Suspension

A mirror suspension system that was evaluated to meet the performance goals defined above is shown in Figure 2-1. The central support element is a circular flexure located with the axis of rotation coincident with the mirror center of gravity. This configuration provides minimum coupling of lateral or rotational vibration to mirror tilt, a key consideration since the optical system is highly sensitive to secondary mirror tilt and the corresponding image motion in the focal plane. It thus provides a good decoupling from structural vibrations in orbit.

A simple form of this central flexure capable of motion about two orthogonal intersecting axes is shown in Figure 2-1.

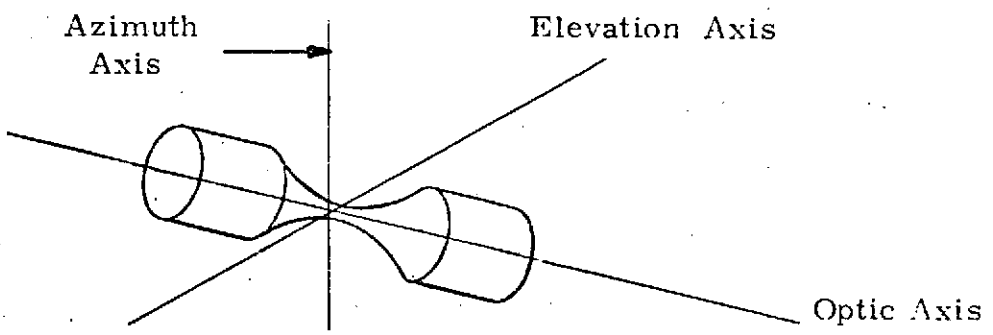

Figure 2-1. Universal Circular Flexure

The flexure, however, has relatively low strength along its longitudinal axis (z axis). Torsional strength about this longitudinal axis is also poor, as is stiffness to lateral loads.

In order to increase strength along the longitudinal axis the configuration of Figure 2-1 can be modified, as shown in Figure 2-2. Here, simple single-axis flexures were combined with an intermediate member.

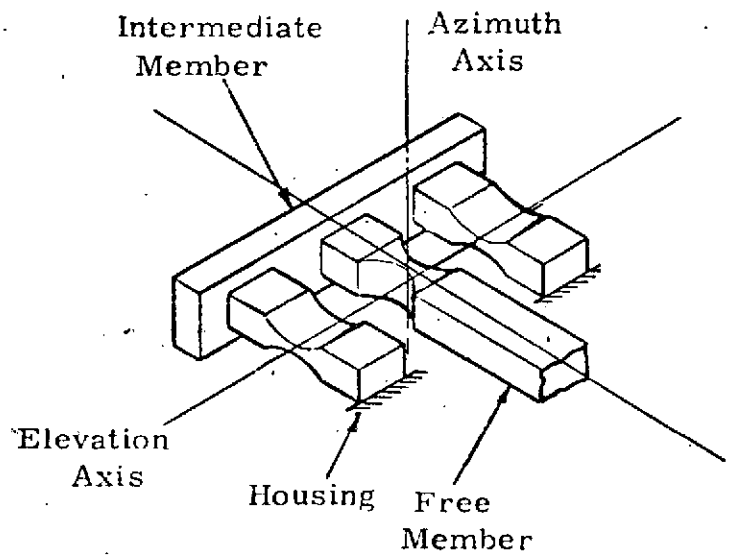

Figure 2-2. Compound Single-Axis Flexures

This improved configuration has proven to be effective in a Perkin-Elmer precision mirror suspension system, but requires additional support against rotation about the mirror optical axis and lateral motion perpendicular to the optic axis. The addition of lateral flexures to provide this support produced the suspension system shown in Figure 2-3.

Analysis of this concept however disclosed undesirable characteristics relative to the interaction of flexure loads on the mirror figure. Flexure attachments at several widely spaced points across the mirror can strain the mirror as a function of manufacturing tolerances or thermal gradients in the structure.

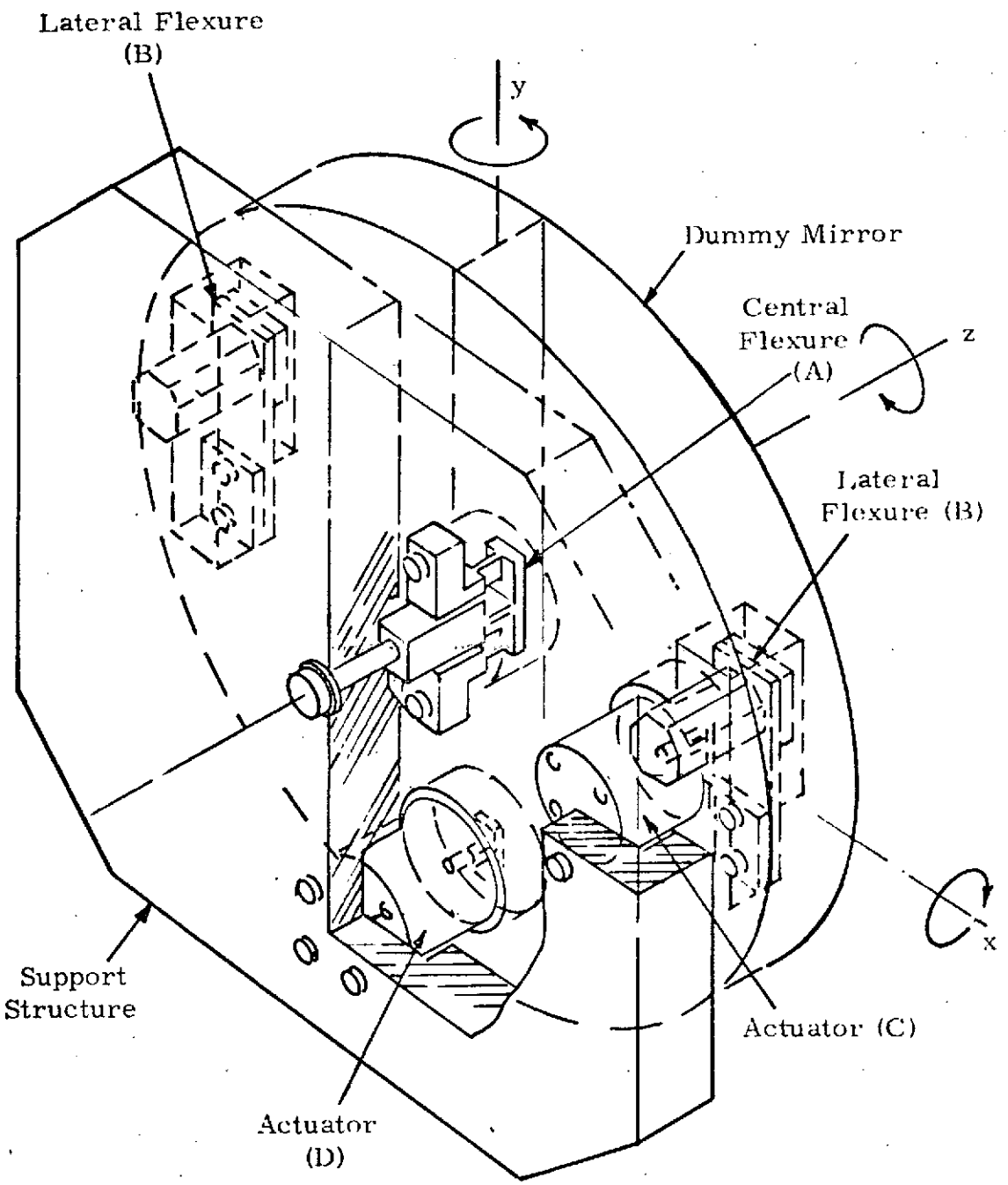

Figure 2-3. Secondary Mirror Actuating System

The overall telescope optical performance is a function of the accumulated effects of surface tolerance on the primary and secondary mirrors. Since the secondary mirror is much smaller in size than the primary mirror, the secondary mirror will be manufactured to surface tolerances that approach the limit of the state of the art, thereby making a greater part of the surface tolerances available to the primary mirror. Accordingly, the secondary mirror suspension must assure minimum degradation of the mirror figure. The cruciform flexure suspension concept was developed to meet this requirement.

2.2.2 Cruciform Flexure Suspension

An optimum mirror suspension configuration consists of a mechanism that provides the required restraint or compliance in all six degrees of freedom with all interface loads at the non-critical central area. The two-axis cruciform flexure (Figure 2-4) meets these requirements.

A cruciform consists of two intersecting planes. The structural characteristics are high stiffness and lateral load capacity (edge loading of the plates) and high compliance to torsion about the intersecting axis of the planes (twist of the plates).

The configuration shown in Figure 2-4 provides rotational freedom about two orthogonal axes (azimuth and elevation) together with high stiffness and load capacity in the remaining rotational mode (rotation about the optical axis). High stiffness in all three lateral modes is provided.

This configuration provides the following significant advantages:

- Precise location of axis of rotation for mirror balance
- Negligible free play
- High compliance and low hysteresis about two orthogonal axes of rotation
- High stiffness and load capacity in remaining four degrees of freedom

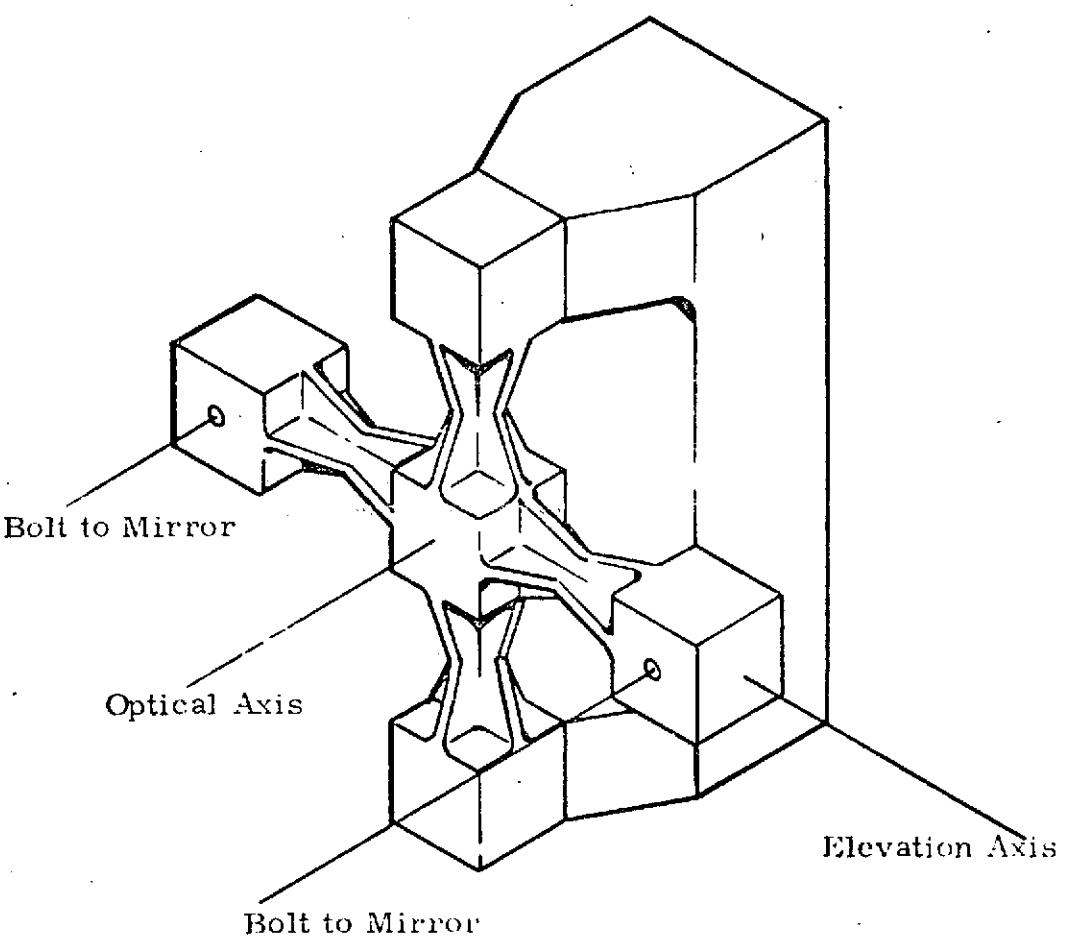

Figure 2-4. Two-Axis Cruciform Flexure (Sheet 1 of 2)

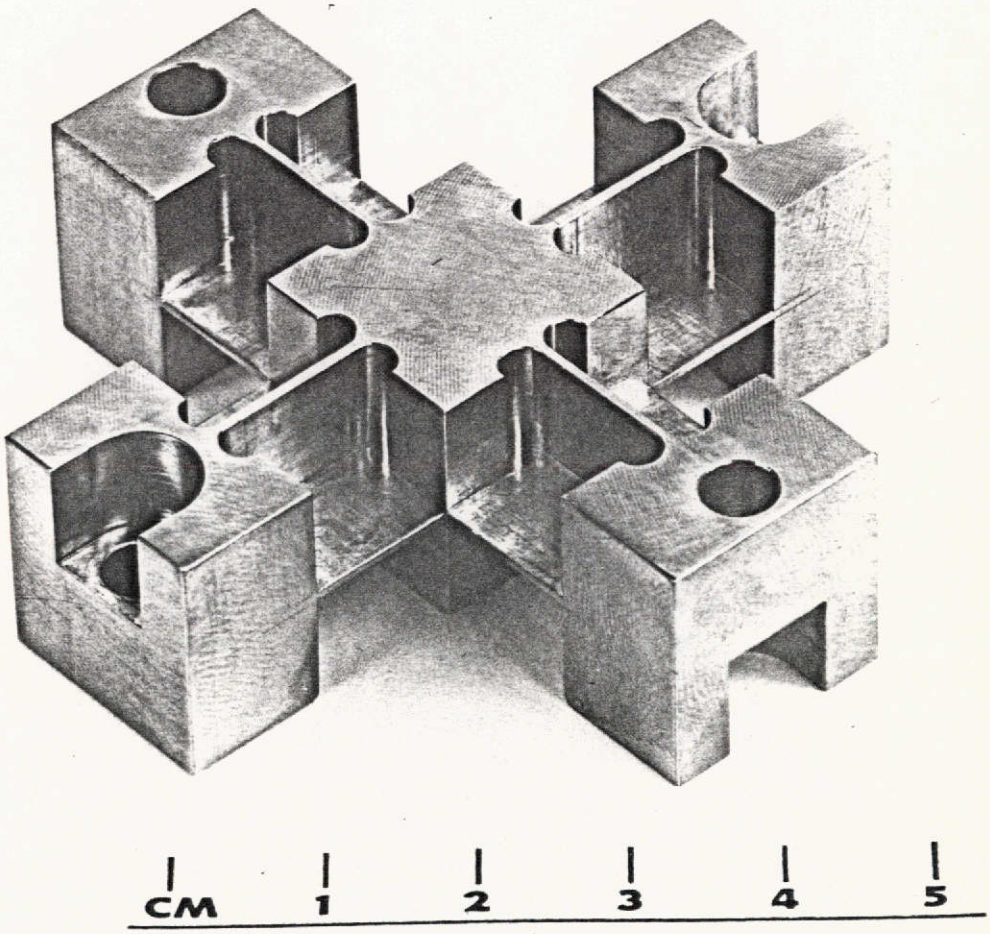

Figure 2-4. Two-Axis Cruciform Flexure (Sheet 2 of 2)

- o High reliability, low stress. Entire mechanism manufactured from single part
- o All interface loads applied at non-critical central area of mirror.

2.3 IMAGE MOTION CONTROL DRIVE ACTUATORS

Previous programs conducted at Perkin-Elmer have required precise position control of mirrors and lenses. Two types of actuators that have demonstrated good operating characteristics in similar applications are described in the following section.

2.3.1 Piezoelectric Translator (Figure 2-5)

Piezoelectric translators are available in several configurations. All utilize a ceramic material that changes a physical dimension upon application of static voltage. Typical configurations consists of cylindrical or disk segments. The segments are wired in parallel and stacked so that the total displacement is the summation of the displacement of each segment. The relationship between total displacement and voltage is controlled by the number of segments in the stack.

This type of actuator has the following significant advantages for use in precision mirror position control.

- o The translator can be designed with stroke compatible with direct coupling to mirror - Typical stroke: extension 12.6 x 10^{-6} meters at 1000 volts.
- o Very good position resolution. Resolution to 0.4 x 10^{-8} meters has been demonstrated.
- o Very high stiffness and force gain - Typical actuator force required for maximum tilt 0.2 newton. Available translator force 5000 newtons.
- o Simple mechanical configuration and structural reliability.

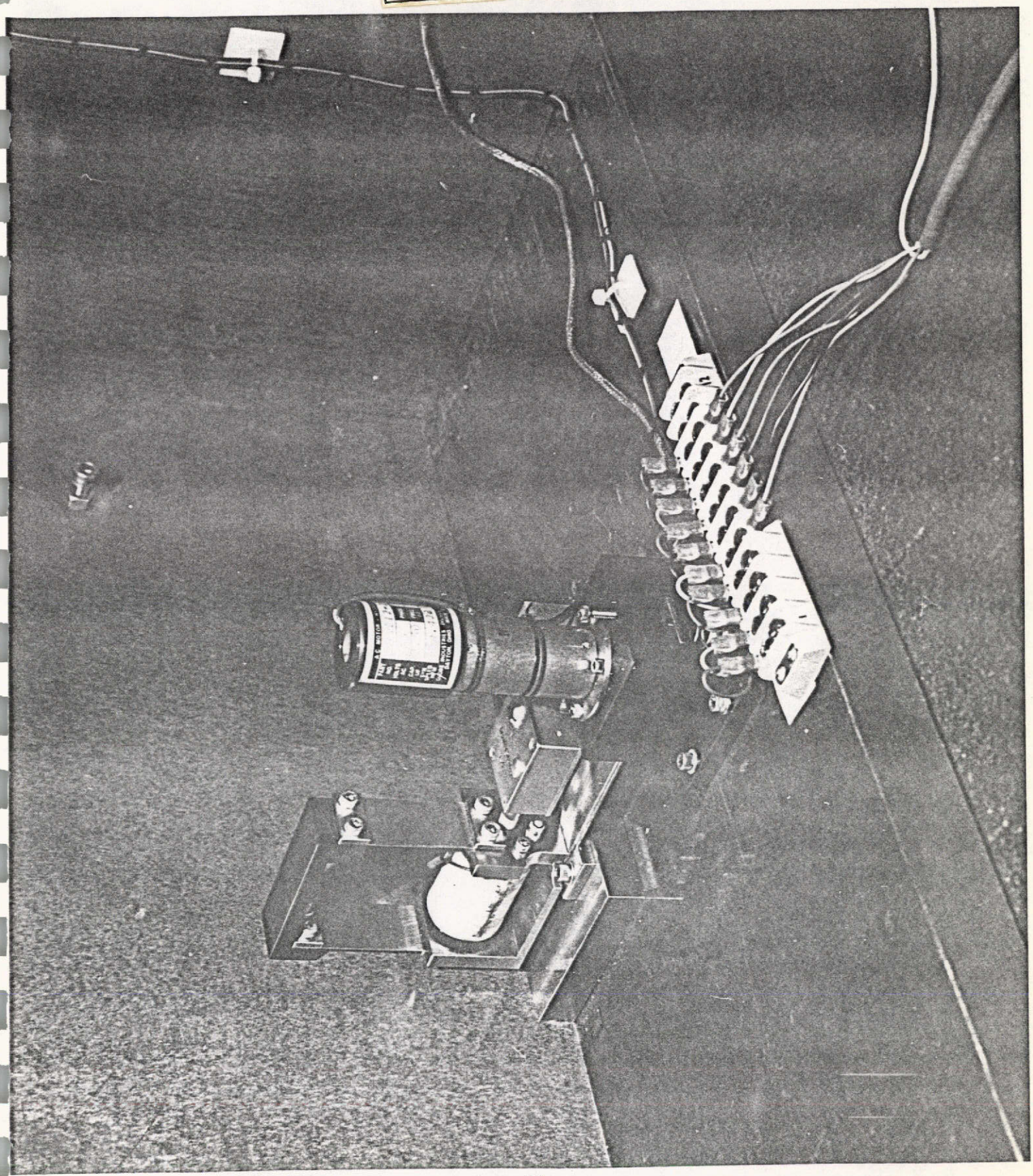

Figure 2-5. Piezoelectric Translator

- Flat frequency response to better than 10,000 Hz.
- Small size - typical envelope 2.5 cm diameter by 3 cm long.

The very high stiffness and force gain of this type of actuator minimizes position errors caused by friction or extraneous loads in the mirror suspension system. The actuator is a simple and effective structural member when not electrically active. This characteristic is effective in surviving launch vibration and can be used to provide electrical redundancy by stacking two translators in a series mechanical arrangement.

PZT materials have a hysteresis characteristic of position relative to voltage that can be undersirable in some applications. This characteristic is not objectionable in a closed-loop application.

2.3.2 Flexure Torque Motor Actuators

The flexure torque motor actuator consists of a permanent magnet armature suspended on flexures in an electromagnetic field. A typical actuator is shown on Figure 2-6. This type of actuator has the following operating characteristics:

- Relatively high stroke - Typical stroke $\pm 1.5 \times 10^{-4}$ meters (± 0.006 in)
- Good linearity and low hysteresis - Typical value 2 percent
- Spring constant controlled by design
- Relatively low force. Typical force at center = 9 newtons (2 pounds)

The high stroke, low force characteristic is compatible with the requirement for precise mirror postion control. This enables the frequency response and stiffness to ground of the mirror suspension to be improved by driving the mirror through a high reduction flexure linkage.

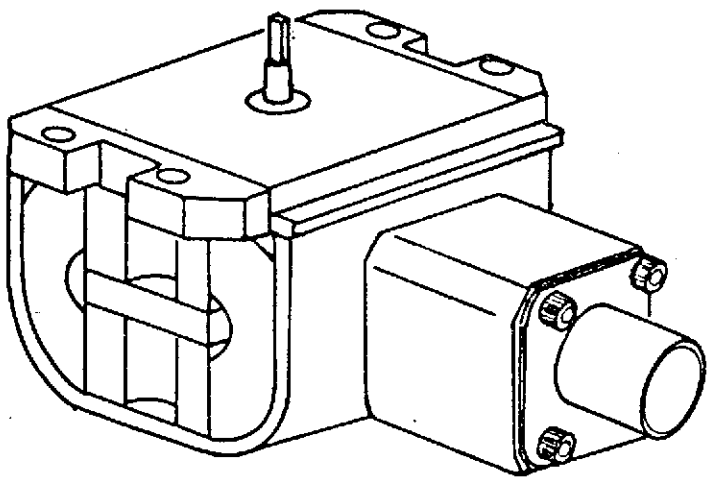

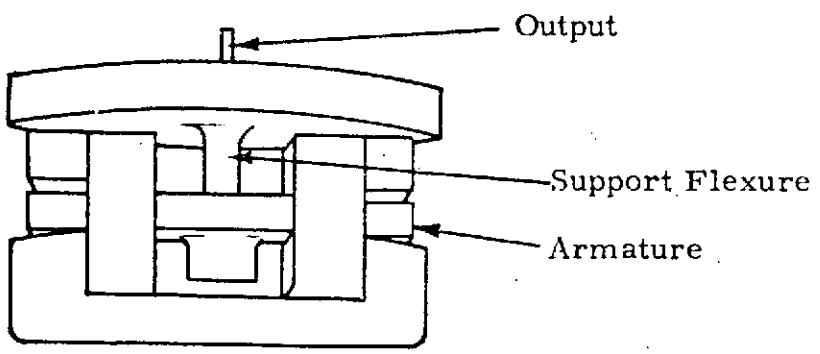

Figure 2-6. Typical Flexure Torque Motor Actuator

The magnetic circuit has a negative spring characteristic. This opposes the positive spring constant of the armature support flexure so that the actuator spring constant can be designed to be negative, zero, or positive.

The acceleration forces required to drive the mirror are negligible because of the low amplitude and frequency. The forces required of the actuator are predominantly those to deflect the support flexure. Although the actuator force is relatively low (9 newtons), it is high relative to the required force (0.2 newton). Maximum power requirement is approximately 1.4 watts.

2.4 ALIGNMENT DRIVE SYSTEM

The two axis tilt alignment is provided by a differential beam microposition mechanism. The output motion of the microposition mechanism biases the position of each image motion control actuator. The design concept is based upon the use of two relatively long thin flexures mounted back-to-back and riveted at one end. If one blade is bent in an arc, the other blade on the outside of the arc and the free ends of the blades will be displaced depending upon the arc parameters and thickness of the blades. The design is shown in Figure 2-7. The radius of the arc may be either positive or negative, giving a positive or negative range of adjustment.

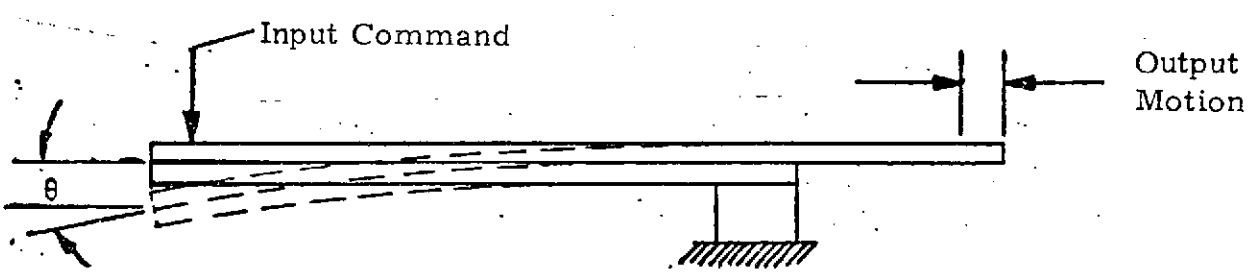

Figure 2-7. Differential Beam Microposition Mechanism

2.5 MIRROR ARTICULATION SYSTEM SELECTED FOR MANUFACTURE AND TEST

The final system design envolved from the elements described above. The mirror suspension consists of a centrally mounted cruiform flexure. The alignment drive consists of a differential beam micropositioner remotely controlled by a gear motor and cam. Interchangeable installation of stabilization actuators of two different types is provided. The piezo ceramic actuator configuration is shown in Perkin-Elmer Engineering drawing 660-0267. The flexure torque motor configuration is shown in drawing 660-0301.

3.0 SYSTEM DESIGN

3.1 MIRROR MASS PROPERTIES

3.1.1 Simulated Mirror Weight

Conditions Mirror Diameter = 0.508 meter (20 inches)

Mirror Thickness = $\frac{D}{6} = \frac{0.508\ m}{6} = 0.0846\ m$

Mirror Density CerVit (2.50 $\frac{gm}{cm^3}$ machined to reduce weight to 40 percent solid weight.

$$\text{Volume} = \frac{\pi d^2}{4} \times \ell = \frac{3.14\ (50.8\ cm)^2}{4} \times 8.46\ cm$$
$$= \underline{17{,}138\ cm^3}$$

$$\text{Weight} = 0.4 \times 17{,}138\ cm^3 \times 2.50\ \frac{gm}{cm^3}$$
$$= 17{,}138\ gm\ (37.79\ lbs)$$

3.1.2 Simulated Mirror Inertia

$$\text{Inertia (I)} = \frac{m}{12}\ (3r^2 + h^2)$$

$$I = \frac{17.138\ Kgm}{12}\ \left[(3 \times 0.254m)^2 + (0.0846m)^2\right]$$

$$I = 0.8394\ (Kgm)\ (m^2)$$

The mass properties of the mirror were simulated in the test system by an assembly of aluminum plate 1.27 cm (0.5 in) thick.

Weight (considered as mass)

Front and back plates:

$$\text{Volume} = \frac{\pi d^2}{4} \times \ell \times 2$$

$$= \frac{\pi\ (50.8\ cm)^2}{4} \times 1.27\ cm \times 2 = 5145.54\ cm^3$$

Central Hub:

Volume = 8.89 cm x 8.89 cm x 5.72 cm = 452 cm^3

Ribs:

Volume = 20.95 cm x 5.84 cm x 1.27 cm x 4 = 621.53 cm^3

Total Volume = 5145.54 cm^3 + 452 cm^3 + 621.53 cm^3 = 6219 cm^3

Total Weight = 6219 cm^3 x 2.702 $\frac{gm}{cm^3}$ = 16,804 g

16.804 Kg (37.05 lbs)

Inertia

$Ig = Ig_1, - Ig_2$

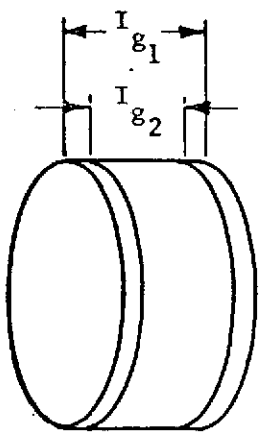

$Ig = \frac{m}{12}(3r^2 + h^2)$

$V_1 = \frac{\pi d^2}{4} \ell_1 = \frac{\pi(50.8\ cm)^2}{4}\ 8.57\ cm = 17{,}361\ cm^3$

$M_1 = 17{,}361\ cm^3 \times 2.702\ \frac{gm}{cm^3} = 46{,}909\ gm$

$Ig_1 = \frac{m_1}{12}(3r^2 + h^2)$

$= \frac{46.9\ Kgm}{12}\ [3(0.254\ m)^2 + (0.086\ m)^2]$

$$Ig_1 = 3.908 \text{ Kgm } (0.1935 \text{ m}^2 + 0.0074 \text{ m}^2)$$

$$Ig_1 = 0.7851 \text{ (Kgm) } (\text{m}^2)$$

$$V_2 = \frac{\pi d^2}{4} \ell = \frac{\pi(50.8 \text{ cm})^2}{4} \times 6.03 \text{ cm}$$

$$= 12{,}215.6 \text{ cm}^3$$

$$M_2 = 12{,}215.6 \text{ cm}^3 \times 2.702 \frac{\text{gm}}{\text{cm}^3} = 33{,}006 \text{ gm}$$

$$Ig_2 = \frac{M_2}{12} (3r^2 + h^2)$$

$$= \frac{33.006}{12} \text{ Kgm } [3(0.254 \text{ m})^2 + (0.0603 \text{ m})^2]$$

$$= 2.750 \text{ Kgm } [0.1935 \text{ m}^2 + 0.0036 \text{ m}^2]$$

$$= 0.542 \text{ (Kgm) } (\text{m}^2)$$

$$\text{Ig total} = Ig_1 - Ig_2$$

$$= 0.7851 - 0.542$$

$$= 0.2431 \text{ (Kgm) } (\text{m}^2)$$

3.2 MIRROR SUPPORT FLEXURE DESIGN

The central flexure compliance was determined by test of a single axis flexure of the same size but different material. The flexure characteristics were corrected for the dual axis configuration and material change (aluminum to steel).

3.2.1 Flexure Compliance along Optic Axis

Test flexure stiffness (aluminum) axial compliance = $3.833 \times 10^{-6} \frac{\text{in}}{\text{lb}}$ (Ref. Appendix D).

$$\text{Axial Compliance} = 3.833 \times 10^{-6} \frac{\text{in}}{\text{lb}} \times 2.54 \times 10^{-2} \frac{\text{meter}}{\text{in}} \times \frac{1}{4.448} \frac{\text{lb}}{\text{newton}}$$

Axial Compliance $= 2.1888 \times 10^{-8} \frac{\text{meter}}{\text{newton}}$ in aluminum

$$K(\text{single axis in steel}) = \frac{1}{2.1888 \times 10^{-8}} \frac{\text{meter}}{\text{newton}} \times \frac{29}{10.6} = 1.2499 \times 10^{8} \frac{\text{newton}}{\text{meter}}$$

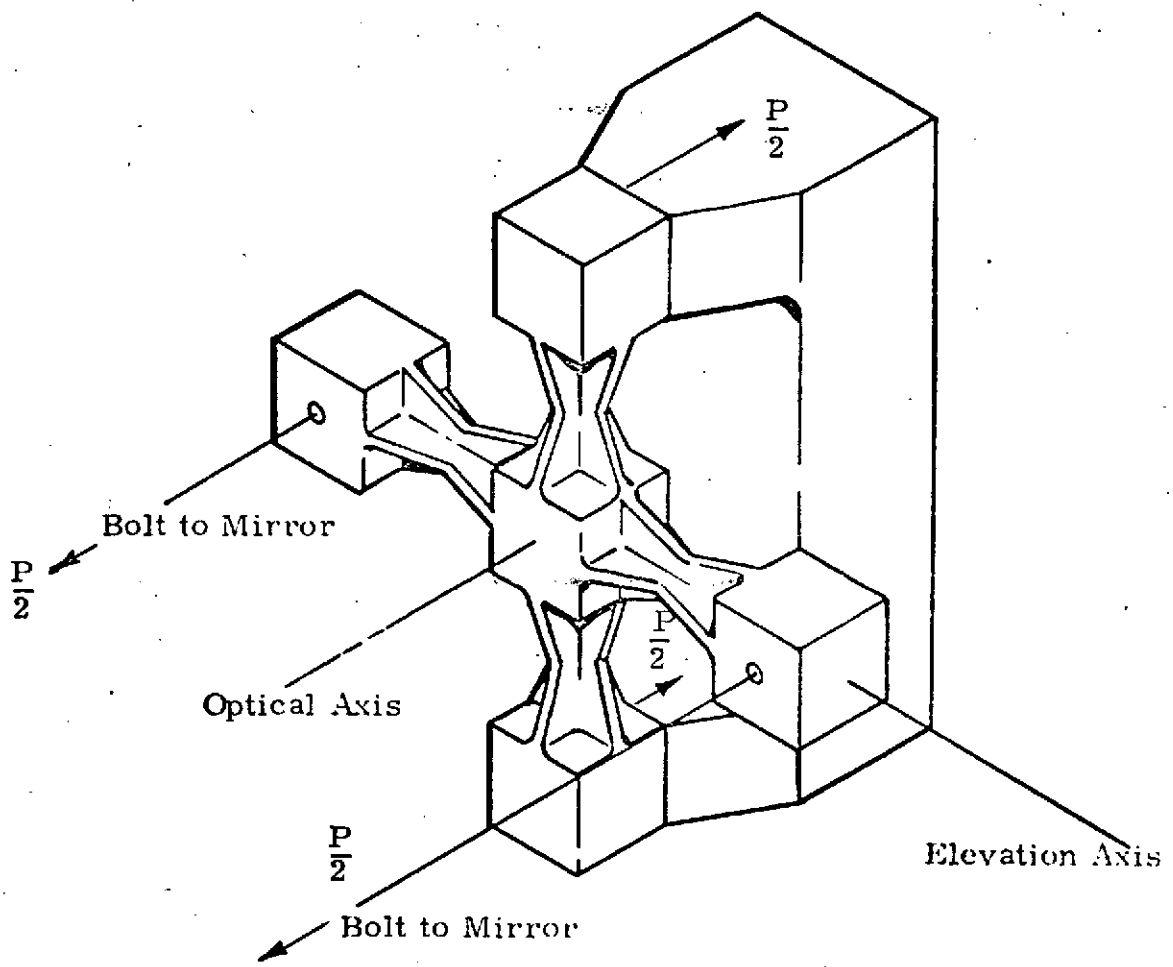

$K_{\text{axial (Dual Axis)}}$

$$\frac{1}{K_T} = \frac{1}{K_1} + \frac{1}{K_2} = \frac{1}{1.2499 \times 10^{8}} + \frac{1}{1.2499 \times 10^{8}}$$

$$K_3 = 0.6249 \times 10^{8} \frac{\text{newton}}{\text{meter}}$$

3.2.2 Radial Compliance

$$\frac{1}{K_{\text{radial}}} = \frac{1}{K_1 + K_2} + \frac{1}{K_3}$$

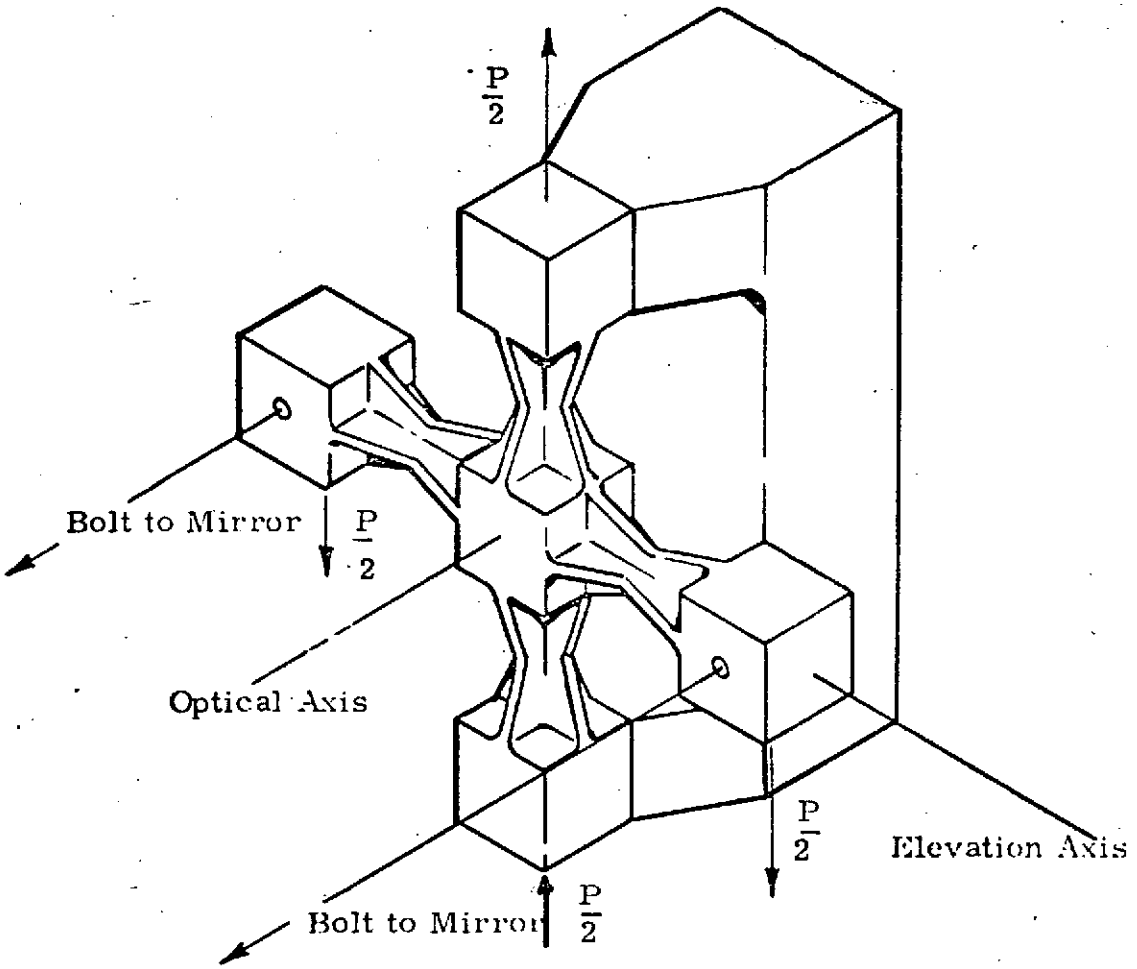

$$\delta_1 = \delta_2 = \frac{PL}{AE}$$

Let $P = \frac{P_1}{2} = 1$ newton

$\ell = 1.27$ cm

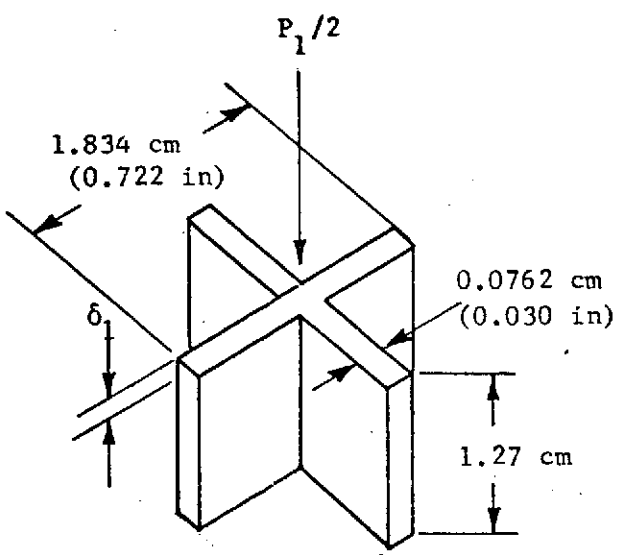

$$A = 1.834 \text{ cm} \times 0.0762 \text{ cm} + 1.758 \text{ cm} \times 0.0762 \text{ cm}$$

$$= 0.1397 + 0.1339 = 0.2736 \text{ cm}^2$$

$$\delta_1 = \frac{PL}{AE} = \frac{1 \text{ newton} \times 1.27 \text{ cm}}{0.2736 \text{ cm}^2 \times 19.63 \times 10^6 \frac{\text{newtons}}{\text{cm}^2}}$$

$$\delta_1 = 0.2364 \times 10^{-6} \frac{\text{cm}}{\text{newton}}$$

$$K_1 = \frac{1}{\delta_1} = \frac{1}{0.2364 \times 10^{-6} \frac{\text{cm}}{\text{newton}}} = 4.230 \times 10^6 \frac{\text{newton}}{\text{cm}}$$

$$= 423.0 \times 10^6 \frac{\text{newton}}{\text{meter}}$$

$$\frac{1}{K_{radial}} = \frac{1}{K_1 + K_2} + \frac{1}{K_3}$$

$$\frac{1}{K_{radial}} = \frac{1}{2(4.23 \times 10^8 \frac{\text{newton}}{\text{meter}})} + \frac{1}{1.2499 \times 10^8 \frac{\text{newton}}{\text{meter}}}$$

$$\frac{1}{K_{radial}} = 1.182 \times 10^{-9} \frac{\text{meter}}{\text{newton}} + 8.000 \times 10^{-9} \frac{\text{meter}}{\text{newton}}$$

$$= 9.182 \times 10^{-9} \frac{\text{meter}}{\text{newton}}$$

$$K_{radial} = \frac{1}{9.182 \times 10^{-9} \frac{\text{meter}}{\text{newton}}} = 1.089 \times 10^8 \frac{\text{newton}}{\text{meter}}$$

3.2.3 Compliance About Azimuth and Elevation Axes

$$K_4 = 283 \frac{\text{in-lb}}{\text{Rad}} \quad \text{(Ref. Appendix E aluminum flexure)}$$

$$K_4 = 283 \frac{\text{in-lb}}{\text{Rad}} \times \frac{29}{10.6} \times 2.54 \times 10^{-2} \frac{\text{meter}}{\text{in}} \times 4.448 \frac{\text{newton}}{\text{lb}}$$

$$= 0.8747 \frac{\text{meter newton}}{\text{Rad.}}$$

3.2.4 Resonant Frequency of Simulated Mirror Supported by Cruciform Flexure

3.2.4.1 Axial Direction

$$f_n = \frac{1}{2\pi}\sqrt{\frac{K}{M}}$$

$$f_n = \frac{1}{2\pi}\sqrt{\frac{0.6249 \times 10^8 \ \frac{\text{newton}}{\text{meter}}}{17.138 \text{ Kg}}}$$

$$= 304.06 \text{ Hz}$$

3.2.4.2 Radial Direction

$$f_n = \frac{1}{2\pi}\sqrt{\frac{1.089 \times 10^8 \ \frac{\text{newton}}{\text{meter}}}{17.138 \text{ Kg}}}$$

$$= 401.39 \text{ Hz}$$

3.2.5 Actuator Stroke

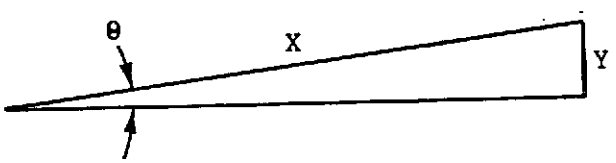

$$\theta = 3 \text{ arc-sec} \times 4.848 \times 10^{-6} \ \frac{\text{rad}}{\text{sec}}$$

$$= 14.544 \times 10^{-6} \text{ rad.}$$

X = Mirror Rad = 0.254 meters

$$Y = \theta x = 14.544 \times 10^{-6} \text{ rad} \times 0.254 \text{ meter}$$

$$= 3.694 \times 10^{-6} \text{ meter } (145.4 \times 10^{-6} \text{in})$$

Actuator Stroke = $\pm$ 3.694×10^{-6} meter.

3.2.6 Actuator Load Due to Cruciform Flexure Stiffness

$$\theta_{max} = \theta \text{ stabilization} + \theta \text{ alignment}$$

$$= 3 \text{ arc-seconds} + 5 \text{ arc-seconds}$$

$$= 8 \text{ arc-seconds} \times 4.848 \times 10^{-6} \frac{\text{rad}}{\text{sec}}$$

$$= 38.784 \times 10^{-6} \text{ radian}$$

$$Q = K\theta = 0.8747 \frac{\text{meter newton}}{\text{rad}} \times 38.784 \times 10^{-6} \text{ rad.}$$

$$= 3.392 \times 10^{-5} \text{ meter newton.}$$

$$F_{act} = \frac{Q}{R} = \frac{3.392 \times 10^{-5} \text{ meter newton}}{0.254 \text{ meter}}$$

$$= 1.335 \times 10^{-4} \text{ newton } (3.002 \times 10^{-5} \text{ lb})$$

3.2.7 Alignment Drive Design

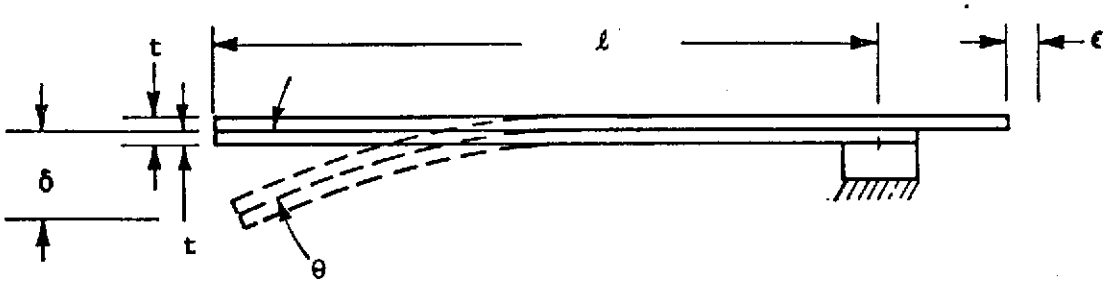

From beam theory,

$$\theta = \frac{F\ell^2}{2\,EI} \qquad \delta = \frac{F\ell^3}{3\,EI}$$

Then,

$$\theta = \frac{3}{2}\frac{\delta}{\ell}$$

For small value of θ

$$\varepsilon = \theta t = \frac{3t\delta}{2\ell}$$

Required stroke (ε) for 10-arc-second alignment range

$$\varepsilon = \text{alignment angle} \times \text{actuator attachment radius}$$

$$= 10\text{-arc-second} \times 4.848 \times 10^{-6} \frac{\text{rad}}{\text{sec}} \times 22.23 \text{ cm}$$

$$= 1077.5 \times 10^{-6} \text{ cm}$$

$$\delta = \frac{2\ell\varepsilon}{3t} \qquad \text{let } \ell = 8.64 \text{ cm}, \quad t = 0.096 \text{ cm}$$

$$= \frac{2 \times 8.64 \text{ cm} \times 1.077 \times 10^{-3} \text{cm}}{3 \times 0.096 \text{ cm}} = 6.462 \times 10^{-2} \text{ cm}$$

Cam angle θ:

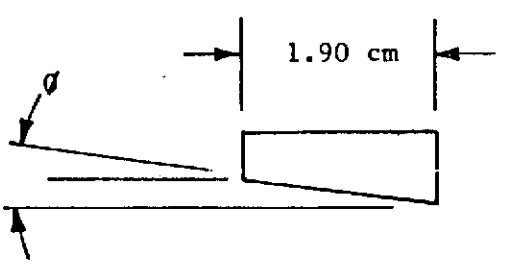

$$\theta = \frac{\delta}{d} = \frac{6.42 \times 10^{-2} \text{ cm} \times 1.6 \text{ (overtravel)}}{1.9 \text{ cm}}$$

$$= 5.44 \times 10^{-2} \text{ rad (3.1 degree)}$$

3.2.8 Thermal Design

The simulated mirror was designed to represent the weight and inertia of a lightweight CerVit mirror. Aluminum plates were selected for two major reasons

- Minimum manufacturing cost
- Low density permits thicker plates and greater stiffness without exceeding weight and inertia limits.

The high coefficient of expansion can cause high sensitivity of mirror angle to temperature change.

The best material for minimum thermal sensitivity would have a low coefficient of expansion, such as Invar. Cost and weight, however, would not be acceptable.

An alternate concept was to balance the effect on mirror angle by selecting elements in the thermal loop from either aluminum or stainless steel in such a way that all thermal dimensional changes add to zero. This provides a structure that is capable of operating over a wide temperature range without a mirror angle index change. Since small and large elements will respond dimensionally at different rates to a temperature change, the structure must be permitted to stabilize at the environmental temperature prior to operation.

The thermal response of the system is determined by adding the dimensional change of each element in the mirror position loop. Reference to Perkin-Elmer drawing 660-0267 for dimensions and material.

Thermal coefficient of expansion are as follows:

Stainless Steel 17-4 PH H1075	= 6.3×10^{-6} in/in/°F
Stainless Steel Type 304	= 9.6 in/in/°F
Aluminum 2024 T4	= 11.74 in/in/°F
Stainless Steel Type 310	= 8.0 in/in/°F
PZT Material	= 2.222 in/in/°F

$$\Delta X = -(3.236 - 0.36)\text{ in} \times 8.0 \frac{\mu\text{ in}}{°F} + (4.06 - 3.50)\ 9.6 \frac{\mu\text{ in}}{°F}$$

$$-[0.718 - (2.12 - 1.62 - 0.25)]\ 8.0 \frac{\mu\text{ in}}{°F} + (0.200)\ 9.6 \frac{\mu\text{ in}}{°F}$$

$$+(1.200)\ 2.22 \frac{\mu\text{ in}}{°F} + (1.85)\ 9.6 \frac{\mu\text{ in}}{°F} + (2.05)\ 11.74 \frac{\mu\text{ in}}{°F}$$

$$-(0.722)\ 6.3 \frac{\mu\text{ in}}{°F} - (1.62)\ 11.74 \frac{\mu\text{ in}}{°F} - (0.36)\ 11.74 \frac{\mu\text{ in}}{°F}$$

$$\Delta X = -2.759 \frac{\mu\text{ in}}{°F}$$

$$\Delta\theta = \frac{3.0\text{ arc-sec}}{128\ \mu\text{ in}} \times -2.759 \frac{\mu\text{ in}}{°F} = -0.0646 \frac{\text{arc-sec}}{°F}$$

$$= (-0.1163 \frac{\text{arc-sec}}{°C})$$

4.0 SYSTEM TEST

4.1 SUMMARY

System testing was performed in accordance with Report No. 11783, Test Procedure - LST Secondary Mirror Actuation System. This document defines test procedures to verify the calibration and performance of components and system. Appendix A documents the results of system testing of the PZT actuator configuration. Appendix B documents results of system testing of the flexure torque motor actuator configuration. This testing was performed using test instruments calibrated in conventional units. Therefore, the data and data reduction in the appendices is in conventional units. Significant performance characteristics derived are listed in the preferred SI units in this section. Appendix C describes a test performed using a precise interferometric angle sensing device that confirmed system performance.

4.2 SYSTEM TEST - PZT ACTUATOR CONFIGURATION - 660-0267 (REFERENCE APPENDIX A)

The component schematic diagram is shown in Figure 4-1. A Hewlett-Packard Model 202A Ultra Low Frequency Signal Generator was used to drive a Burleigh PZ-70 High Voltage Operational Amplifier in each axis. Mirror position was monitored by four position transducers. All four were basically Brown and Sharp Model 599-986 Super Gage Sensors and Brown and Sharp Model 599-991 amplifiers. During system calibration, the position sensors that are provided to monitor alignment drive position in each axis were relocated to sense mirror angle. A position sensor is built into each axis (azimuth and elevation). B and S Model 599-986 gage heads were disassembled to remove the magnetic core and sensing coils. The core was mounted to the mirror and the sensing coils were mounted to the support structure. This was done to eliminate sensor force that could affect mirror position. Since such disassembly could invalidate the manufacturer's calibration, the remaining two gage heads were calibrated by the Perkin-Elmer Quality Control Department and used to monitor mirror position. Two monitor gages were mounted to measure mirror tilt angle in each axis during calibration. The average of the two monitor gages was used to determine a scale factor for the single gages built into each axis. The test setup is shown in Figure 4-2. Results of the test are tabulated in Table 4-I.

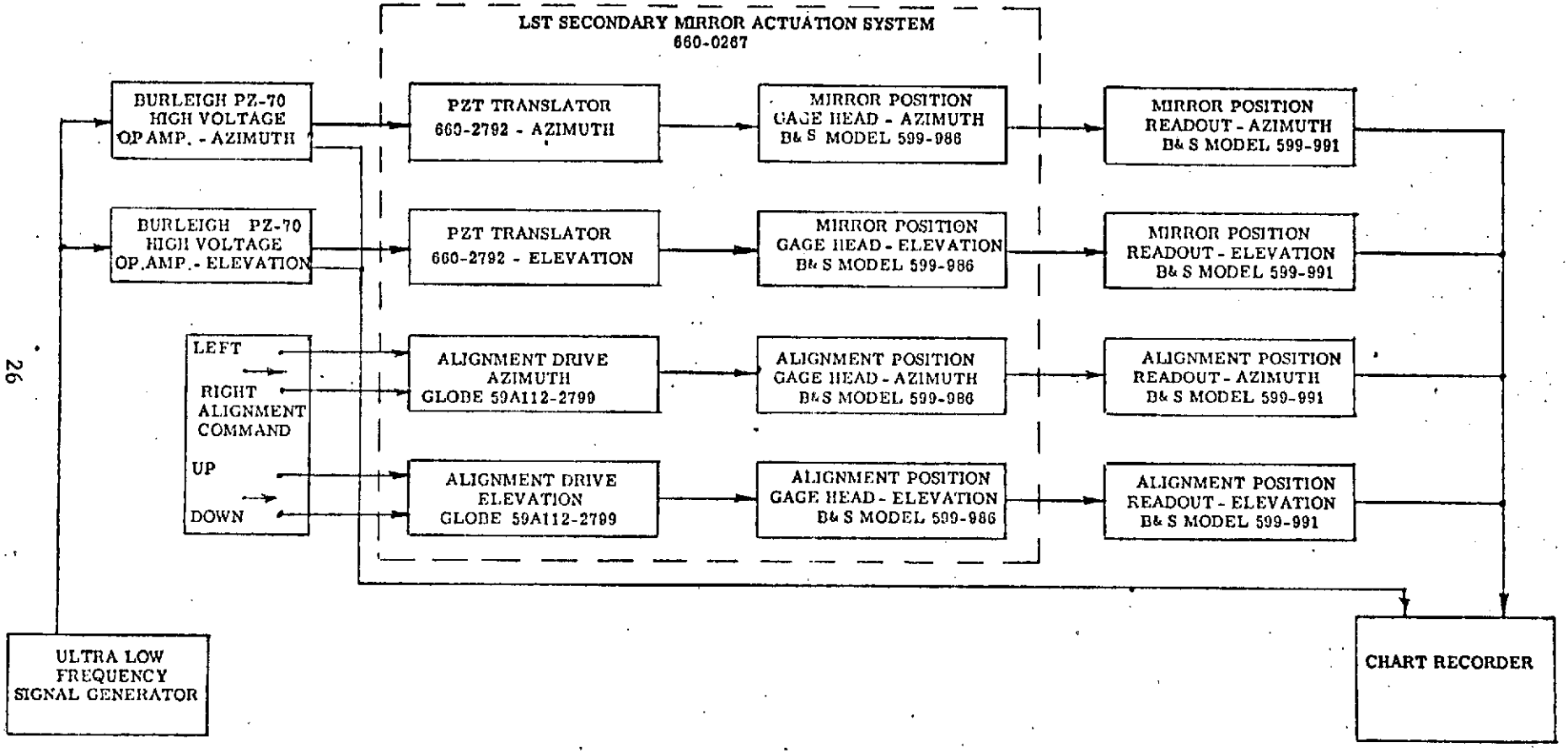

Figure 4-1. Component Schematic Piezo Ceramic Actuator Configuration

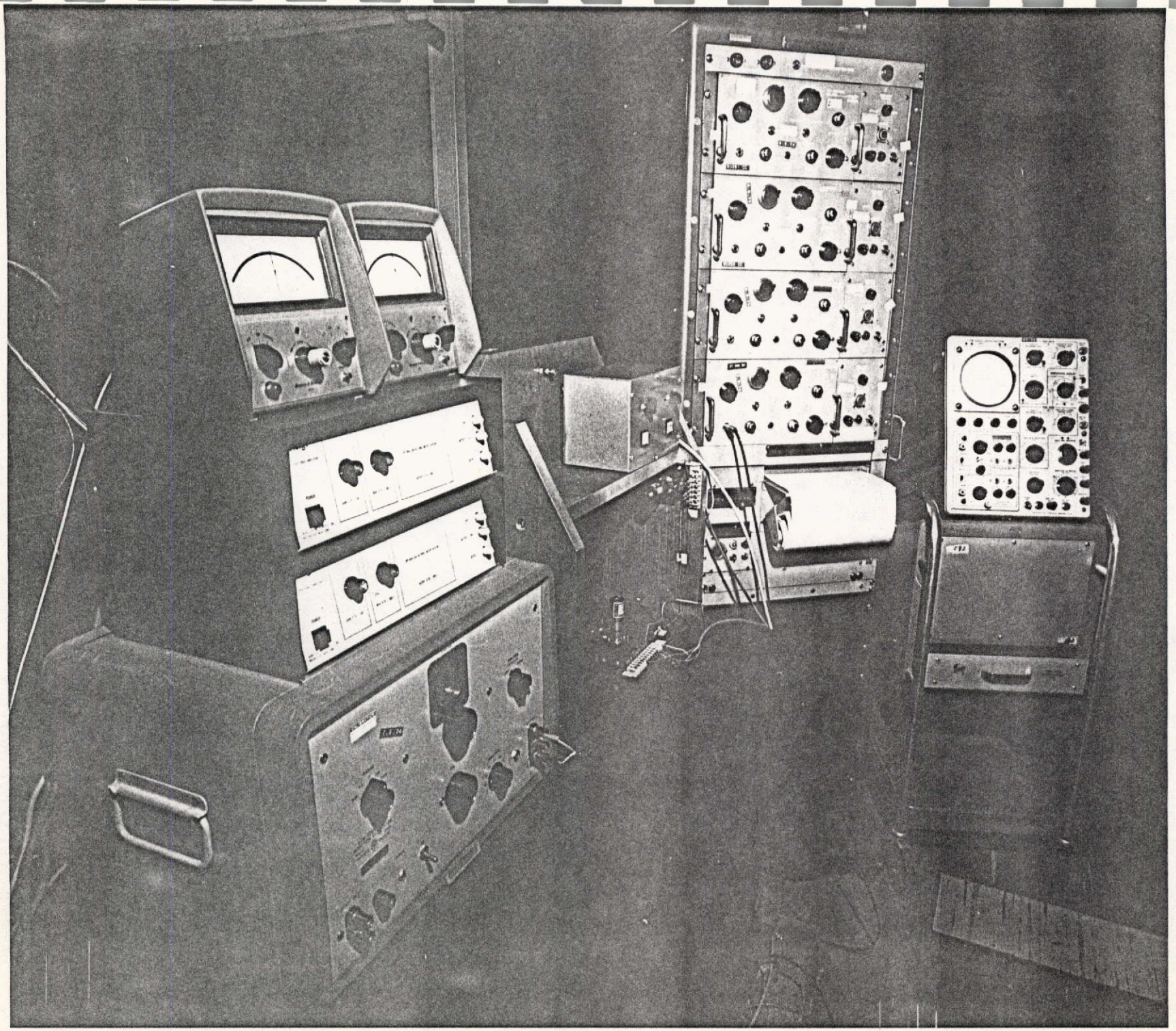

Figure 4-2. PZT Actuator Configuration Test Setup (Sheet 1 of 2)

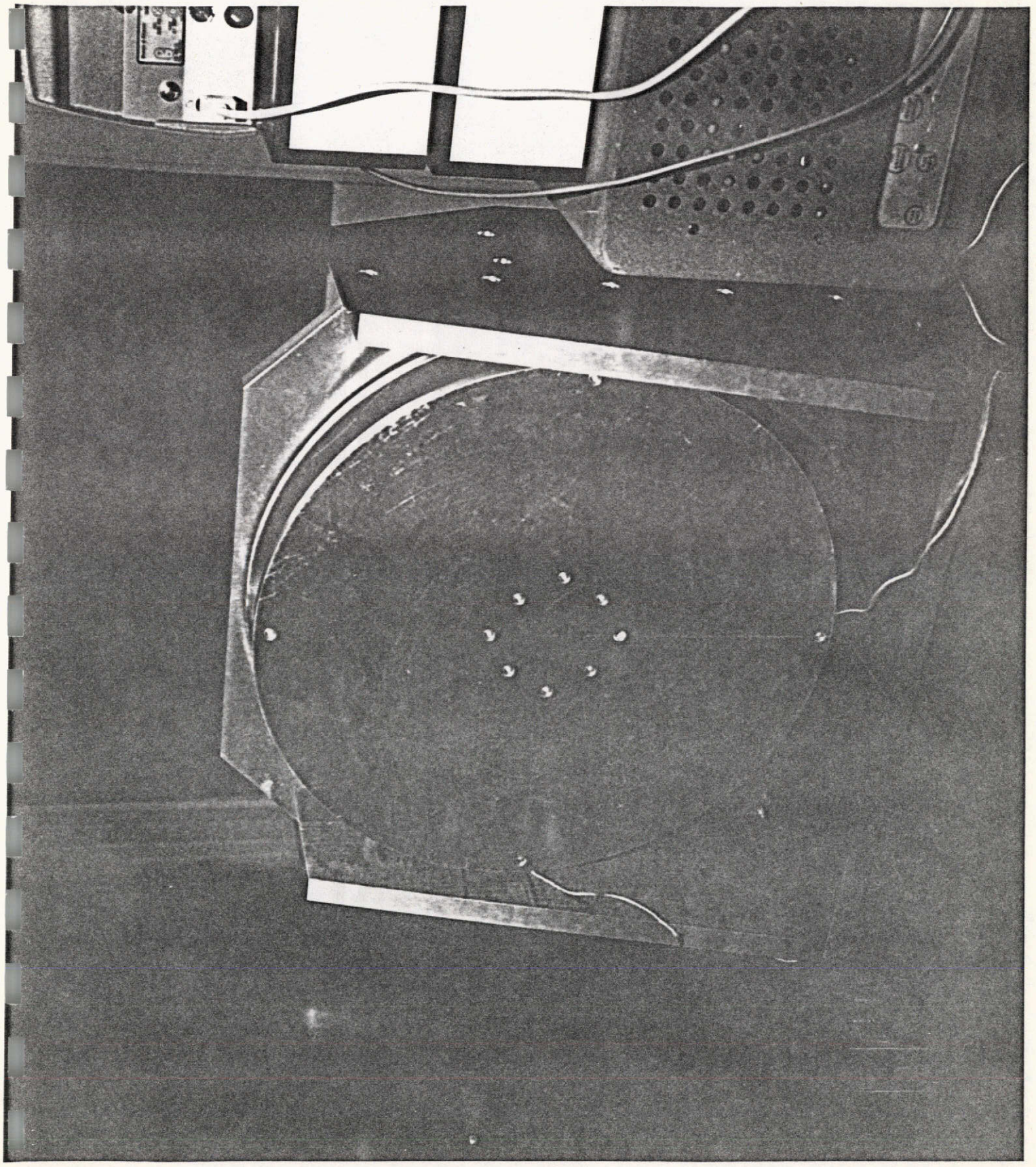

Figure 4-2. PZT Actuator Configuration Test Setup (Sheet 2 of 2)

TABLE 4-I. TABULATION OF TEST RESULTS

Characteristic	Spec	PZT Configuration AZ	PZT Configuration EL	Flex Torque AZ	Flex Torque EL
Alignment					
Total Range	±5 arc-sec	±6.04 arc-sec	±5.83 arc-sec	±5.83 arc-sec	±5.042 arc-sec
Threshold	0.1 arc-sec	0.042 arc-sec	0.052 arc-sec	0.08 arc-sec	0.063 arc-sec
Response	10 arc-sec/min	10.36 arc-sec/min	10.001 arc-sec/min	10.003 arc-sec/min	8.664 arc-sec/min
Stabilization					
Total Range	±3 arc-sec	±7.58 arc-sec	±7.3 arc-sec	±3.93 arc-sec	±3.26 arc-sec
Response	3 db @ 4 Hz	+1.86 db @ 70 Hz	-0.26 db @ 70 Hz	-2.59 db @ 20 Hz	-2.0 db @ 20 Hz
Threshold	±0.005 arc-sec	±0.0007 arc-sec	±0.0007 arc-sec	±0.003 sec	±0.0017 arc-sec

4.3 SYSTEM TEST - FLEXURE TORQUE MOTOR ACTUATOR CONFIGURATION - 660-0301 (REFERENCE APPENDIX B)

The component schematic diagram for this configuration is shown in Figure 4-3. The test procedure was the same as that used for the PZT actuator configuration. The detailed test results are documented in Appendix B and tabulated in Table 4-I.

4.4 TEST OF MIRROR SUSPENSION STIFFNESS PZT ACTUATOR CONFIGURATION (660-0267)

The stiffness of the mirror suspension system to ground was measured by placing the mirror system on the isolation table with the optic axis vertical. Weights were placed on the mirror surface at a 9.9-inch radius, directly over the supporting actuator. A position transducer sensed deflection at the point of load application. The relationship between applied load and mirror deflection is shown on Figure 4-4.

The mirror support stiffness is:

$$\theta = \frac{500 \times 10^{-6} \text{ in}}{9.9 \text{ in}} = 50.5 \times 10^{-6} \text{ rad}$$

$$Q = 5.5 \text{ lb} \times 9.9 \text{ in} = 54.45 \text{ in lb}$$

$$\text{Stiffness} = \frac{50.5 \times 10^{-6} \text{ rad}}{54.45 \text{ in lb}} = 0.927 \times 10^{-6} \frac{\text{rad}}{\text{in-lb}}$$

$$= \left(8.21 \times 10^{-6} \frac{\text{rad}}{\text{meter-heating}}\right)$$

NOTE

Bracket (Item 3, 660-0267) was found to cause excessive compliance. It was replaced with a stiffer bracket (660-2855) for test of the 660-0301 configuration. The 660-0267 configuration was not retested with the stiffer bracket.

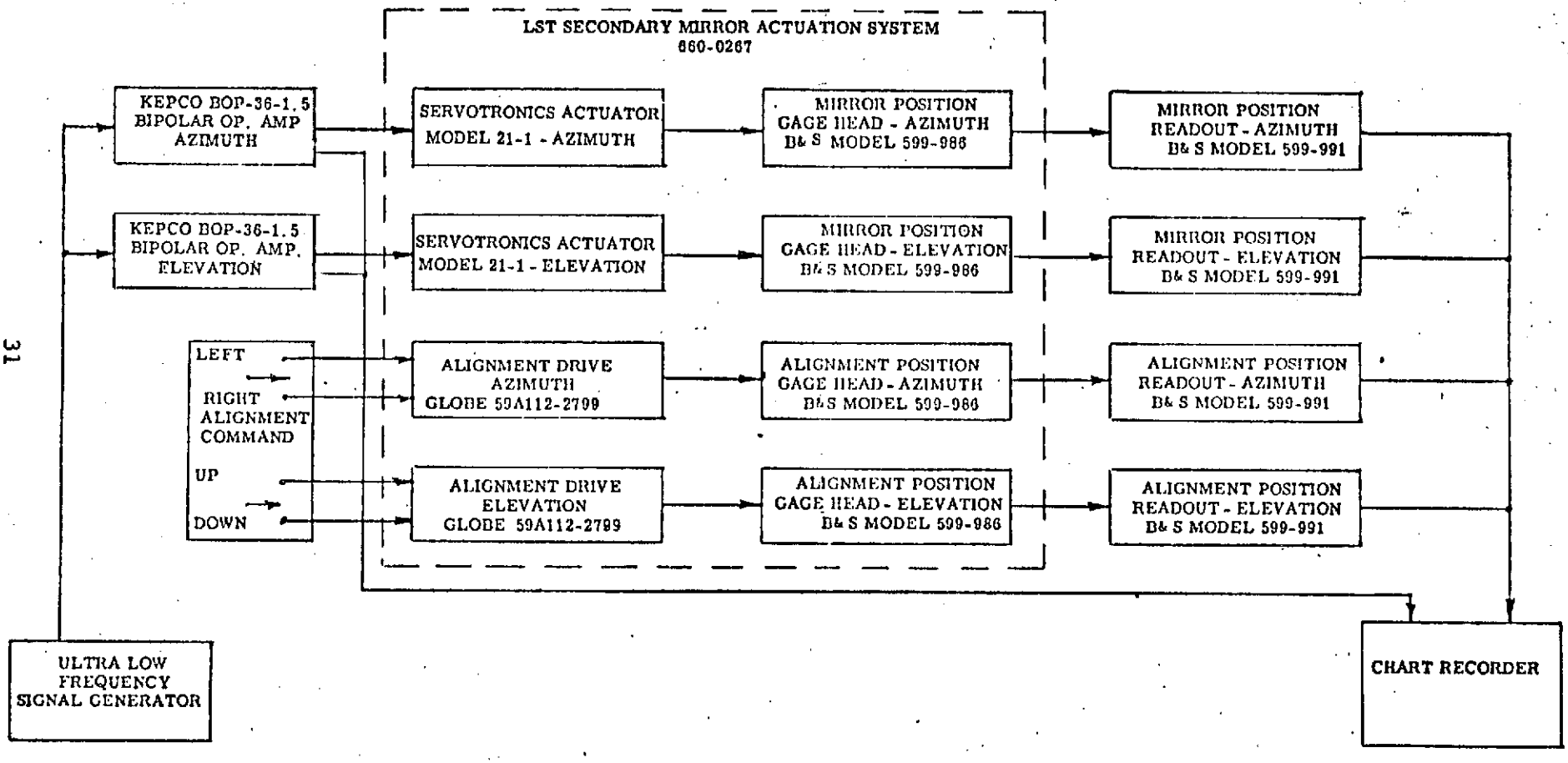

Figure 4-3. Component Schematic Flexure Torque Motor Actuator Configuration

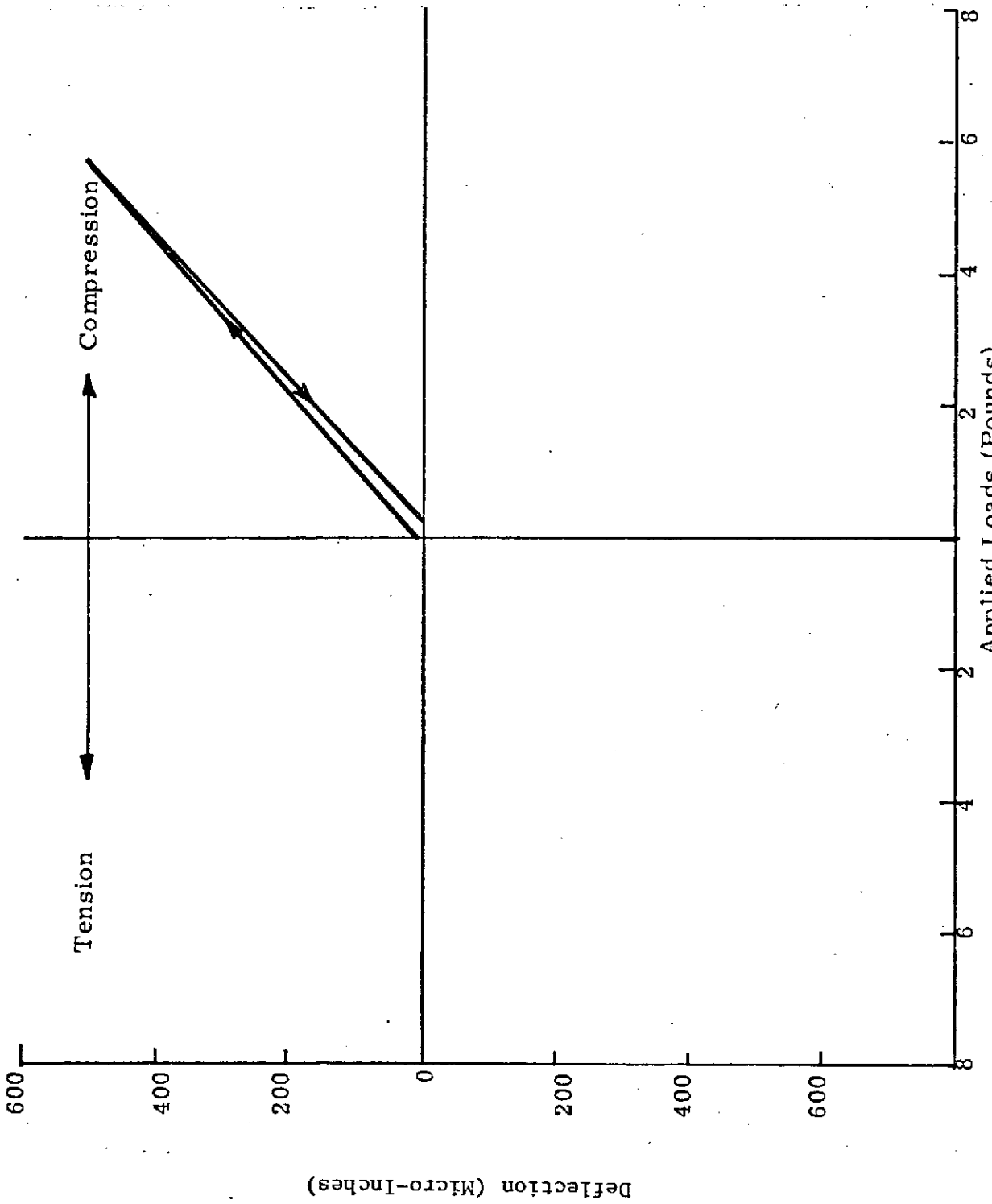

Figure 4-4. LST Secondary Mirror (Elevation Axis), Mirror Deflection versus Applied Load

4.5 TEST OF MIRROR SUSPENSION SYSTEM - FLEXURE TORQUE MOTOR CONFIGURATION (660-0301)

The stiffness of the mirror suspension system with the flexure torque motor actuators was measured using the same method. The relationship between applied load and mirror deflection is shown in Figure 4-5.

The mirror stiffness is

$$\theta = \frac{550 \times 10^{-6} \text{ in}}{9.9 \text{ in}} = 55.55 \times 10^{-6} \text{ rad}$$

$$Q = 8.37 \text{ lb} \times 9.9 \text{ in} = 82.86 \text{ in-lb}$$

$$\text{Stiffness} = \frac{55.55 \times 10^{-6} \text{ rad}}{82.86 \text{ in-lb}} = 0.67 \times 10^{-6} \frac{\text{rad}}{\text{in-lb}}$$

$$= \left(5.93 \times 10^{-6} \frac{\text{rad}}{\text{meter newton}}\right)$$

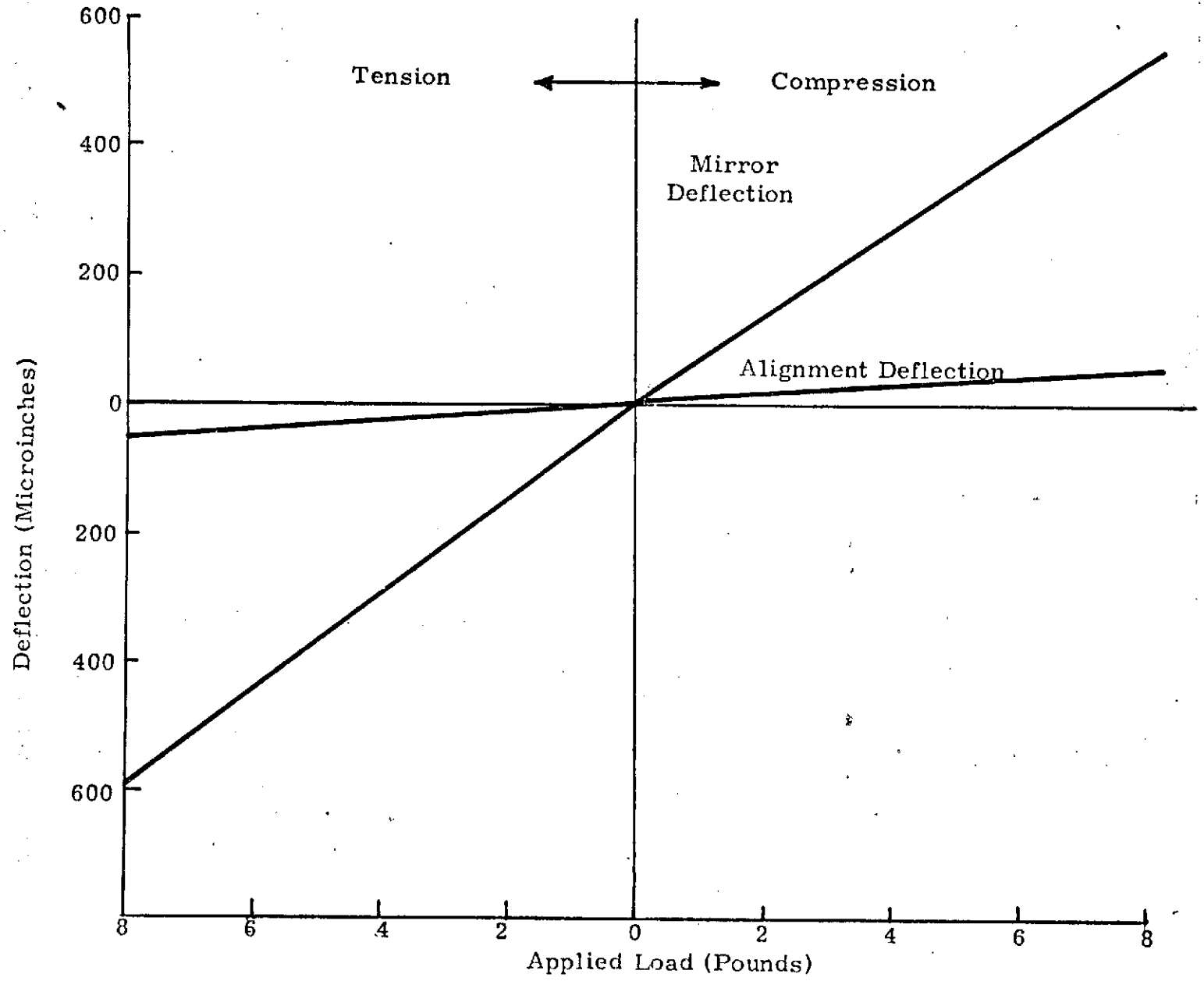

Figure 4-5. LST Secondary Mirror (Elevation Axis), Mirror Deflection and Alignment Drive Deflection versus Applied Load

5.0 CONCLUSIONS AND RECOMMENDATIONS

Review of the test results leads to the following conclusions.

5.1 CONCLUSION

5.1.1 Piezo Ceramic (PZT) Actuator Performance

The piezo ceramic actuator demonstrated position resolution that significantly exceeded the specified requirements. The maximum range was 2.5 times the required ±3 arc-seconds. The threshold was 7 times better than the required ±0.005 arc-second. The resolution range was 10,800 to 1 compared to the required 600 to 1. It is probable that the resolution limit demonstrated was determined by the position sensors rather than the mirror position control system.

The high stiffness and force capability of the PZT actuator provides very high frequency response capability. The response of the system tested was limited by a structural resonance at 70 to 90 Hz. This was traced to excessive compliance in an actuator support bracket. The bracket was replaced for test of the flexure torque motor (FT) actuator.

The PZT actuator demonstrated a high hysteresis characteristic approximately 14 percent. The percentage hysteresis is relatively constant for all amplitudes so that good response at very small amplitudes is possible. This characteristic must be considered in the design of a closed loop control system.

5.1.2 Flexure Torque Motor (FT) Actuator Performance

The position resolution of the FT actuator also significantly exceeded the specified requirements. The maximum range was slightly greater than the required ±3 arc-seconds and is limited by the stiffness of actuator stroke reducing flexures and the reduction in actuator force as the actuator approaches the stroke limit. These factors affect linearity of actuator current relative to mirror angle at maximum mirror angle. The resolution range is approximately 1500 to 1 compared to the required 600 to 1. Hysteresis was approximately 2 percent.

The frequency response of the FT actuator system was not as flat as the PZT actuator configuration. Refer to the response plot in Appendix B. The amplitude is +3 db at 2 Hz and falls rapidly above 10 Hz. Structural resonance was 100 to 120 Hz.

5.1.3 Alignment Drive Performance

The alignment drive performed with good precision and stability. Minimum pulse was approximately 0.05 arc-second and was limited by the start-stop characteristic of the motor. A stepper motor drive could provide better resolution if required.

5.1.4 Mirror Suspension System

The cruciform flexure performance was excellent. Cross coupling, and hysteresis were negligible.

5.1.5 Position Sensing Components

The Brown and Sharpe electromagnetic position sensors performed with resolution that exceeded expectation. The meter provided for visual indication of position is limited to approximately 1 microinch resolution. By taking the modulated 10,000-Hz carrier from the gage amplifier, filtering, and examining on a Type 502 HP oscilloscope, it was possible to resolve better than 0.04 microinch. It is significant to note that these measurements were accomplished under typical laboratory environmental conditions of atmospheric pressure turbulence, and temperature gradients.

5.2 RECOMMENDATIONS

Although both actuator configurations demonstrated the capability of meeting all performance requirements, the configuration considered to have the greatest overall merit is the piezo ceramic actuator configuration. The cruciform flexure suspension and flexure microposition alignment drive were common to both configurations tested. Performance of these common elements was excellent throughout testing of both actuator configurations.

The performance characteristics that favor the PZT actuator are listed below. The differences are not so significant that the flexure torque motor actuator should not receive further consideration for the LST application.

- o PZT actuators had best range and resolution
- o Structural simplicity and reliability of the PZT actuator approaches that of simple structural members. Redundancy can be accomplished by series stacking of actuator components.
- o Stroke range is compatible with direct coupling of actuator to mirror.
- o High stiffness and load capacity provides launch survival without caging devices.
- o High force and frequency response better than 10,000 Hz provide capability to follow square wave forms.

5.3 DOCUMENTATION LIST

Engineering drawings and reports covering both actuator mechanisms are listed below:

Drawing Number	Title
660-0267	LST Secondary Mirror Actuation System (PZT Actuator)
660-0301	LST Secondary Mirror Actuation System (Flexure Torque Motor)
660-0306	System Wiring Diagram - LST Secondary Mirror
660-2792	PZT Translator Assembly
660-2841	Alignment Control Panel
660-2855	Support, Flexure
Reports	
11602A	Proposal - LST Secondary Mirror Articulation System
11783	Test Procedure - LST Secondary Mirror Actuation System

APPENDIX A

PZT ACTUATOR TEST DATA

A

THE PERKIN-ELMER CORPORATION

SENSOR SYSTEMS

Scientific Payloads Department

74-SS-1468

January 23, 1974

TO: File - LST Secondary Mirror

FROM: W. E. Kohman

SUBJECT: FINAL ACCEPTANCE TEST
LST SECONDARY MIRROR ACTUATION SYSTEM
PZT ACTUATOR CONFIGURATION
660-0267

REFERENCE: (1) Contract NAS 8-29723 SPO 33117

The attached data sheets and calculation sheets document the final acceptance test of the subject LST Secondary Mirror actuation system. This test confirms that the system meets the requirements of the Reference (1) contract and is accepted and approved for disassembly and conversion to the flexure torque motor configuration 660-0301.

W E Kohman

W. E. Kohman — Perkin-Elmer Engineering

A. Menzies — Perkin-Elmer Quality Assurance

John E Golley

Paul Golley — MSFC Engineering

WEK:mb

Attachments

BY W.K. Johnson DATE 1/25/74 SUBJECT TEST PROCEDURE — 6ST SECONDARY MIRROR — ER 11783 — SHEET NO. 1 OF 8

CHKD. BY ____ DATE ____ — JOB NO. ____

I DETERMINE VOLTAGE GAIN — ELEVATION.

1. MIRROR EL = $\frac{(+387 + 320)\ \text{MIN.}}{800\ \text{VOLTS}} = .883 \times 10^{-6}\ \frac{\text{IN}}{\text{VOLT}}$

2. MIRROR AZ — 0

3. MONITOR BOTTOM = $\frac{+160 + 410}{800} = .713 \times 10^{-6}\ \frac{\text{IN}}{\text{VOLT}}$

4. MONITOR TOP = $\frac{255 + 295}{800} = .6875 \times 10^{-6}\ \frac{\text{IN}}{\text{VOLT}}$

5. AVERAGE MONITOR GAIN.

$$\frac{(.713 + .6875)\times 10^{-6}\ \text{IN/VOLT}}{2} = .70025 \times 10^{-6}\ \frac{\text{IN}}{\text{VOLT}}$$

MONITOR ACCURACY = ± 1.82 PERCENT

6. SCALE FACTOR - MIRROR EL.

$$S.F = \frac{.70025}{.883} = .79304$$

II 4.2.1.1 TOTAL ANGULAIR RANGE & RATE

BY_____ DATE_____ SUBJECT_____ SHEET NO. 1 OF 10

CHKD. BY_____ DATE_____ JOB NO._____

PEAK TO PEAK AMPLITUDE = 245 + 165 = 410×10^{-6} IN.

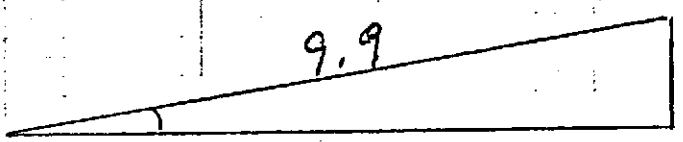

$$\theta = \frac{410 \times 10^{-6} \text{ IN}}{9.9 \text{ IN}} = 41.414 \times 10^{-6} \text{ RAD}$$

$$\theta = \frac{41.414 \times 10^{-6} \text{ RAD}}{4.848 \times 10^{-6} \frac{\text{RAD}}{\text{SEC}}} = 8.542 \text{ SEC P-P}$$

± 4.271

INCREASE GAIN OF ALIGNMENT CAM

PEAK TO PEAK AMPLITUDE $+100 + 460 = 560 \times 10^{-6}$ IN.

$$\theta \quad \frac{560 \times 10^{-6} \text{ IN}}{9.9 \text{ IN}} = 56.565 \times 10^{-6} \text{ RAD.}$$

$$\theta = \frac{56.565 \times 10^{-6} \text{ RAD}}{4.848 \times 10^{-6} \frac{\text{RAD}}{\text{SEC}}} = 11.667 \text{ SEC}$$

± 5.834 SEC

PERIOD = 140 SEC

4.2.1.2 THRESHOLD

$$\text{MIN PULSE} = \frac{(192 - 187) \times 10^{-6}\ \text{IN}}{2} = 2.5 \times 10^{-6}\ \text{IN.}$$

$$\theta = \frac{2.5 \times 10^{-6}\ \text{IN}}{9.9\ \text{IN}} = .2525 \times 10^{-6}\ \text{RAD}$$

$$\theta = \frac{.2525 \times 10^{-6}\ \text{RAD}}{4.845 \times 10^{-6}\ \frac{\text{RAD}}{\text{SEC}}} = \underline{0.0521\ \text{SEC}}$$

4.2.2.1 TOTAL ANGULAR RANGE

$$\text{RANGE} = 700.25 \times 10^{-6}\ \frac{\text{IN}}{1000\ \text{VOLTS}}$$

$$\theta = \frac{700.25 \times 10^{-6}\ \text{IN}}{9.9\ \text{IN}} = 70.732 \times 10^{-6}\ \text{RAD.}$$

$$\theta = \frac{70.732 \times 10^{-6}\ \text{RAD}}{4.848 \times 10^{-6}\ \frac{\text{RAD}}{\text{SEC}}} = 14.59\ \text{SEC}$$

OR ± 7.295 SEC

4.2.2.2 FREQUENCY RESPONSE

FREQ (CPS)	ACT VOLTS	MIRROR POS. VOLTS	DB
1	± 210	0.34 P-P	0
4		0.36	+.212
10		0.30	-.545
20		0.24	-1.52
30		0.26	-1.17
40		0.26	-1.17
50		0.28	-.846
60		0.28	-.846
70	↓	0.32	-.264

$$db = 10 \log \frac{I_1}{I_0} = 10 \log \frac{0.30}{0.34} =$$
(10 Hz)

$$= 10 \log .882$$

$$= 10(-.0545) = -0.545 \text{ db.}$$

$$db = 10 \log \frac{0.24}{0.34} = 10 \log .7058$$
(20 Hz)

$$= 10(-.1512)$$

$$= -1.512 \text{ db.}$$

$$db = 10 \log \frac{0.32}{0.34} = 10 \log 0.941$$
70 Hz

$$= 10(-.0264)$$

$$= -.264 \text{ db.}$$

4.2.2.3 THRESHOLD

$$\text{DISPLACEMENT} = 0.70025 \times 10^{-6} \frac{IN}{VOLT} \times 0.1 \text{ VOLT}_{P-P}$$

$$= .070025 \times 10^{-6} IN \text{ P-P.}$$

$$\theta = \frac{.070025 \times 10^{-6} IN}{9.9 IN} = .0070732 \times 10^{-6} \text{ RAD.}$$

$$\theta = \frac{.0070732 \times 10^{-6} RAD}{4.848 \times 10^{-6} \frac{RAD}{SEC}} = 0.00146 \text{ SEC}_{P-P}$$

III DETERMINE VOLTAGE GAIN – AZIMUTH

1. MIRROR – ELEVATION = 0

2. MIRROR AZIMUTH = $\frac{(257 + 340)\,10^{-6}\,IN}{800\ VOLT} = .74625\ \frac{10^{-6}\,IN}{VOLT}$

3. MONITOR LEFT = $\frac{(175 + 400)\,10^{-6}\,IN}{800\ VOLT}$

$= .71875 \times 10^{-6}\ \frac{IN}{VOLT}$

4. MONITOR RIGHT = $\frac{(230 + 360)\,10^{-6}\,IN}{800\ VOLT}$

$= .7375 \times 10^{-6}\ \frac{IN}{VOLT}$

5. AVERAGE MONITOR GAIN

$\frac{(.71875 + .7375)\,10^{-6}\,IN/VOLT}{2} = .72813 \times 10^{-6}\ \frac{IN}{VOLT}$

MONITOR VARIATION = $\frac{.7375}{.72813} = 1.01287$

$\pm 1.28\ \%$

6. SCALE FACTOR – AZIMUTH

$\frac{.72813}{.74625} = .9757$

BY _____ DATE _____ SUBJECT _____ SHEET NO. 5 OF 12

CHKD. BY _____ DATE _____ JOB NO. _____

4.2.1.1 TOTAL ANGULAR RANGE & RATE

P-P AMPLITUDE = $(250 + 330)\,10^{-6}$ IN = 580×10^{-6} IN

$$\Theta = \frac{580 \times 10^{-6}\ \text{IN}}{9.9\ \text{IN}} = 58.5858 \times 10^{-6}\ \text{RAD}$$

$$\Theta = \frac{58.5858 \times 10^{-6}\ \text{RAD}}{4.848 \times 10^{-6}\ \frac{\text{RAD}}{\text{SEC}}} = 12.084\ \text{SEC}$$

$$= \pm 6.042\ \text{SEC}.$$

PERIOD = 140 SEC

4.2.1.2 THRESHOLD

MIN PULSE = 2.0×10^{-6} IN.

$$\Theta = \frac{2 \times 10^{-6}\ \text{IN}}{9.9\ \text{IN}} = 0.202 \times 10^{-6}\ \text{RAD}.$$

$$\Theta = \frac{0.202 \times 10^{-6}\ \text{RAD}}{4.848 \times 10^{-6}\ \frac{\text{RAD}}{\text{SEC}}} = 0.0416\ \text{SEC}$$

4.2.2.1 TOTAL ANGULAR RANGE

RANGE $.72813 \times 10^{-6}\ \frac{\text{IN}}{\text{VOLT}}$

$$\Theta = \frac{728.13 \times 10^{-6}\ \text{IN}/1000\ \text{VOLT}}{9.9\ \text{IN}.} = 73.548 \times 10^{-6}\ \text{RAD}$$

BY _____ DATE _____ SUBJECT _____ SHEET NO. 1 OF 2

CHKD. BY _____ DATE _____ JOB NO. _____

$$\theta = \frac{73.543 \times 10^{-6}\ \text{RAD}}{4.848 \times 10^{-6}\ \frac{\text{RAD}}{\text{SEC}}} = 15.170\ \text{SEC} \pm 7.585\ \text{SEC.}$$

VOLTAGE GAIN = $15.17\ \frac{\text{SEC}}{1000\ \text{VOLTS}}$

OR $.01517\ \frac{\text{SEC}}{\text{VOLT.}}$

4.2.2.2 FREQUENCY RESPONSE

$$\frac{\pm 3.0\ \text{SEC}}{.01517\ \frac{\text{SEC}}{\text{VOLT}}} = \pm 197.76\ \text{VOLT} \quad 395.5\ \text{VOLT P-P.}$$

FREQ (CPS)	ACT VOLTS	VOLTS METER READ POS	DB
1	400 P-P	.75	0
4	↓	.80	+.275
10		.60	−.969
20		.50	−1.765
30		.50	−1.765
40		.55	−1.349
50		.60	−.969
60		.80	+.275
70		1.15	+1.86

BY _____ DATE _____ SUBJECT _____ SHEET NO. 8 OF _____

CHKD. BY _____ DATE _____ JOB NO. _____

4.2.2.3 THRESHOLD

RESPONSE FALLS TO ZERO AT .05 TO .1 VOLT P-P AT 4 HZ.

.1 VOLT X .01517 $\frac{\text{SEC}}{\text{VOLT}}$

= .001517 SEC P-P.

TO .00076 SEC P-P.

33

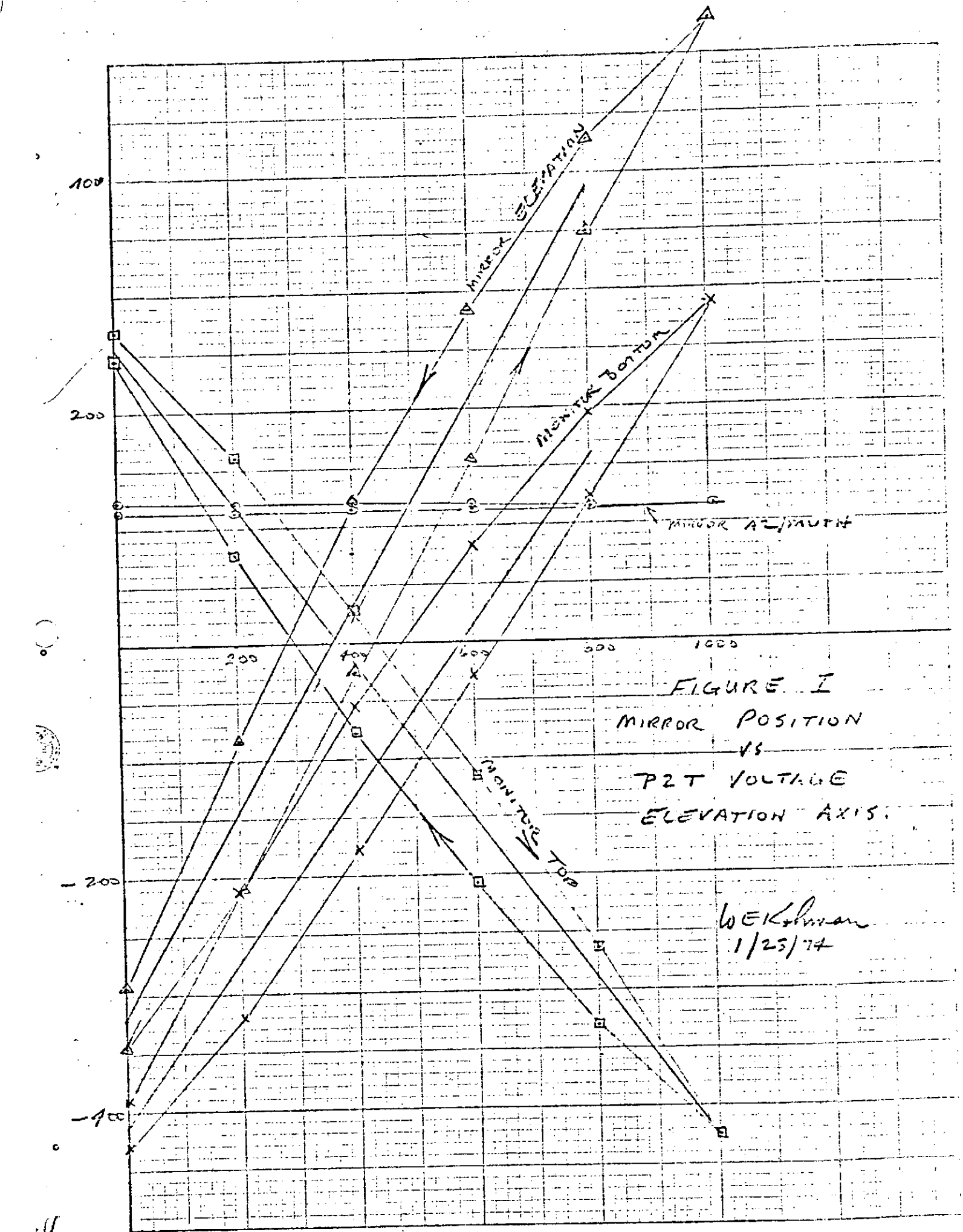

FIGURE I
MIRROR POSITION
VS
PZT VOLTAGE
ELEVATION AXIS.

WEK:hman
1/23/74

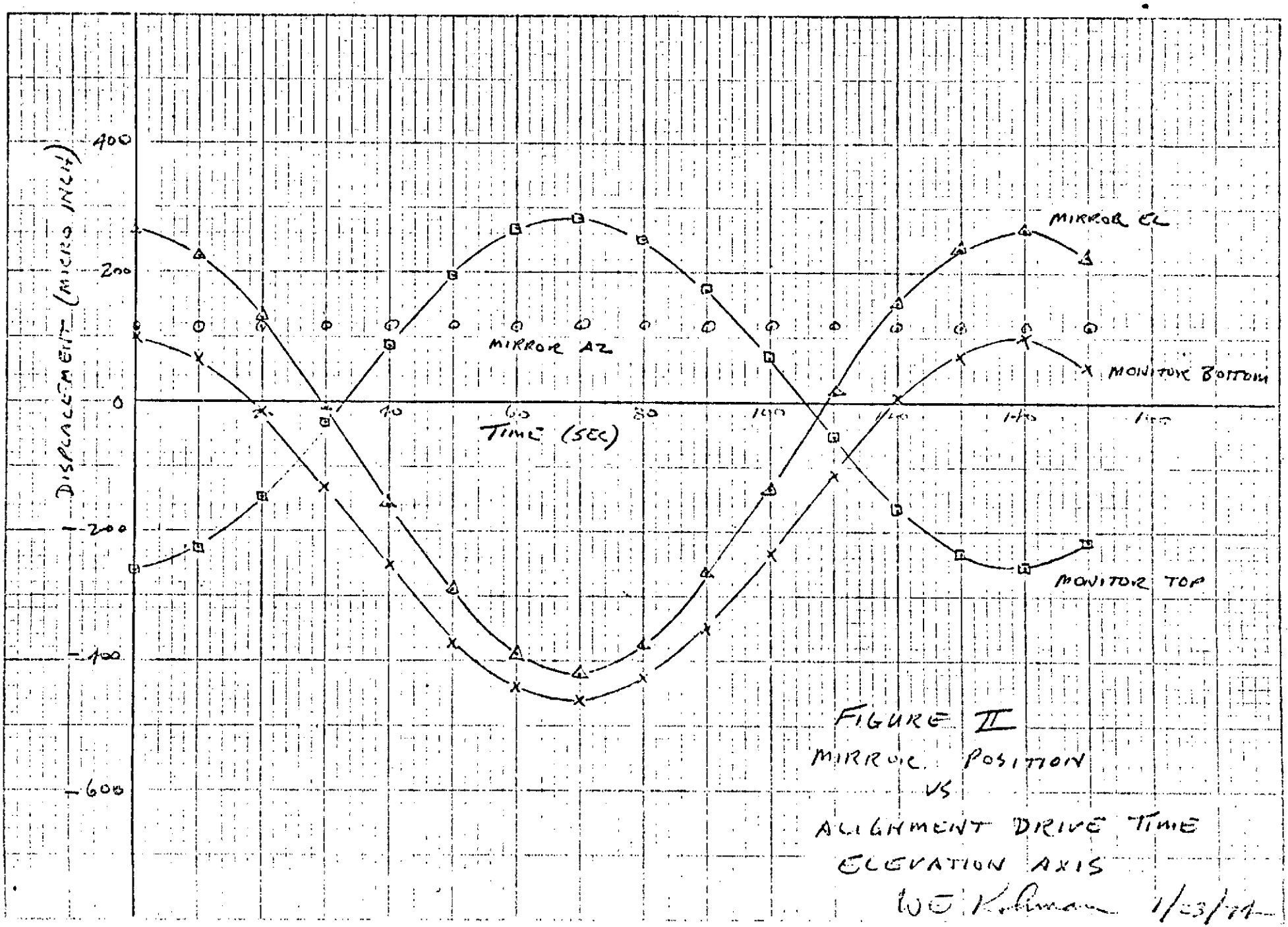

FIGURE II
MIRROR POSITION
VS
ALIGNMENT DRIVE TIME
ELEVATION AXIS
W E Kolman 1/23/74

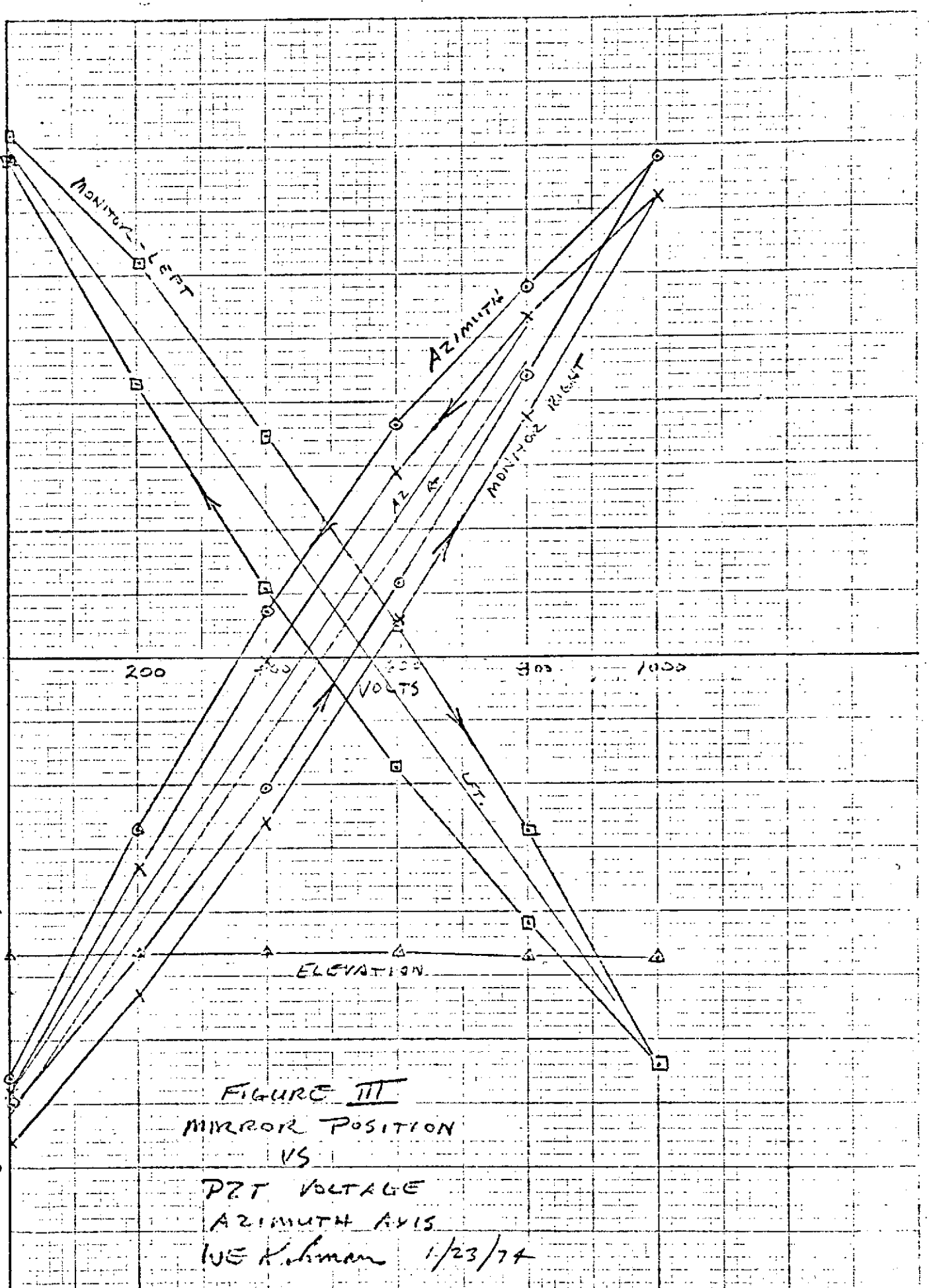

FIGURE III
MIRROR POSITION
VS
PZT VOLTAGE
AZIMUTH AXIS
IUE K. Kirman 1/23/74

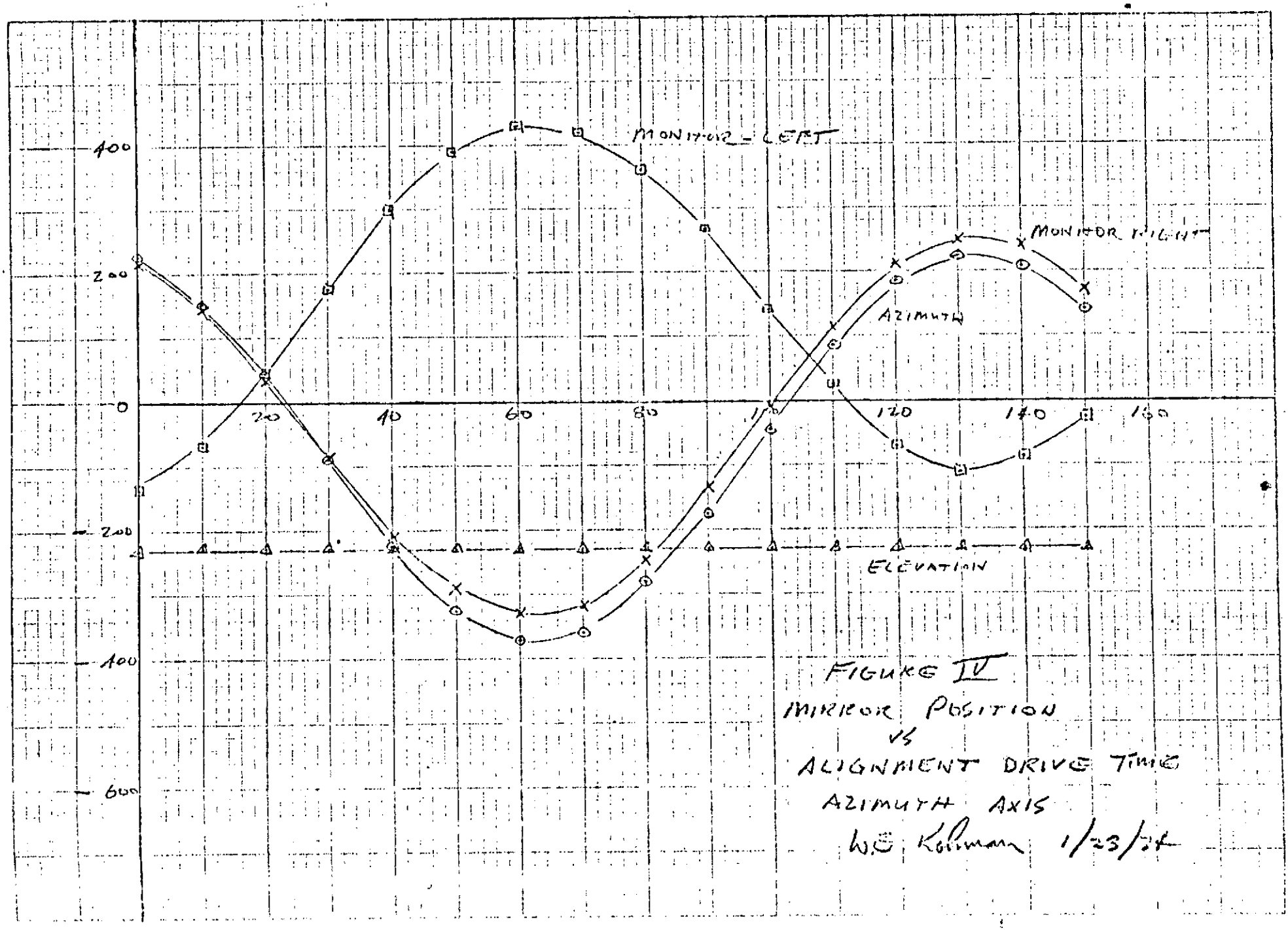

FIGURE IV
MIRROR POSITION
VS
ALIGNMENT DRIVE TIME
AZIMUTH AXIS
W.E. Kahlman 1/23/74

GENERAL DATA SHEET - II

SPC 33117 | SHEET 1 OF 3

TEST: FINAL ACCEPTANCE (PZT - ELEVATION) | SPEC: ER 11783 | PARA: 4.3 | TEST NO:

TEST ITEM: LST SECONDARY MIRROR 660-0267 | DATE: 1/22/71

CLIENT: MSFC | CLIENT REPRESENTATIVE: John L Hodgson | TEMP: LAB. 76°F RH.

TEST EQUIPMENT: (1) DVM HP 3440A S/N 08109 | MODEL NO: | TESTED BY: W E Coleman

INSTRUMENTATION: (2) AC/DC RANGE UNIT HP 3445A S/N 08110 (3) TEKTRONIX TYPE 602 A DUAL BEAM OSC. (4) HP LOW FREQ FUNCT GENERATOR MODEL 202 A S/N 07347 | ENGR. CHECK: QA | SUPV. CHECK:

TOP BOT

	PZT VOLTS	MIRROR POSITION MICRO INCHES A2	EL	MAIN	MON	PZT VOLTS	MIRROR POSITION MICRO INCHES A2	EL	MAIN	MON	TIME SEC.
	-6.19	+138	-324	+170	-430	6.19	+111	-217	+178	-320	
	+2047	+130	-210	+160	-320		+111	-112	+90	-235	10.3
	+401.9	+130	-25	+38	-178		+110	+15	0	-142	20.0
	+601.5	+118	+158	-115	-30		+110	+119	-83	-55	30.0
	+801.1	+117	+350	-263	+123		+109	+197	-142	+12	40.0
	+1003.2	+116	+540	-425	+239		+109	+227	-163	+37	50.1
	+805.6	+115	+430	-330	+195		+109	+198	-141	+13	60.2
	+605.2	+115	+286	-219	+81		+109	+122	-82	-47	70.1
	+404.4	+113	+120	-79	-54		+109	+14	-2	-132	80.0
	+203.3	+113	-82	+78	-212		+109	-113	+89	-229	90.0
	+6.2	+113	-293	+245	-390		+109	-222	+172	-325	100.0
							+109	-295	+228	-380	110.1
							+109	-340	+246	-390	120.2
							+109	-310	+221	-370	130.0
							+109	-225	+171	-320	140.0
							+108	-120	+93	-231	150.0

SKETCH OR NOTES:

GENERAL DATA SHEET - II

SPO:

SHEET: 2 OF 3

TEST: SPEC: PARA: TEST NO:

TEST ITEM: DATE:

CLIENT: CLIENT REPRESENTATIVE: JRH TEMP: LAB. RH.

TEST EQUIPMENT: MODEL NO TESTED BY:

INSTRUMENTATION: ENGR. CHECK: QA

SUPV. CHECK:

	PZT VOLTS	MIRROR POSITION MICRO INCHES AZ	EL	MON LIGHT	MON RIGHT	PZT VOLTS	MIRROR POSITION MICRO INCHES AZ	EL	MON LIGHT	MON RIGHT	TIME SEC.
							+118	+261	-260	+100	0
	THRU SH01 D						+118	+223	-225	- 65	10.0
INPUT	5mV/DIV = 21.4V						+118	+133	-146	- 18	20.1
OUTPUT	4.0 MV P-P						+118	- 7	- 33	-131	30.0
							+118	-160	+ 58	-255	40.0
INPUT	7.0 mV/DIV = 30 MV						+118	-350	+192	-375	50.1
OUTPUT	1.5 MV P-P						+118	-390	+363	-440	60.0
							+119	-420	+283	-460	70.0
INPUT	1.0 MV/DIV = 4.1V						+118	-375	+250	-425	80.1
OUTPUT	SAME OUTPUT						+118	-265	+175	-350	90.2
							+118	-137	+ 67	-235	100.0
							+118	+ 18	- 58	-113	110.0
1 HZ							+118	+153	-167	+ 4	120.0
INPUT	5V/DIV = 310. V						+118	+253	-257	+ 73	130.1
OUTPUT	17 KΩ = 0.34 V P-P						+118	+265	-255	+ 100	140.0
							+118	+221	-218	+ 59	150.0
1 HZ											
INPUT	±1.1V/DIV = 310. MV							PULSE			
OUTPUT	1 2V/DIV = 1.2 V P-P						+115	- 71	+ 32	-180	0
							+115	- 75	+ 31	-187	0.2
10 HZ	SIN ±						+115	- 77	+ 37	-185	
INPUT	1V/DIV = 2.50 V P-P						±115	- 79	+ 38	-192	~ 150

SKETCH OR NOTES:

39

GENERAL DATA SHEET - II

SPO:

SHEET 3 OF 3

TEST:

SPEC:

PARA:

TEST NO:

TEST ITEM:

DATE:

CLIENT:

CLIENT REPRESENTATIVE:

TEMP: LAB. RH.

TEST EQUIPMENT:

MODEL NO:

TESTED BY:

INSTRUMENTATION:

ENGR. CHECK:

SUPV. CHECK:

	PZT VOLTS	MIRROR POSITION MICRO INCHES AZ	EL	MON LEFT	MON RIGHT		PZT VOLTS	MIRROR POSITION MICRO INCHES AZ	EL	MON LEFT	MON RIGHT	TIME SEC.
20	HZ											
IN			± 7.10.0 V									
OUT		1.7, V 2 = 0.24 V PP										
30	HZ	IN	± 7.10 V									
		OUT		0.26 V PP								
40	HZ	IN	± 7.10 V									
		OUT		0.26 V PP								
50	HZ	IN	± 7.10 V									
		OUT		0.25 V PP								
60	HZ	IN	± 7.10 V									
		OUT		0.24 V PP								
70	HZ	IN	± 7.10 V									
		OUT	0.23 V PP									

SKETCH OR NOTES:

40

GENERAL DATA SHEET - II

33117

SHEET 1 OF 2

TEST: FINAL ACCEPTANCE (PZT-AZIMUTH) | SPEC: 11733 | PARA: 4.2 | TEST NO:

TEST ITEM: LST SECONDARY MIRROR 660-0267 | DATE: 1-23-74

CLIENT: MSFC | CLIENT REPRESENTATIVE: John E Hagner | TEMP: LAB. RH: 76

TEST EQUIPMENT: | MODEL NO: | TESTED BY: WE Kuhlman

INSTRUMENTATION: | ENGR. CHECK: QA D. Worley

SUPV. CHECK: 2-03 -370

	PZT VOLTS	MIRROR POSITION MICRO INCHES AZ	EL	MON LEFT	MON RIGHT		PZT VOLTS	MIRROR POSITION MICRO INCHES AZ	EL	MON LEFT	MON RIGHT	TIME SEC.
	+6.1	-350	-232	+210	-330		6.2	+227	-233	-139	+212	0
	+205.1	-232	-232	+310	-265			+155	-232	- 67	+145	10.0
	+595.1	-101	-232	+172	-130			+ 42	-232	+ 47	+ 37	20.1
	+602.2	+ 59	-235	+ 25	+ 27			- 90	-230	+172	- 85	30.0
	+791.8	+232	-237	-136	+188			-222	-230	+300	-210	40.
	+799.5	+390	-257	-320	+360			-325	-227	+390	-272	50.0
	+800.1	+390	-256	-210	+267			-370	-229	+430	-330	60.0
	+595	+181	-235	- 89	+142			-360	-229	+430	-320	70.0
	+397.0	- 37	-233	+ 52	- 4			-280	-229	+360	-245	80.1
	+199.9	-155	-232	+215	-165			-177	-230	+265	-132	90.0
	+ 6.2	-330	-230	+390	-340			- 42	-230	+140	- 9	100.1
								+ 15	-230	+ 22	+114	110.0
								+182	-231	- 75	+219	120.2
								+221	-231	-110	+259	130.1
								+207	-231	- 99	+240	140.1
								+140	-230	- 28	+172	150.0

SKETCH OR NOTES:

GENERAL DATA SHEET - II

SHEET 2 OF 2

TEST: | SPEC: | PARA: | TEST NO:

TEST ITEM: | DATE: 1-23-74

CLIENT: | CLIENT REPRESENTATIVE: | TEMP: LAB. RH.

TEST EQUIPMENT: | MODEL NO: | TESTED BY:

INSTRUMENTATION: | ENGR. CHECK: QA | SUPV. CHECK:

FREQUENCY

PZT THRESHOLD

	÷100 PP INPUT		PP VOLTS OUT			Hz	INPUT PP		OUTPUT PP			
1 Hz	4V	1.5K.5	= .75			1 Hz	0.7V	1.3V1	1.3MV			
4 Hz	4V	1.6K.5	= .80			1 Hz	3.0V	3.0K1	3.0MV			
10 Hz	4V	1.2K.5	= .6			4 Hz	0.05V	.05	.		.00075	75
20 Hz	4V	1.0K.5	= .5			4 Hz	0.1V				.0015	75
30 Hz	4V	1.0K.5	= .5									
40 Hz	4V	1.1K.5	= .55									
50 Hz	4V	1.2K.5	= .60									
60 Hz	4V	1.6K.5	= .80				THRESHOLD					
70 Hz	4V	2.2K.5	= 1.1 5			(-335 ; +3 =0)			(-47)			
1 Hz	0.4V	1.7K.05	.085									
4 Hz	0.4V	"	.085			TIME	PULSE					
10 Hz	0.4V	1.4K.05	.070			0	-44					
20 Hz	0.4V	1.0K.05	.050			1/5	-46 5					
30 Hz	0.4V	"	.050			1/10	-47					
40 Hz	0.4V	1.2K.05	.060			1/20	-50					
50 Hz	0.4V	1.5K.05	.075									
60 Hz	0.4V	2.0K.05	.100									
70 Hz	0.4V	6.0K.05	.300									
2 Hz	0.4V	1.8K.05	.090									

SKETCH OR NOTES:

42

APPENDIX B

FLEXURE TORQUE MOTOR ACTUATOR TEST DATA

"B"

7

PERKIN-ELMER

OPTICAL GROUP
THE PERKIN-ELMER CORPORATION
NORWALK, CONNECTICUT 06852
TELEPHONE: (203) 762-1000
CABLE: PECO-NORWALK

74-SS-1491

March 1, 1974

TO: File - LST Secondary Mirror

FROM: W. E. Kohman

SUBJECT: FINAL ACCEPTANCE TEST
LST SECONDARY MIRROR ACTUATION SYSTEM
FLEXURE TORQUE MOTOR ACTUATOR CONFIGURATION
660-0301

REFERENCE: (1) Contract NAS 8-29723 SPO 33117

The attached data sheets and calculation sheets document the final acceptance test of the subject LST Secondary Mirror actuation system. This test confirms that the system meets the requirements of the Reference (1) contract and is accepted and approved for delivery to MSFC.

W E Kohman

W. E. Kohman Perkin-Elmer
Engineering

J. Mortellaro

J. Mortellaro Perkin-Elmer
Quality Assurance

WEK:mb

Attachments

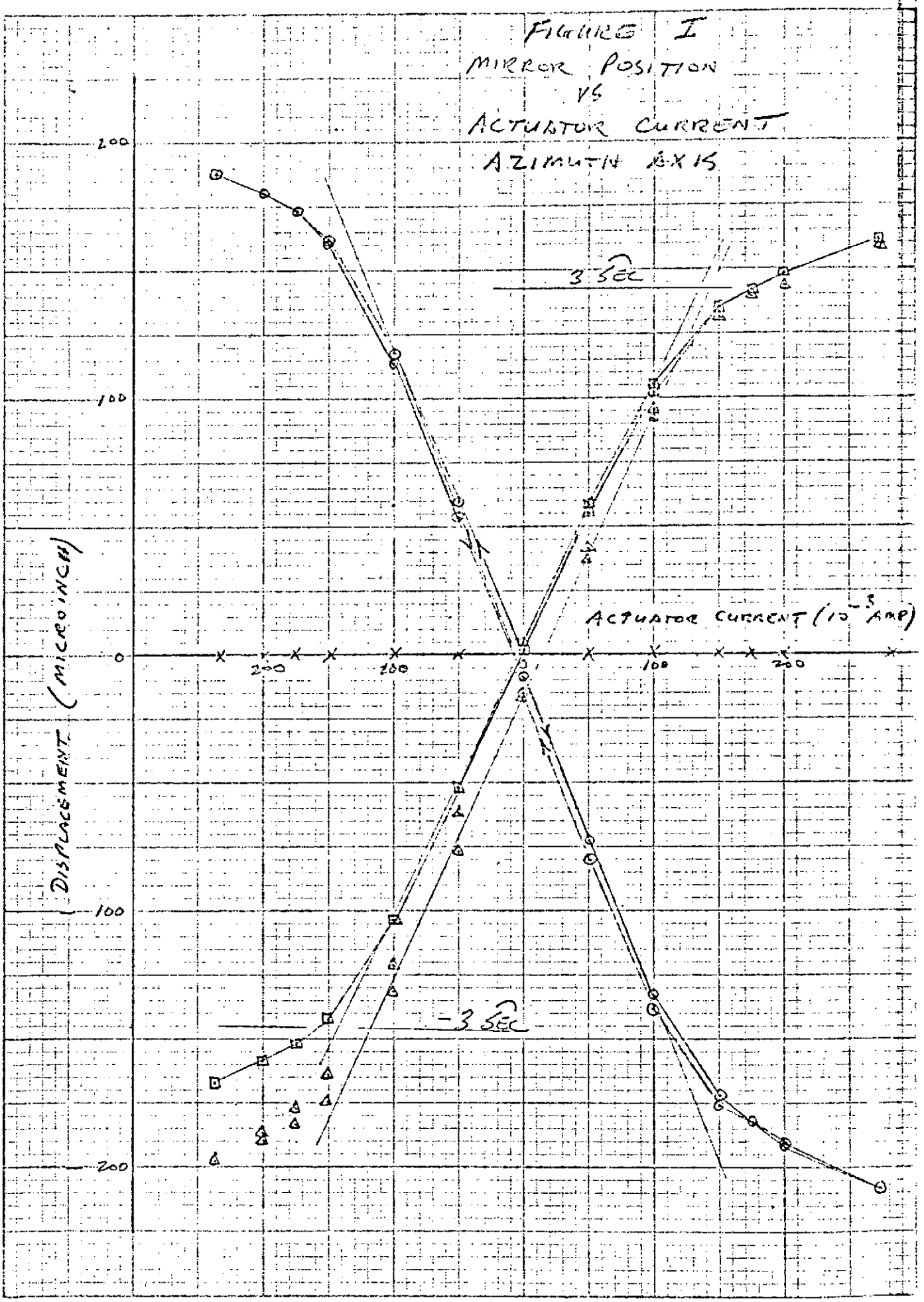
FIGURE I
MIRROR POSITION
VS
ACTUATOR CURRENT
AZIMUTH AXIS
3 SEC
-3 SEC
200
100
0
100
200
DISPLACEMENT (MICROINCH)
ACTUATOR CURRENT (10⁻⁵ AMP)

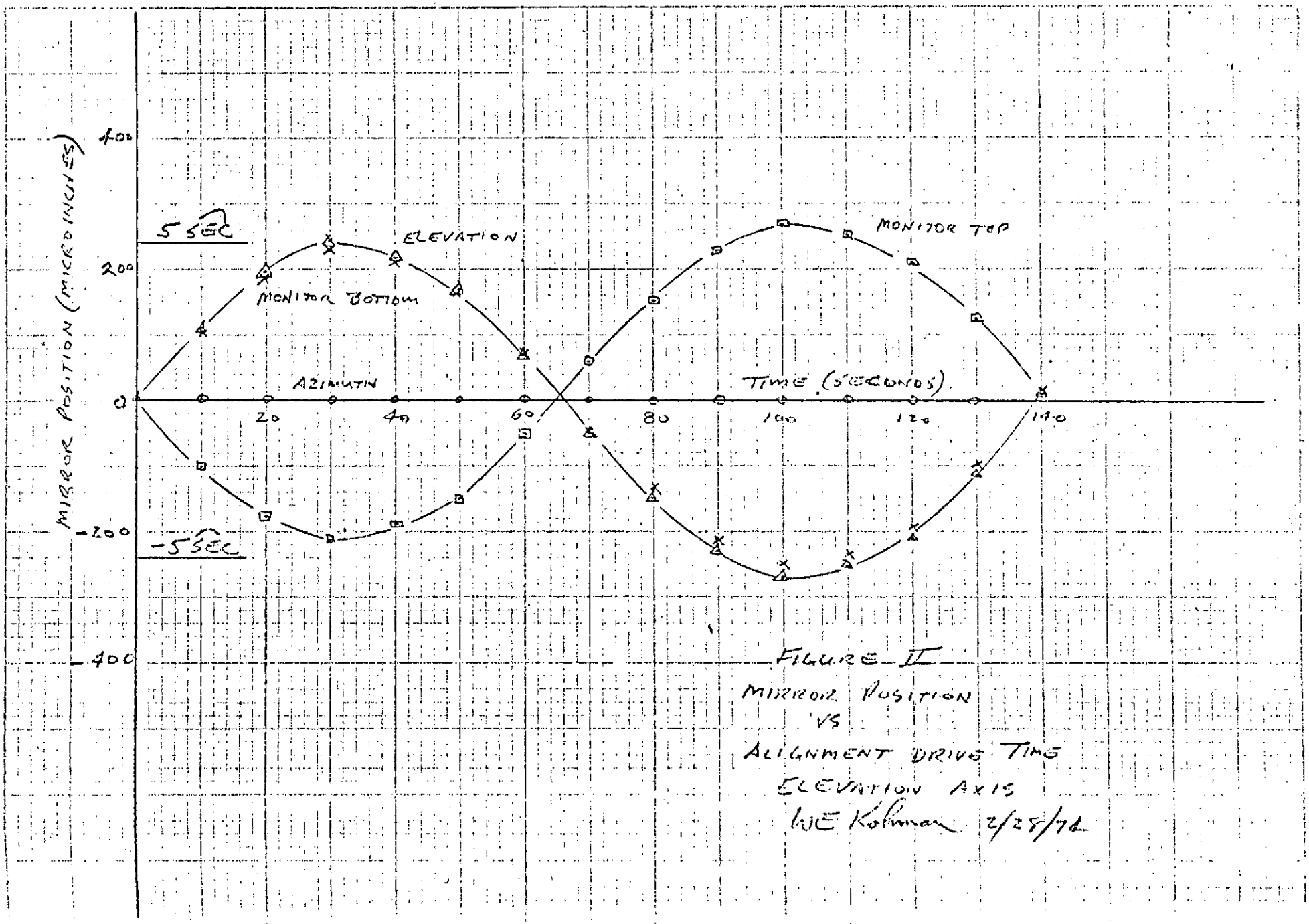

FIGURE II
MIRROR POSITION
VS
ALIGNMENT DRIVE TIME
ELEVATION AXIS
WE Kolman 2/25/72

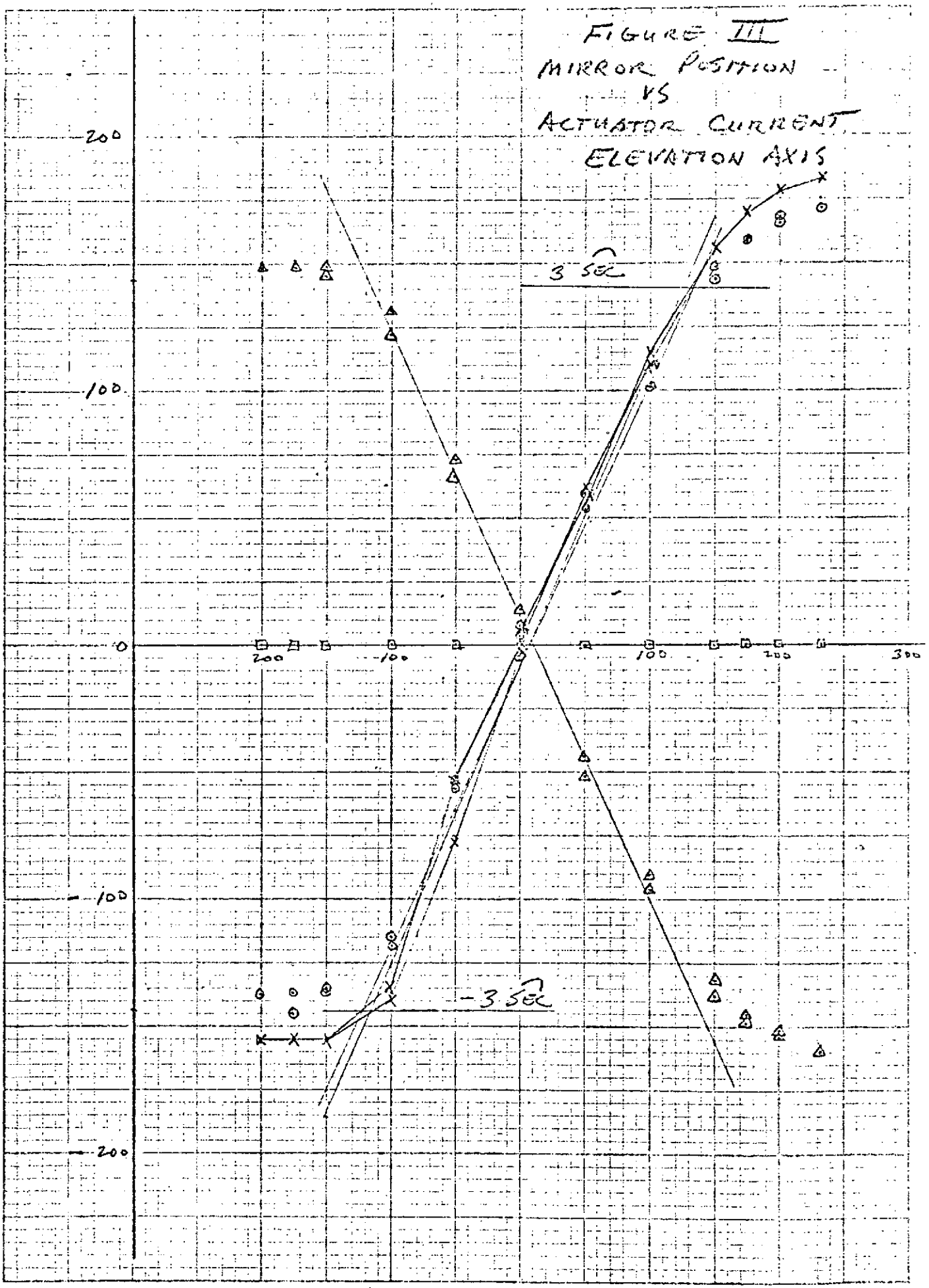
FIGURE III
MIRROR POSITION
VS
ACTUATOR CURRENT
ELEVATION AXIS
3 SEC
-3 SEC
200
100
0
-100
-200
200
100
100
200
300

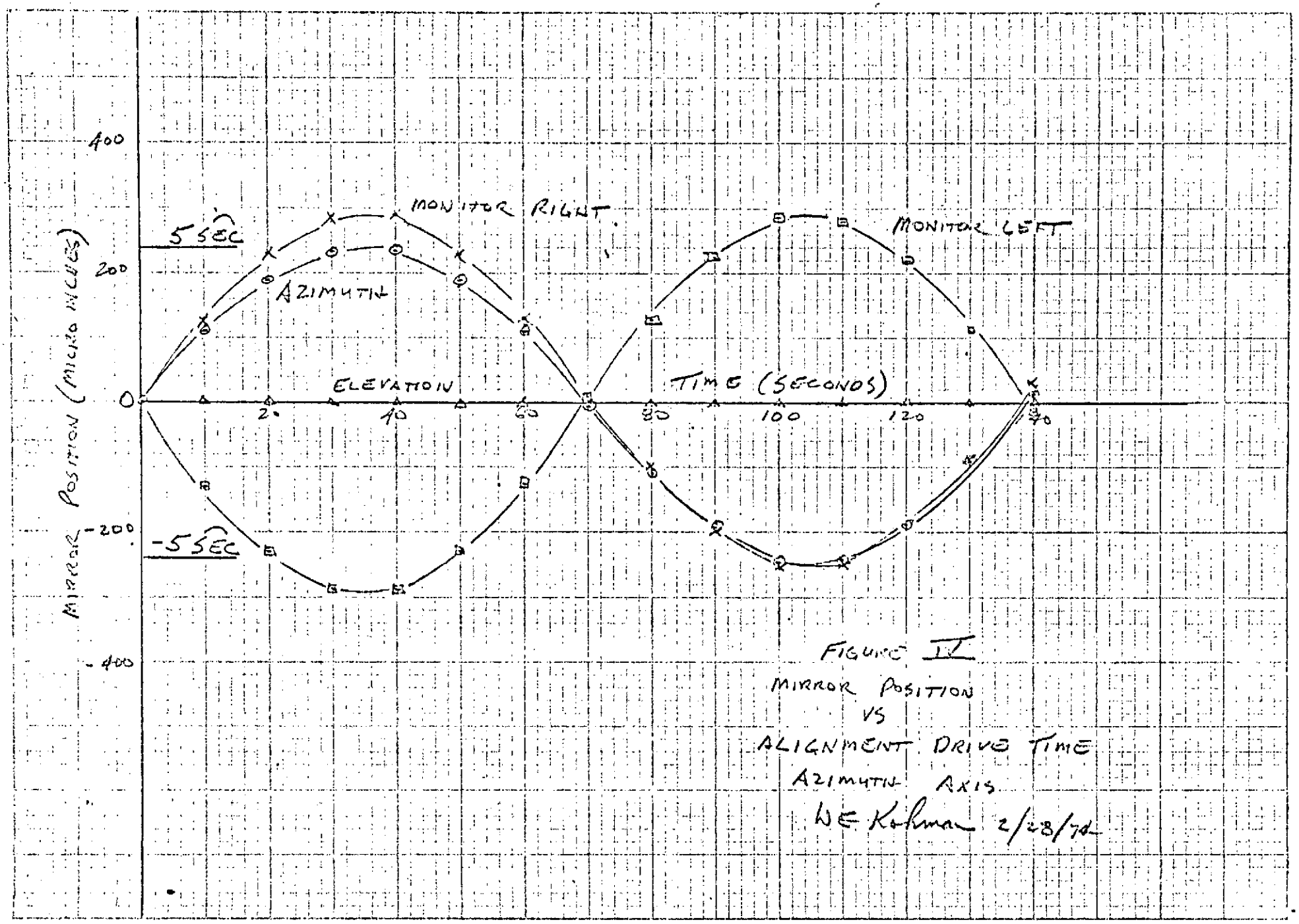

FIGURE IV

MIRROR POSITION
VS
ALIGNMENT DRIVE TIME
AZIMUTH AXIS

W E Kohman 2/28/74

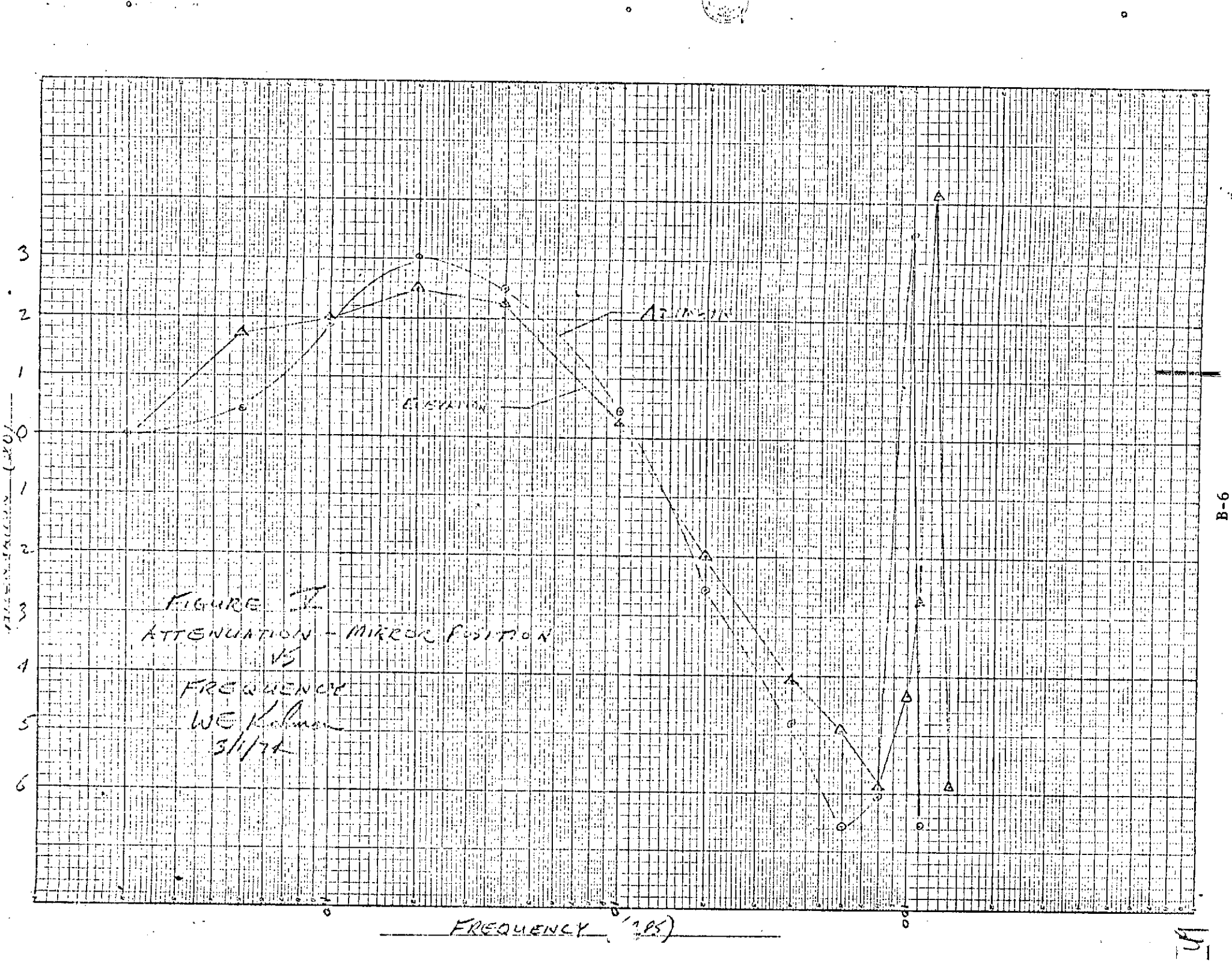

FIGURE 7
ATTENUATION - MIRROR POSITION
VS
FREQUENCY
WG K-Band
3/74

GENERAL DATA SHEET - II

S. 33117

SHEET 1 OF 3

TEST: FINAL ACCEPTANCE (FLEXURE - TORQUE)

SPEC: ER 11783

PARA: 5.0

TEST NO:

TEST ITEM: LST SECONDARY MIRROR 660-0301

DATE: 2/26/74

CLIENT: MSFC

CLIENT REPRESENTATIVE:

TEMP: LAB. RH: 76° F

TEST EQUIPMENT:

MODEL NO:

TESTED BY: WE Kohman

INSTRUMENTATION:

ENGR. CHECK:

SUPV. CHECK:

EL.

ACT CURRENT MA	MON BOT. MIN	MON TOP MIN	AZ MIN	EL MIN	
0	0	0	0	0	
+50	+53	-52	0	+62	
+100	+102	-96	0	+110	
+150	+144	-138	0	+155	
+176	+158	-148	0	+170	
+200	+165	-154	0	+178	
+232	+172	-160	0	+183	
+200	+163	-152	0	+177	
+175	+160	-145	0	+170	
+150	+149	-132	0	+156	
+100	+110	-90	0	+115	
+50	+60	-44	0	+58	
0	+8	+8	0	+2	
-50	-53	+67	+.1	(-53) ?	
-100	-115	+122	+.2	-135	
-150	-135	+145	+.2	-155	
-175	-145	+148	+.2	-155	
-200	-137	+148	+.2	-155	
-175	-137	+148	+.2	-155	
-150	-135	+149	+.1	-155	
-100	-118	+132	+.1	-140	
-50	-57	+73	+.1	-78	

AZ

ACT CURRENT MA	MON LEFT MIN	MON. RIGHT MIN	AZ MIN	EL MIN	TIME
0	0	0	0	0	1315
-50	+60	-62	-52	0	
-100	+118	-121	-103	0	
-150	+162	-165	-142	0	
-175	+173	-177	-152	0	
-200	+180	-187	-159	0	
-233	+183	-197	-167	0	
-200	+180	-190	-159	0	
-175	+172	-184	-152	0	
-150	+160	-175	-194	+1	
-100	+114	-132	-105	+1	
-50	+53	-77	-53	+1	
0	-9	-16	+1	+1	1335
+50	-73	+41	+55	1	
+100	-133	+95	+102	1	
+150	-172	+131	+135	1	
+175	-182	+139	+142	1	
+200	-190	+144	+148	1	
+271	-208	+160	+161	1	
+200	-191	+144	+148	1	
+175	-183	+135	+142	1	
+150	-176	+128	+135	0	
+100	-138	+91	+105	0	
+50	-80	+37	+58	0	
0	-15	-23	+5	0	1400
0	-22.5	-34	-.2	-.5	1635

SKETCH OR NOTES:

0 +4 +15 0 -3

50

PERKIN-ELMER

GENERAL DATA SHEET - II

SPU:

SHEET 2 OF 3

TEST:

SPEC:

PARA:

TEST NO:

TEST ITEM: AZIMUTH

DATE:

CLIENT:

CLIENT REPRESENTATIVE:

TEMP: LAB. RH.

TEST EQUIPMENT:

MODEL NO:

TESTED BY:

INSTRUMENTATION:

ENGR. CHECK:

SUPV. CHECK:

	ACT Current ma.	AZ °	EL △	MON LEFT □	MON RT X	TIME sec.		ACT Current	ACT VOLT (VOLTS)	ACT DISP	freq	VOLTS ACT DISP
	0	0	0	0	0	0	—	121.8	-3.0	+.028	Static	
		+110	0	-132	+132	10.3	—	122	+3.0	-.020	"	
		+190	0	-230	+230	20.2		—	6.0 P-P	.092	1 cps	.28
		+237	0	-288	+288	30.0			6.0	.108	2	.36
		+237	0	-288	+288	40.3			6.0	.096	4	.32
		+190	0	-228	+230	50.3			6.0	.052	10	.20
		+105	0	-124	+133	57.8			6.0	.020	20	.10
		+3	0	+8	+8	70.1			6.0	.008	40	.06
		+108	+2	+129	-109	80.0			6.0	.006	60	.04
		-193	2	+225	-200	90.0			6.0	.004	80	.045
		-212	2	+283	-250	100.2			6.0	.012	100	.40
		-240	2	+290	-247	110			6.0	.002	110	.04
		-188	2	+220	-190	120.1			6.0	.066	0.5	.20
		-93	2	+112	-85	130.1			6.0	.056	0.2	.18
		+15	1.5	-15	+37	140.2						
								THRESHOLD				P-P
		MINIMUM PULSE							P-P .003		4.0	.0001
	0	0	0	0	0	0						
		+.1	0	-.1	3.5	—						
		.7	.1	-1.7	6.9	—						
		1.5	.1	-4.1	11.4							

SKETCH OR NOTES:

51

GENERAL DATA SHEET - II

SPO:

SHEET 3 OF 3

TEST:

SPEC:

PARA:

TEST NO:

TEST ITEM: ELEVATION

DATE:

CLIENT:

CLIENT REPRESENTATIVE:

TEMP: LAB. RH.

TEST EQUIPMENT:

MODEL NO:

TESTED BY:

INSTRUMENTATION:

ENGR. CHECK:

SUPV. CHECK:

← MICRO INCH →

	ACT CURRENT Ma	AZ	EL	MON BOT	MON TOP	TIME SEC		ACT CURRENT Ma	ACT VOLTS	FILTER VOLTS DISP.	FREQ CPS	UNFILTERED VOLTS ACT DISP.
	0	0	0	0	0	0		+129	+3.2	.032		
		0	+110	+105	-100	10		0	0	0		
		0	+199	+190	-178	20		-129	-3.1	.030		
		0	+241	+232	-216	30			6.0 P-P	.097	1 CPS	.30
		0	+219	+210	-190	40				.112	2	.34
		0	+174	+169	-150	50				.102	4	.32
		0	+68	+67	-50	60				.06	10	.20
		0	-50	-45	+60	70				.028	20	.12
		0	-150	-137	+152	80				.010	40	.075
		0	-230	-215	+228	90				.004	60	.060
		0	-270	-252	+267	100				.003	80	.05
		0	-255	-238	+253	110				.003	100	.07
		0	-210	-193	+208	120				.004	110	.10
		0	-117	-100	+121	130				.01	120	.50
		0	+7	+17	+10	140				.002	140	.05
										.076	1.5	.285
		MIN	PULSE						6.0	.064	2	.190
		0	0	0	0	—						
		0	+2.5	3.5	-1				THRESHOLD			
		0	4.7	6.1	-1.5				P-P .002		1	P-P .00225
		0	6.9	9.1	-2.8							

SKETCH OR NOTES:

52

I DETERMINE ACTUATOR CURRENT VS MIRROR ANGLE GAIN — AZIMUTH AXIS

1. MIRROR ELEVATION — 0

2. MIRROR AZIMUTH $= \dfrac{(153 + 153)\,10^{-6}\,IN}{300 \times 10^{-3}\,AMP}$

$= 1.0366 \times 10^{-3}\,\dfrac{IN}{AMP}$

3. MONITOR LEFT $= \dfrac{(182 + 197)\,10^{-6}\,IN}{300 \times 10^{-3}\,AMP}$

$= 1.263 \times 10^{-3}\,\dfrac{IN}{AMP}$

4. MONITOR RIGHT $= \dfrac{(150 + 130)\,10^{-6}\,IN}{300 \times 10^{-3}\,AMP}$

$= 1.100 \times 10^{-3}\,\dfrac{IN}{AMP}$

5. AVERAGE MONITOR GAIN

$= \dfrac{(1.263 + 1.100)\,10^{-3}\,\frac{IN}{AMP}}{2} = 1.1815 \times 10^{-3}\,\dfrac{IN}{AMP}$

6. SCALE FACTOR - MIRROR AZIMUTH

$SF = \dfrac{1.1815}{1.0366} = 1.1398$

7. CALIBRATION - MIRROR AZIMUTH ANGLE VS CURRENT

MIRROR AZIMUTH ANGLE

$$= \frac{1.1815 \times 10^{-3} \frac{IN}{AMP}}{47.995 \times 10^{-6} \frac{IN}{SEC}} = 24.617 \frac{SEC}{AMP}$$

II 4.2.1.1 TOTAL ANGULAR RANGE & RATE - ALIGNMENT

560 $\times 10^{-6}$ IN PEAK TO PEAK

$$\theta = \frac{560 \times 10^{-6} IN}{9.9 IN} = 56.56 \times 10^{-6} RAD$$

$$\theta = \frac{56.56 \times 10^{-6} RAD}{4.848 \times 10^{-6} \frac{RAD}{SEC}} = 11.67 SEC$$

OR $\pm$ 5.83 SEC

PERIOD 140 SEC

AVERAGE ALIGNMENT RATE

$$= \frac{11.67 SEC}{70 SEC} \times 60 \frac{SEC}{MIN} = 10.003 \frac{SEC}{MIN}$$

4.2.1.2 THRESHOLD

$$\text{MIN PULSE} = \frac{11.4 \times 10^{-6} IN}{3 \text{ PULSES}} = 3.80 \times 10^{-6} \frac{IN}{PULSE}$$

$$\theta = \frac{3.80 \times 10^{-6} \text{ IN}}{9.9 \text{ IN}} = .3838 \times 10^{-6} \text{ RAD}$$

$$\frac{.3838 \times 10^{-6} \text{ RAD}}{4.848 \times 10^{-6} \frac{\text{RAD}}{\text{SEC}}} = 0.079 \frac{\text{SEC}}{\text{PULSE}}$$

4.2.2.1 TOTAL ANGULAR RANGE – STABILIZATION

$$\frac{377 \times 10^{-6} \text{ IN}}{9.9 \text{ IN}} = 38.08 \times 10^{-6} \text{ RAD}$$

$$\frac{38.08 \times 10^{-6} \text{ RAD}}{4.848 \times 10^{-6} \frac{\text{RAD}}{\text{SEC}}} = 7.855 \text{ SEC}$$

OR $\pm$ 3.93 SEC

4.2.2.2 FREQUENCY RESPONSE

10 Log $\frac{I_1}{I_0}$

FREQ	ACT VOLTS	ACT CURRENT	MIRROR POS VOLTS	I_1/I_0	Db
0.2	6.0 P-P	244 MA P-P	.18	1.0	0
0.5	↓	↓	.20	1.11	+.45
1			.28	1.55	+1.90
2			.36	2.0	+3.01
4			.32	1.78	+2.50
10			.20	1.11	+.45
20			.10	0.55	−2.59
40			.06	0.33	−4.81
60			.04	0.22	−6.57
80			.045	0.25	−6.02
100			.40	2.22	+3.46
110			.04	0.22	−6.57

BY_____DATE_____ SUBJECT_____ SHEET NO. 4 OF 8

CHKD. BY_____DATE_____ JOB NO._____

4.2.2.3 THRESHOLD

AMPLITUDE RATIO @ 1 HZ

$$24.617 \frac{\text{SEC}}{\text{AMP}} \times .294 \text{ amp P-P} \times \frac{.096}{.048} \times \frac{.003 \text{ VOLT P-P}}{6.0 \text{ VOLT P-P}}$$

$$= 0.0060 \text{ SEC P-P OR } \pm .003 \text{ SEC}$$

II. DETERMINE ACTUATOR CURRENT VS MIRROR ANGLE

1 GAIN - ELEVATION AXIS

1. MIRROR EL = $\frac{(168 + 183)10^{-6}\,IN}{(150 + 150)10^{-3}\,AMP} = \frac{351 \times 10^{-6}\,IN}{300 \times 10^{-3}\,AMP} =$

$= 1.170 \times 10^{-3}\,\frac{IN}{AMP}$

2. MIRR AZ = 0

3. MONITOR BOTTOM = $\frac{(160 + 175)10^{-6}\,IN}{300 \times 10^{-3}\,AMP} = \frac{335 \times 10^{-6}\,IN}{300 \times 10^{-3}\,AMP}$

$= 1.117 \times 10^{-3}\,\frac{IN}{AMP}$

4. MONITOR TOP = $\frac{(178 + 155)10^{-6}\,IN}{300 \times 10^{-3}\,AMP} = \frac{333 \times 10^{-6}\,IN}{300 \times 10^{-3}\,AMP}$

$= 1.110 \times 10^{-3}\,\frac{IN}{AMP}$

5. AVERAGE MONITOR GAIN

$$\frac{(1.117 + 1.110)10^{-3}\,\frac{IN}{AMP}}{2} = 1.1135 \times 10^{-3}\,\frac{IN}{AMP}$$

6. SCALE FACTOR - MIRROR ELEVATION

$$S.F. = \frac{1.1135}{1.170} = 0.9517$$

7. CALIBRATION – MIRROR ELEVATION ANGLE VS CURRENT

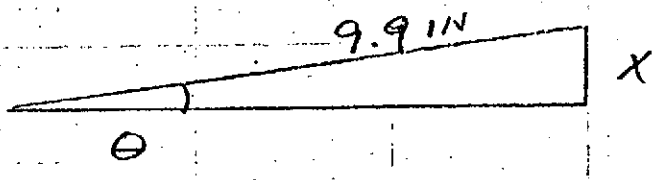

LET $\theta = 1 \overset{\frown}{SEC} = 4.848 \times 10^{-6} \frac{RAD}{\overset{\frown}{SEC}}$

$X = 4.848 \times 10^{-6} RAD \times 9.9 IN = 47.995 \times 10^{-6}$

MIRROR ELEV. ANGLE

$$= \frac{1.1135 \times 10^{-3} \frac{IN}{AMP}}{47.995 \times 10^{-6} \frac{IN}{\overset{\frown}{SEC}}} = 23.2 \frac{\overset{\frown}{SEC}}{AMP}$$

5.2.1.1 TOTAL ANGULAR RANGE & RATE

$$\frac{184 \times 10^{-6} IN}{9.9 IN} = 18.88 \times 10^{-6} RAD$$

$$\theta = \frac{18.88 \times 10^{-6} RAD}{4.848 \times 10^{-6} \frac{RAD}{\overset{\frown}{SEC}}} = 10.084 \overset{\frown}{SEC}$$

OR $\pm 5.042 \overset{\frown}{SEC}$

PERIOD = 140 SEC

AVERAGE ALIGN RATE

$$= \frac{10.084 \overset{\frown}{SEC}}{70 SEC} \times 60 \frac{SEC}{MIN} = 8.644 \frac{\overset{\frown}{SEC}}{MIN}$$

5.2.1.2 THRESHOLD

$$\text{MIN PULSE} = \frac{9.1 \times 10^{-6}\ \text{IN}}{3\ \text{PULSES}} = 3.033 \times 10^{-6}\ \frac{\text{IN}}{\text{PULSE}}$$

$$\theta = \frac{3.033 \times 10^{-6}\ \text{IN}}{9.9\ \text{IN}} = .3064 \times 10^{-6}\ \text{RAD}$$

$$= \frac{.3064 \times 10^{-6}\ \text{RAD}}{4.848 \times 10^{-6}\ \frac{\text{RAD}}{\text{SEC}}} = 0.063\ \frac{\text{SEC}}{\text{PULSE}}$$

5.2.2.1 TOTAL ANGULAR RANGE – STABILIZATION

$$\frac{313 \times 10^{-6}\ \text{IN}}{9.9} = 31.56 \times 10^{-6}\ \text{RAD}$$

$$\frac{31.56 \times 10^{-6}\ \text{RAD}}{4.848 \times 10^{-6}\ \frac{\text{RAD}}{\text{SEC}}} = 6.509\ \text{SEC}$$

OR ± 3.255 SEC

5.2.2.2 FREQUENCY RESPONSE

FREQ	ACT VOLTS	ACT CURRENT	MIRROR POS VOLTS	I/I_0	$10 \log \frac{I_1}{I_0}$ DB
.2	6.0 P-P	258 ma P-P	.19	1.0	0
.5			.285	1.5	+1.76
1			.30	1.58	+1.98
2			.34	1.79	+2.53
4			.32	1.68	+2.25
10			.20	1.05	+ .21
20			.12	.63	−2.0
40			.075	.39	−4.08
60			.060	.32	−4.94
80			.05	.26	−5.85
100			.07	.37	−4.32
110			.10	.53	−2.75
120			.50	2.63	+4.19
140			.05	.26	−5.85

BY_____DATE_____ SUBJECT_____ SHEET NO. 8 OF 9

CHKD. BY_____DATE_____ JOB NO._____

5.2.2.3

THRESHOLD

$$23.2 \frac{\text{SEC}}{\text{AMP}} \times .258 \text{ AMP P-P} \times \frac{.32}{.19} \times \frac{.002 \text{ VOLT P-P}}{6.0 \text{ VOLT P-P}}$$

$$= .00336 \text{ SEC P-P OR } \pm .00168 \text{ SEC}$$

APPENDIX C

PRECISION ANGLE INSTRUMENT

INTER-COMPANY COMMUNICATION

PERKIN-ELMER

Date: February 8, 1974

cc: CMinihan, JBeardsley, JDixon, JCallahan, CMorser, DRehnberg, DMcCarthy, WRizzi, WArmstrong

To: RCBabish

From: RCrane

Subj: PRECISION ANGLE INSTRUMENT

The attached write-up titled "Interferometric Angle Sensing" describes a very precise angle measuring technique which was used to monitor a secondary mirror control system on the LST Program. This memo is being circulated in the hope of finding other applications and markets for an instrument using this technique.

Comments are solicited.

R. Crane

RC:em

attachment

0-0532-02

Interferometric Angle Sensing

Experimental Data

An optical experiment was conducted to demonstrate an ability to measure small angle variations in the alignment of a large mirror using an equal-path interferometer. The optical arrangement, as shown in Figure 1, included a solid-glass interferometer which has an even number of reflections in each beam path, with the result that the output fringe pattern is uniphase for all angles of the mirror under test. An equal path arrangement was used so that the output fringe pattern would be independent of the input beam angle. Output fringe phase for a given wavelength is determined by the angle between the interferometer output face and the mirror surface. For small values of the angle, θ, one fringe is generated by a mirror rotation of:

$$\theta = \frac{\lambda}{2d}$$

The following constants were used:

$$\lambda = 6328\ \text{Å}$$
$$d = 2\ \text{inch}$$

Experiment procedure consisted of first varying θ over an angle large enough to generate more than one fringe, which provided the data needed to calculate the calibration factor C_θ, where:

$$C_\theta = \frac{1}{2\pi}\left(\frac{d}{\lambda}\right) V^{-1}$$

where: d = separation of two beams at the mirror
λ = wavelength
V = detector peak-to-peak output

This calibration, as indicated by Figure 2, is correct over an angular range small compared to that which generates one fringe.

Figure 3 shows typical results from testing the LST secondary mirror mock-up. Trace 3a shows a calibration scan generated by a triangular-wave cyclic scan of the mirror. This shows a peak-to-peak output of V = 32 mm, which resulted in

$$C_\theta = 6.8 \times 10^{-8} \left(\frac{\text{radian}}{\text{mm}}\right)$$

The second and third traces show ambient mechanical noise in mirror angle position and typical signal response for a sine wave drive applied to the mirror actuators.

Figure 4 was generated with a second arrangement in which the laser beam of 10^{-4} watts was fed directly into the interferometer with no collimator. For this arrangement

$$C_\theta = 2\tfrac{1}{2} \times 10^{-7} \quad \left(\frac{\text{radian}}{\text{volt}}\right)$$

The middle trace in Figure 4 shows details of the ambient noise with a recording speed of 100 mm per second. The cyclic signal is characteristic of band limited noise. In this case this is the response of the high-Q mirror mount to the local mechanical ambient, i.e. building noise. This was measured to be approximately 1/300 sec peak-to-peak. The bottom trace shows the mirror system response generated by a truck starting up at a light on the local highway. The quiescent noise level was approximately 0.001 sec peak-to-peak. Intrinsic noise of the interferometer sensor as determined by the detector and laser photon noise was calculated for a bandwidth of 1000 cps to be 2 orders of magnitude below building noise.

$\theta = \frac{1}{2\pi}\left(\frac{\lambda}{D}\right)\left(\frac{S}{N}\right)^{-1}$ (rad rms)

Figure 5 shows the output of the interferometer displayed on an oscilloscope. The top picture shows calibration data in which the upper trace is the mirror actuator control signal and the lower trace is the interferometer output. This picture indicates

$$C_\theta = 3\tfrac{1}{2} \times 10^{-7} \quad \left(\frac{\text{radian}}{\text{volt}}\right)$$

The middle picture in Figure 5 shows the square wave response of the mirror system with the drive at the top and the response at the bottom. Note the effect of the high-Q in the mirror suspension which caused severe ringing. This data indicates a mechanical Q of approximately 12. The bottom trace of Figure 5 shows the response to a low level control signal. Signal and noise are both approximately 0.007 sec peak-to-peak.

This interferometer has essentially equal paths so it will operate well with quasi-coherent light. Therefore a Gallium Arsnide LED was tried. Results are shown in Figure 6 where the top trace is calibration data indicating:

$$C_\theta = 1\tfrac{1}{2} \times 10^{-6} \quad \left(\frac{\text{radian}}{\text{volt}}\right)$$

Note that the mirror was scanned over several fringes which produced a variable fringe contrast. This is due to the fact that the LED does not have a long coherent length. The equal path position is at the right-hand side of the recording. The bottom trace in Figure 6 shows ambient noise again, with an indicated level of approximately 1/300 sec peak-to-peak.

Application Notes

If an angle sensor of this type is to be used as an absolute angle meter it will be necessary to resolve the ambiguity due to the multiple fringes. This can be done using a white light source. Because the interferometer is equal-path this source need not be well collimated and a small lamp may be used. Figure 7 shows 2 interferograms gnnerated using a tungsten lamp made by Sylvania and a silicon detector made by EG&G. In this case the equal path fringe is dark and readily recognized at the center of the pattern.

If an equal path interferometer is to be considered for precision angle measurements such as described above it should be recognized that these measurements were made in subdued light and with less than 1 mm air space between the interferometer face and the rotating mirror. This technique can be extended to high ambient light conditions or outdoor operation by modulating the LED with a carrier frequency.

The limited dynamic range indicated by Figure 2 may not be adaquate for many applications. This can be extended to several min by incorporating an optical frequency shifter in one arm of the interferometer combined with electronic fringe phase detection, as described in Perkin-Elmer Report 10692.

Angle measurements thru an air path to a precision of seconds of arc or less require very very careful stabilization of the air path. This should be kept in mind in considering applications of the technique.

Conclusion

Very precise angle measurements can be made with relatively simple optical and electronic equipment plus careful attention to air stabalization. Figure 8 is a photograph

of the experimental interferometer with an LED source and a silicon photo-detector. In this picture the rotatable mirror has been removed to permit a better view of the interferometer. Limiting precision will be determined in most applications by the ability to minimize a) ambient mechanical vibrations; b) air path thermal fluctuations.

An instrument based upon the simple configuration of Figure 8, i.e. solid-glass equal-path interferometer (per PE Patent Disclosure Docket D-1557), with a modulated LED source will be capable of providing the following performance specification:

Dynamic Range	1 $\widehat{\text{sec}}$
Precision	10^{-10} radian rms uncertainty
Response Time	$<$ 10 msec
Output	analog voltage
Operation	very stable air environment

An interferometer with the added complexity of an optical frequency shifter (per PE Patent No. 3536374), a white light source, plus an electronic phase detector could be made capable of providing the following performance specification.

Dynamic Range	3 $\widehat{\text{min}}$
Precision	10^{-10} radian rms or 0.1% full scale
Accuracy	0.1% of full scale
Response Time	$<$ 10 msec
Output	digital display
Operation	very stable air environment

The latter configuration would have a linear response with scale changes to accomodate the full dynamic range in accordance with Figure 9.

106

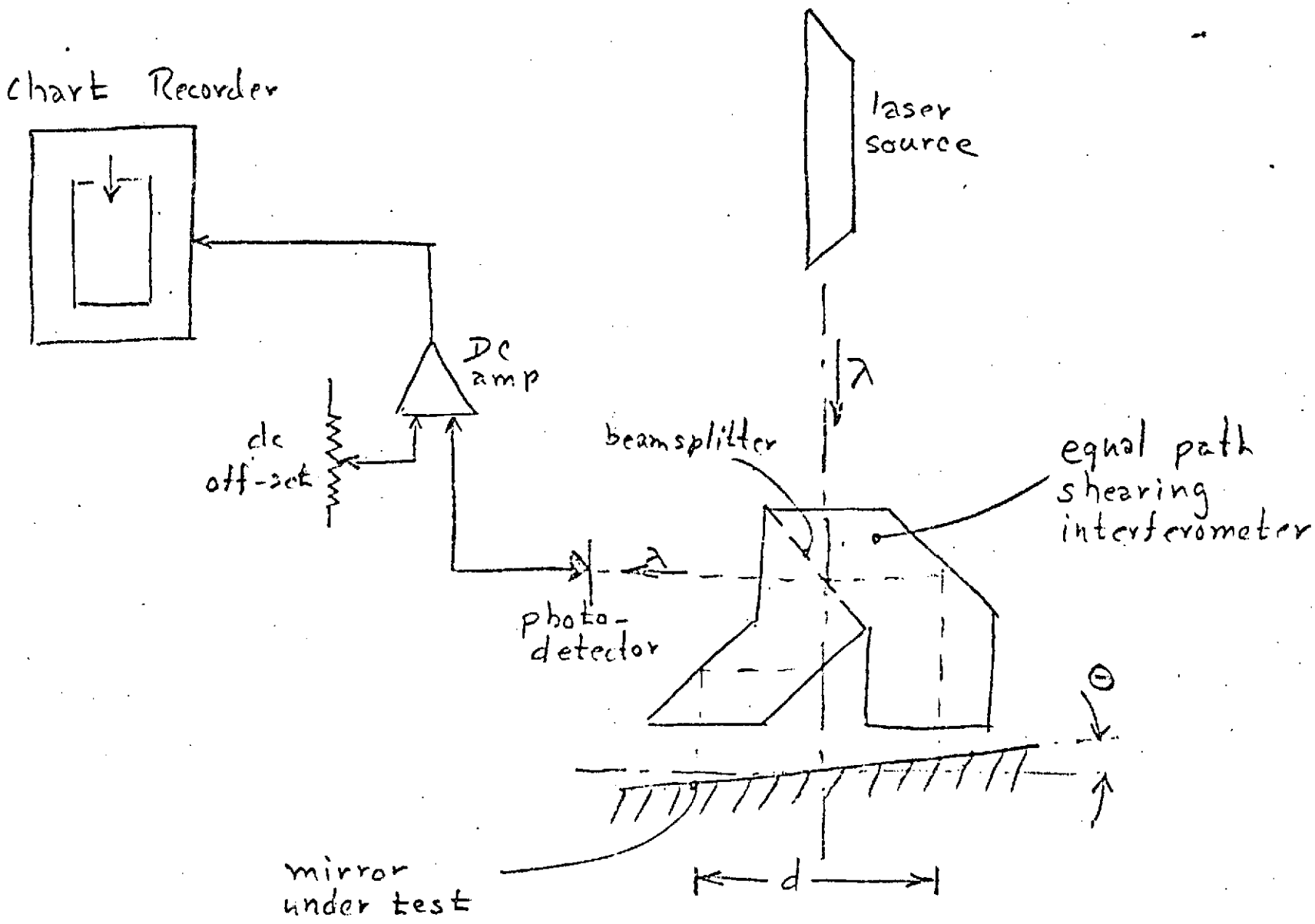

Figure 1 Block Diagram

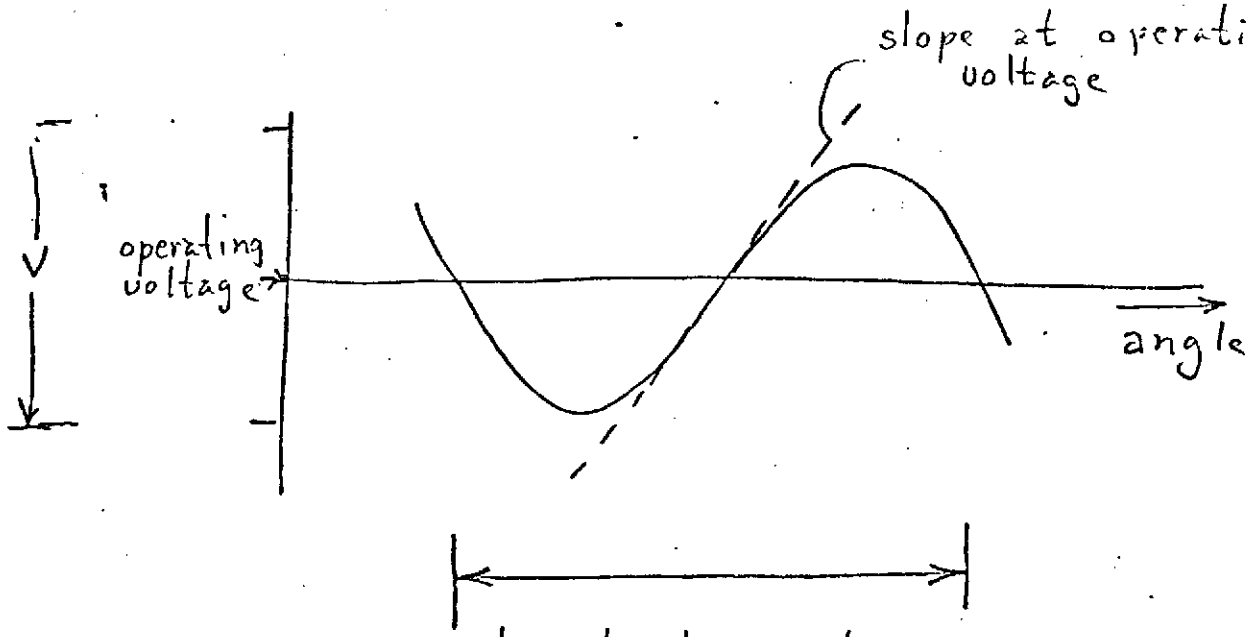

$\frac{1}{2}\lambda$ displacement
or
1λ of OPD
or
1 fringe

Calibration, $C_\theta = \dfrac{1}{\left(\frac{\text{fringes}}{\text{radian}}\right) \times \left(\frac{\text{volts}}{\text{fringe}}\right)}$

where: $\dfrac{\text{fringes}}{\text{radian}} = 2\dfrac{d}{\lambda}$

$\dfrac{\text{volts}}{\text{fringe}} = \text{slope} = \pi V$

Therefore,

$$C_\theta = \frac{1}{2\pi}\left(\frac{\lambda}{d}\right) V^{-1} \quad \left(\frac{\text{radian}}{\text{volt}}\right)$$

68 Fig 2 - Calibration Derivation

Figure 5 - Example Data

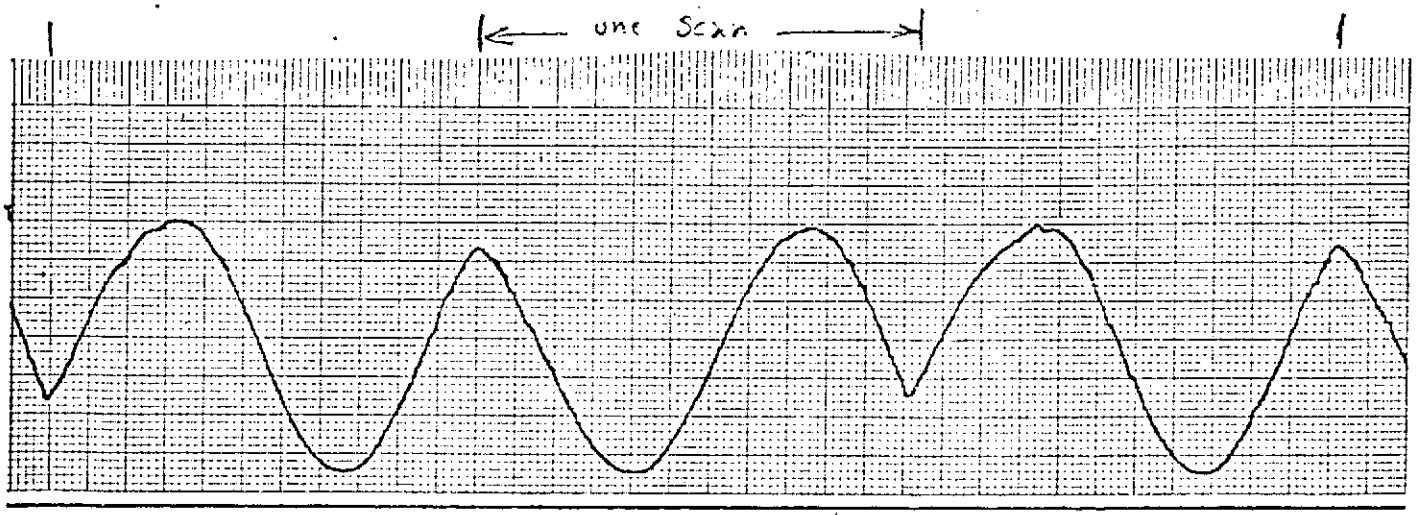

a. Calibration curve showing a peak to peak deflection of V = 32 mm; $C_o = 7 \times 10^{-8}$ radian/mm

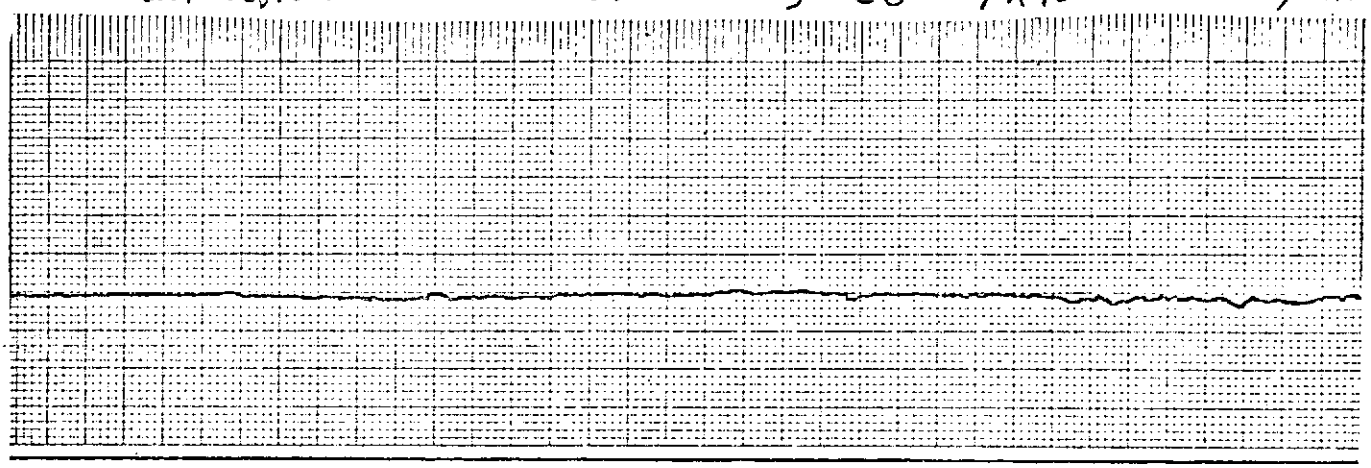

b. Ambient noise at same gain setting

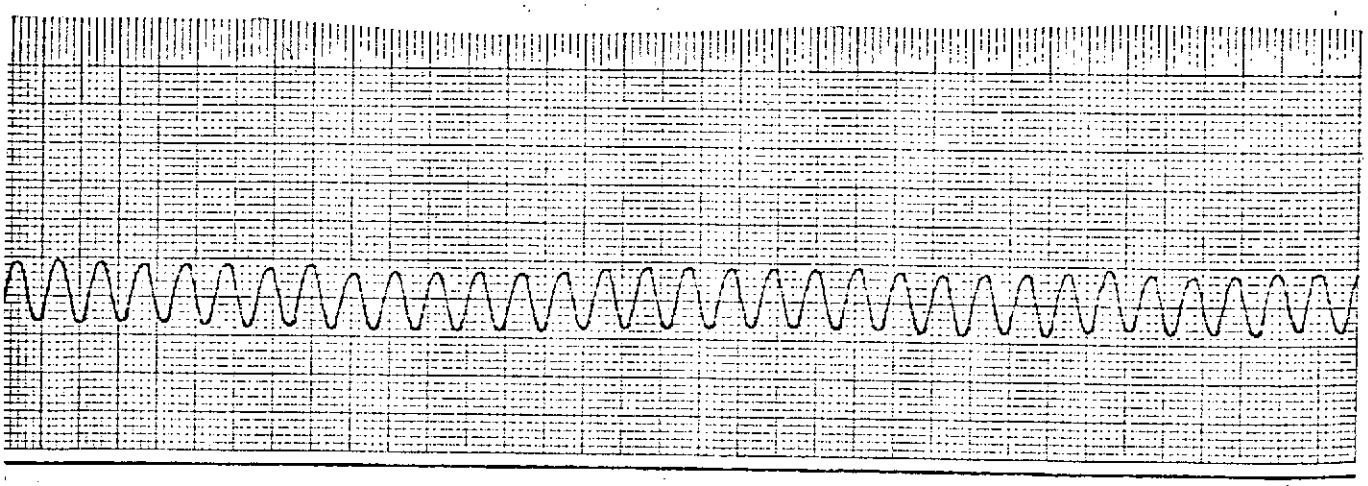

c. Typical mirror deflection indication, where signal = $4\frac{1}{2} \times 10^{-7}$ radian p-p

69

Figure 4 - Example Data

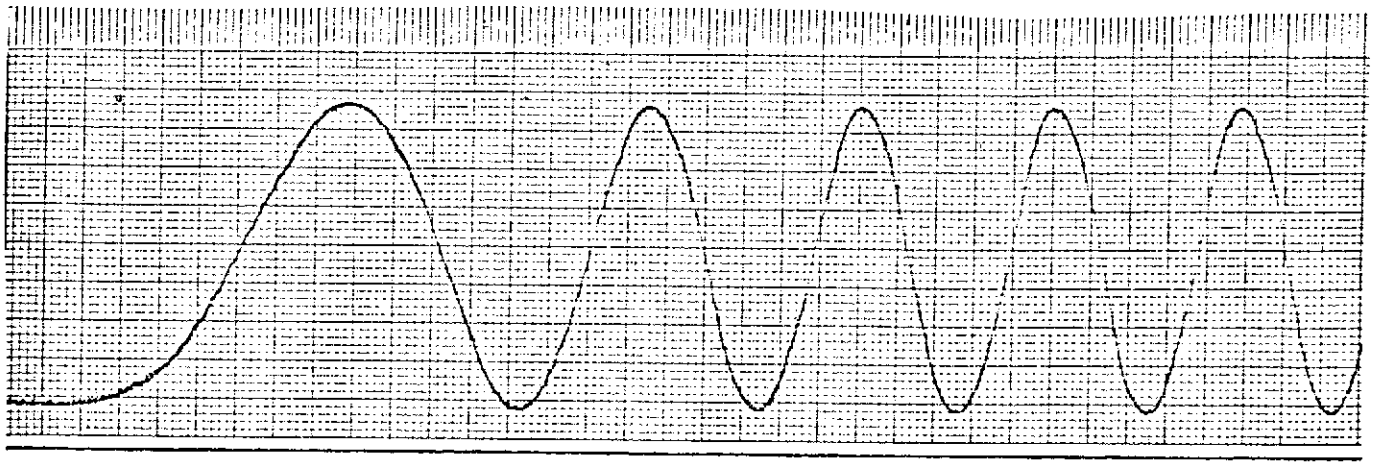

a. Calibration data with gain set at 2 volt/cm showing $C_\Theta = 2\frac{1}{2} \times 10^{-7}$ radian/volt

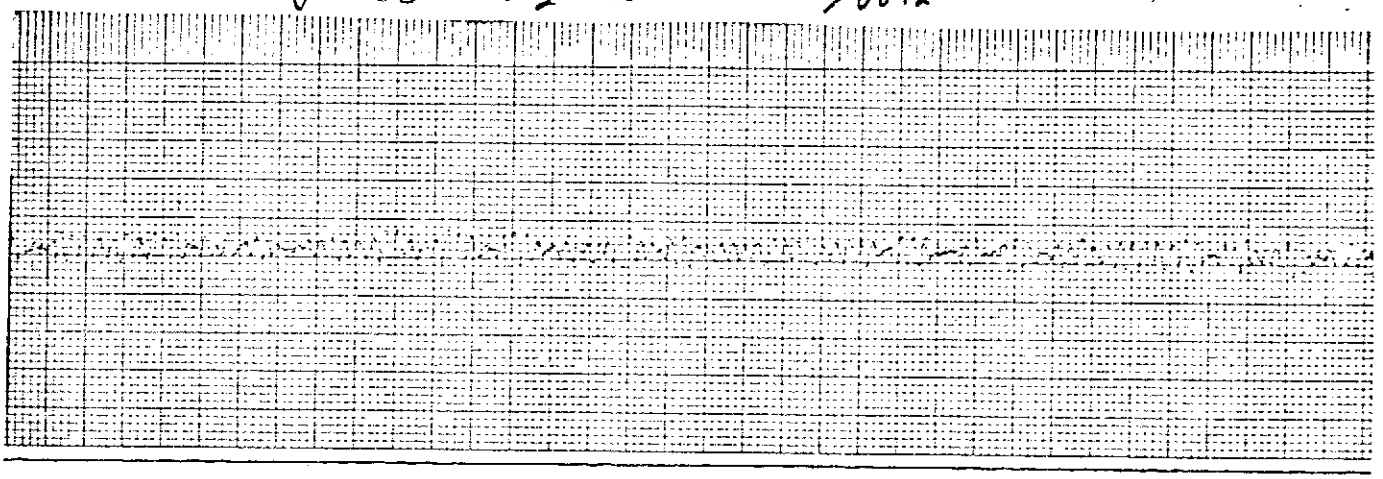

b. Ambient noise with gain at 20 mv/mm and chart speed of 100 mm/sec

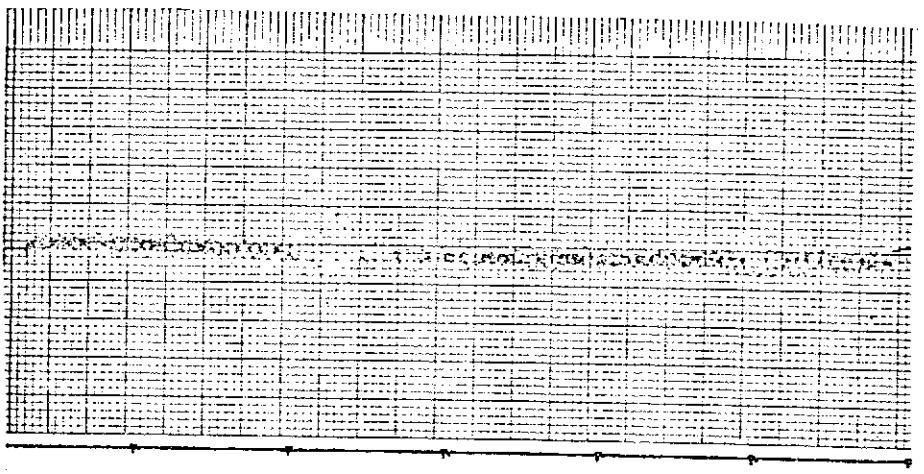

c. Example of transient caused by a truck on local highway, approximately $\frac{1}{100}$ sec p-p

1. Calibration showing
$C = 3\frac{1}{2} \times 10^{-7}$ $\frac{\text{radian}}{\text{volt}}$
gain set at $1\ \frac{v}{cm}$

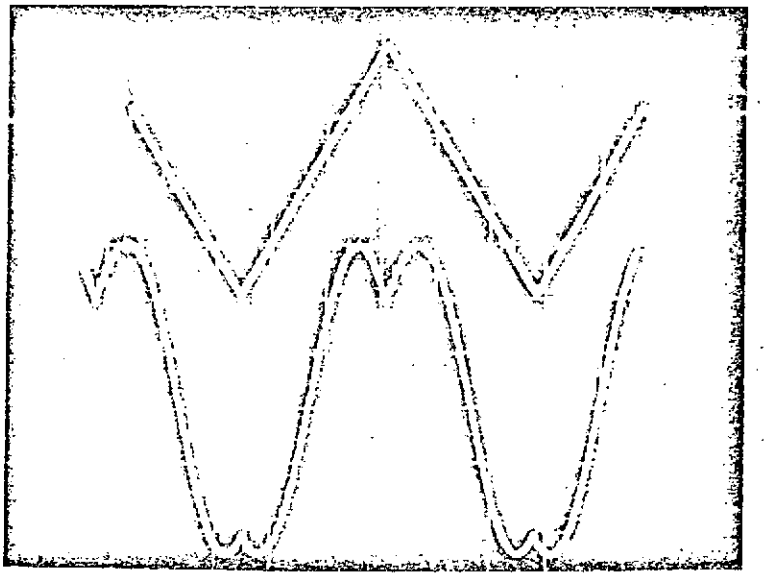

2. Square wave signal showing ringing due to high Q of mechanical resonance.
gain set at $1.0\ \frac{v}{cm}$

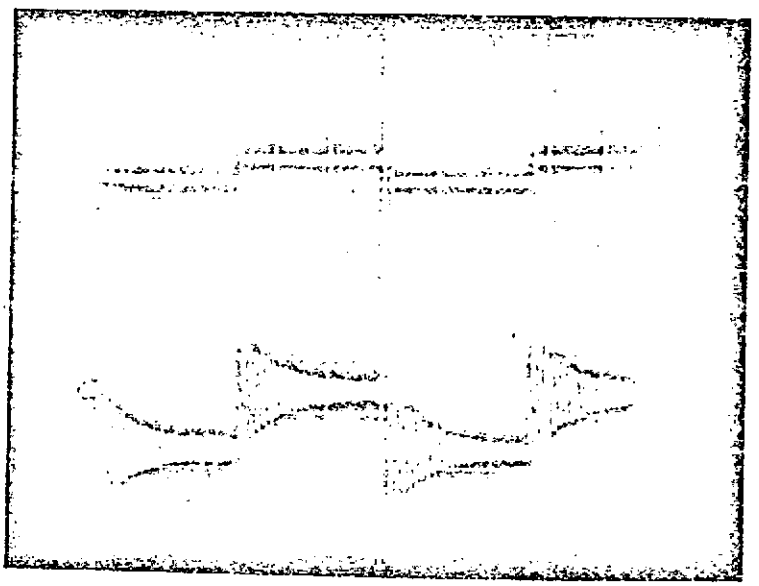

3. Low level signal and ambient noise
signal = 0.007 sec p-p
noise = 0.007 sec p-p
gain set at $0.2\ \frac{v}{cm}$

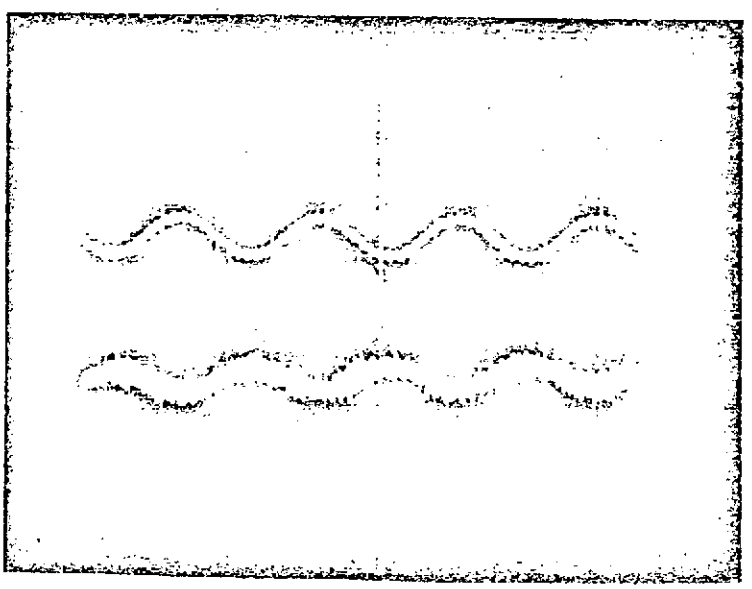

Fig 5 - Example Data, Oscilloscope Display

a. Calibration

Gain: 0.5 v/cm

$C_\theta = 1\frac{1}{2} \times 10^{-6} \frac{\text{rad}}{\text{volt}}$

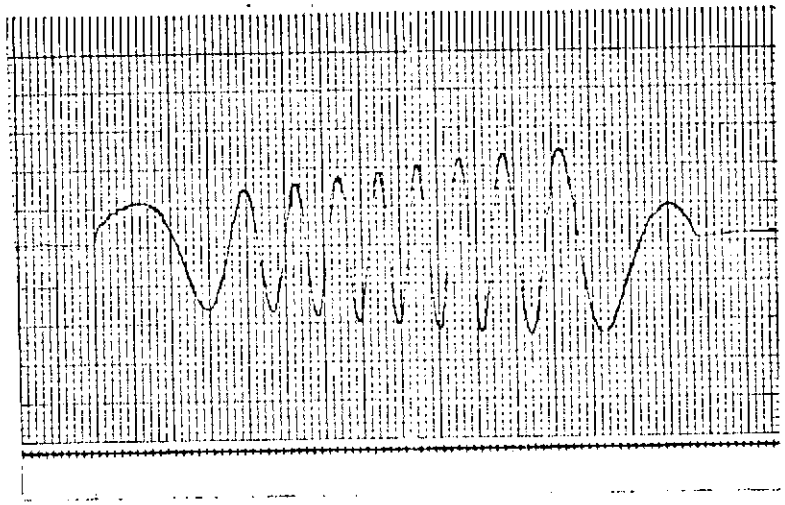

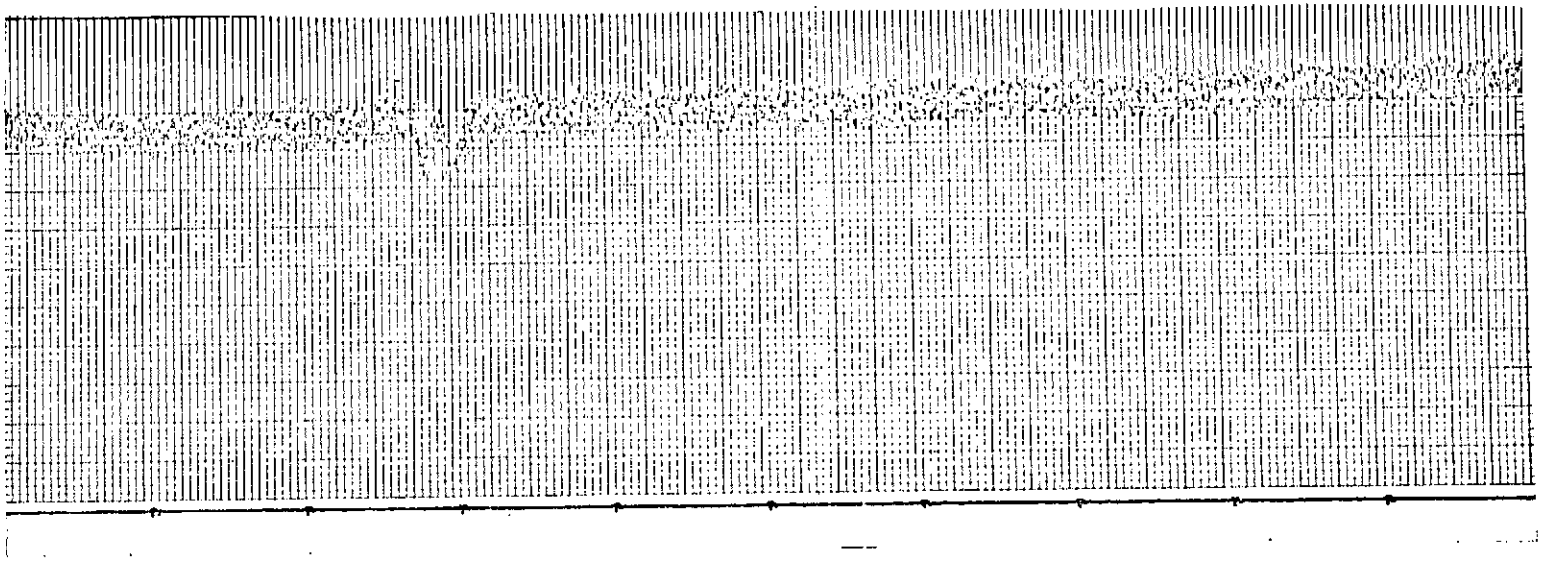

b. Ambient noise with gain set at 2 mv/mm. Average noise is approximately 1/300 sec p-p

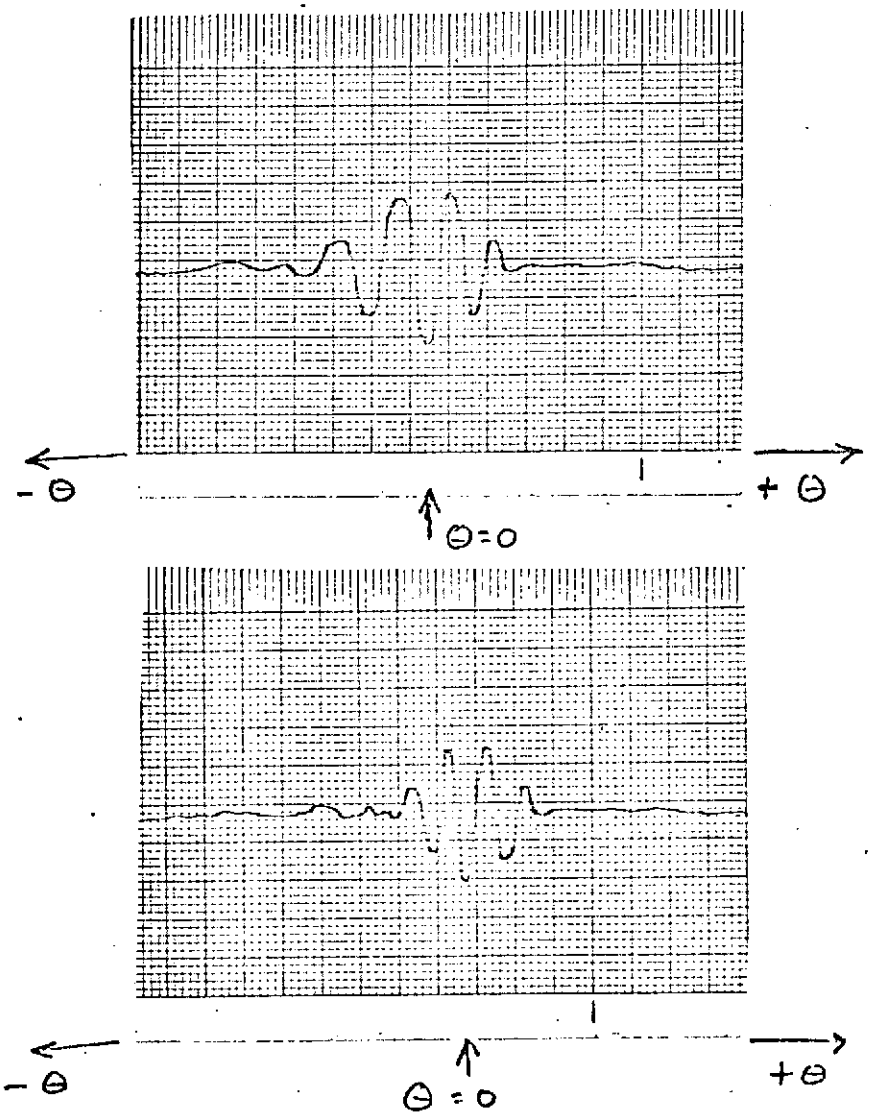

Fig 7 - Example Interferogram generated with linear mirror scan and a white light source showing waveform from which $\Theta = 0$ reference may be determined on absolute basis

73

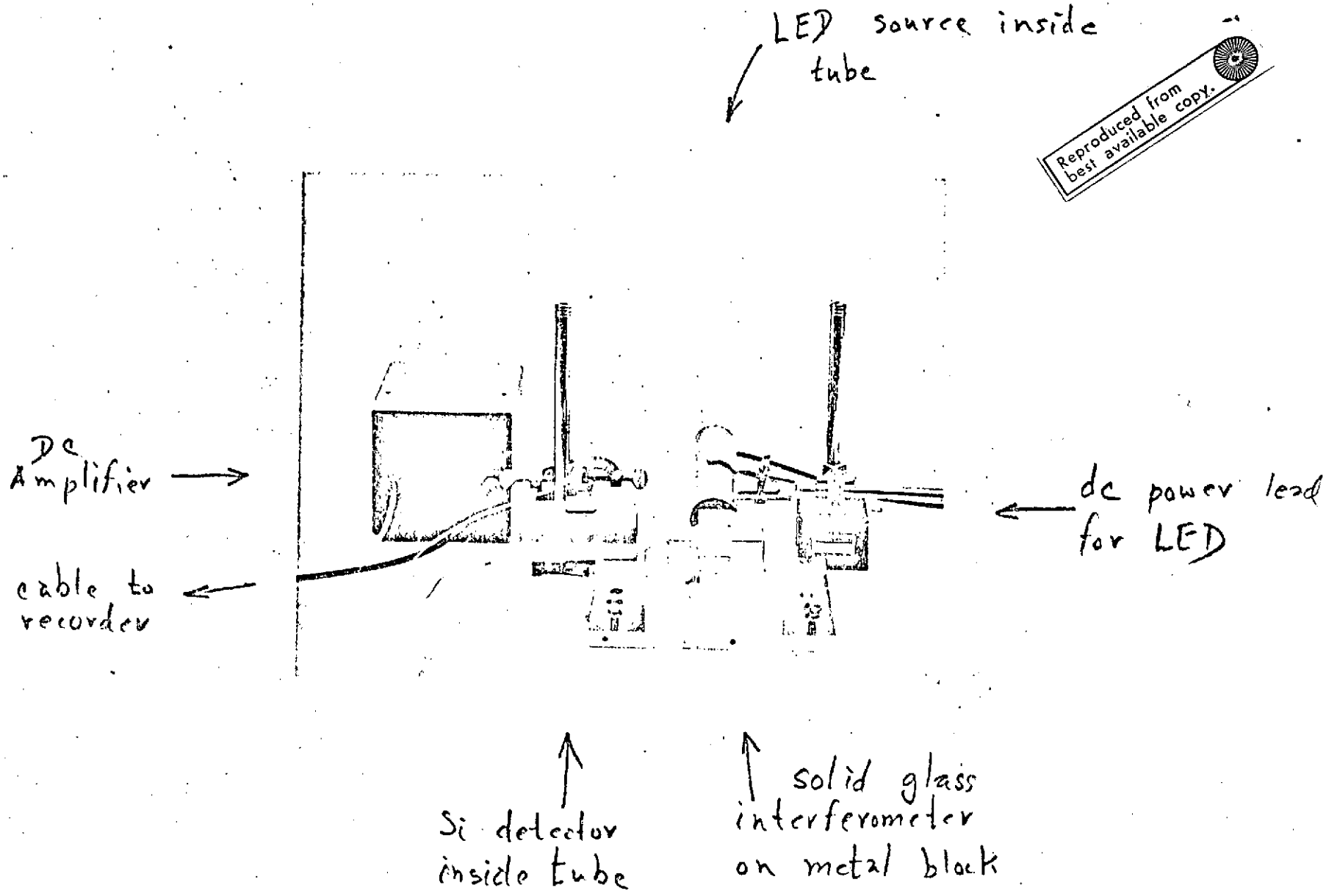

Fig 8 - Experimental Components

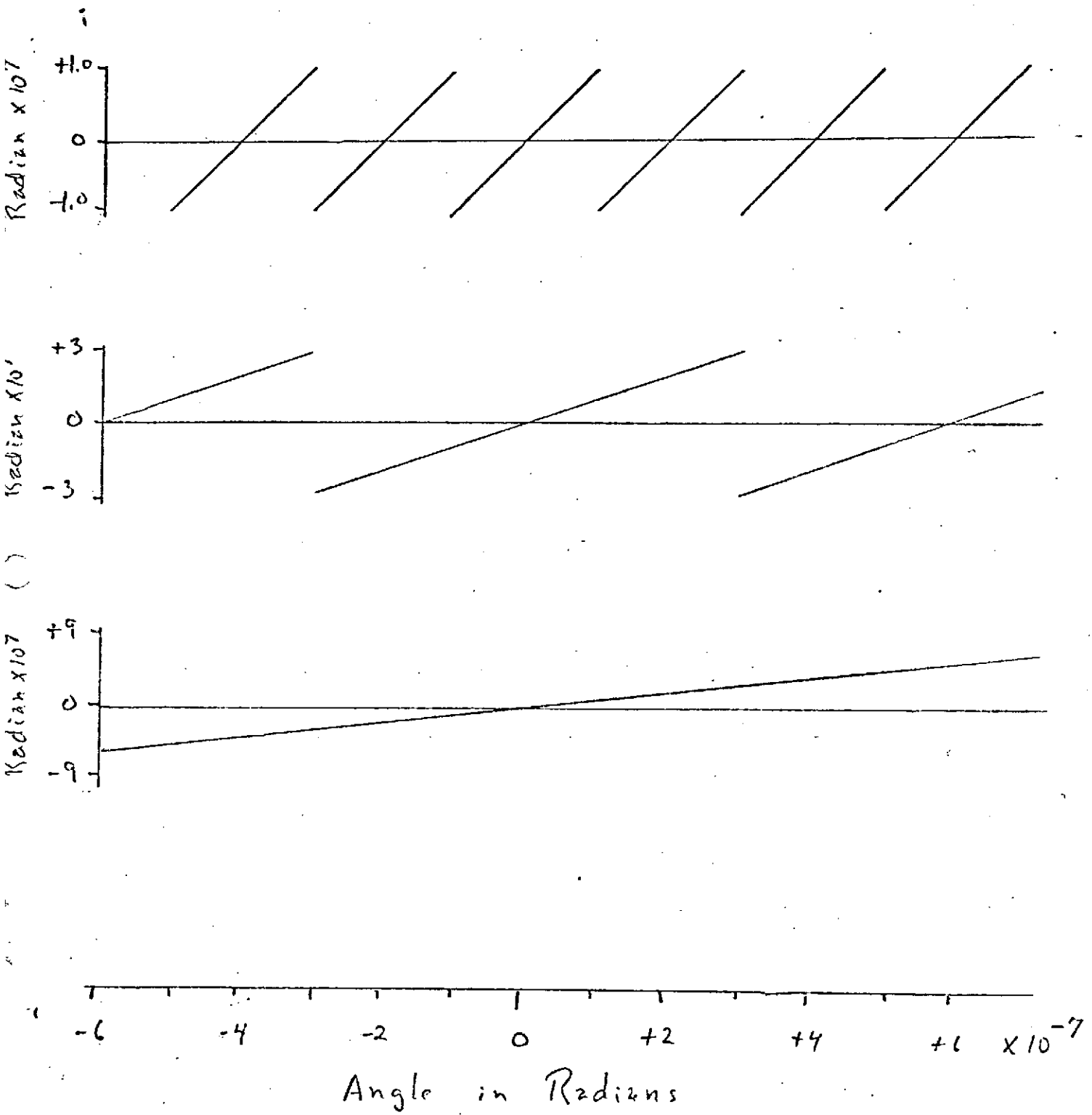

Figure 9 - Example Output Indication Showing Linear Response and Scale Changes

APPENDIX D

LATERAL STIFFNESS - CRUCIFORM FLEXURE

GENERAL DATA SHEET - II

SPO: 33117

SHEET 2 OF

TEST: LATERAL STIFFNESS "B"

SPEC:

PARA:

TEST NO:

TEST ITEM: CRUCIFORM FLEXURE

DATE: 11/6/73

CLIENT: MSFC

CLIENT REPRESENTATIVE:

TEMP: LAB. RH.

TEST EQUIPMENT:

MODEL NO:

TESTED BY: D E Kline

INSTRUMENTATION:
START 1540
STOP 1603

ENGR. CHECK:

SUPV. CHECK:

WT OZ	X_1 10^{-6} IN	X_2 10^{-6} IN	ΔX
0	0	0	
16	-2.5	0	
32	-6	+1	
48	-9.5	+11	
32	-4.5	-3	
16	-0.5	-5	
0	+3.5	-3	
16	+1.5	-8	
32	-2	-1	
48	-6.5	+7	
32	-1.5	-5	
16	+3	-7	
0	+7	-5	
16	+9.5	-11	
32	+0.5	+0.5	
48	-3	+5	
32	+1	-12.5	
16	+5.5	-12.5	
0	+9.5	-7	

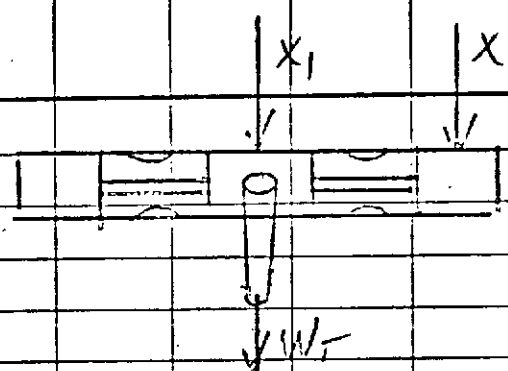

SKETCH OR NOTES:

UNIFORM FLEXURE - LATERAL STIFFNESS B

$$\text{SLOPE} = \frac{11.5 \times 10^{-6}\ \text{IN}}{3\ \text{LB}} = 3.8333 \times 10^{-6}\ \frac{\text{IN}}{\text{LB}}$$

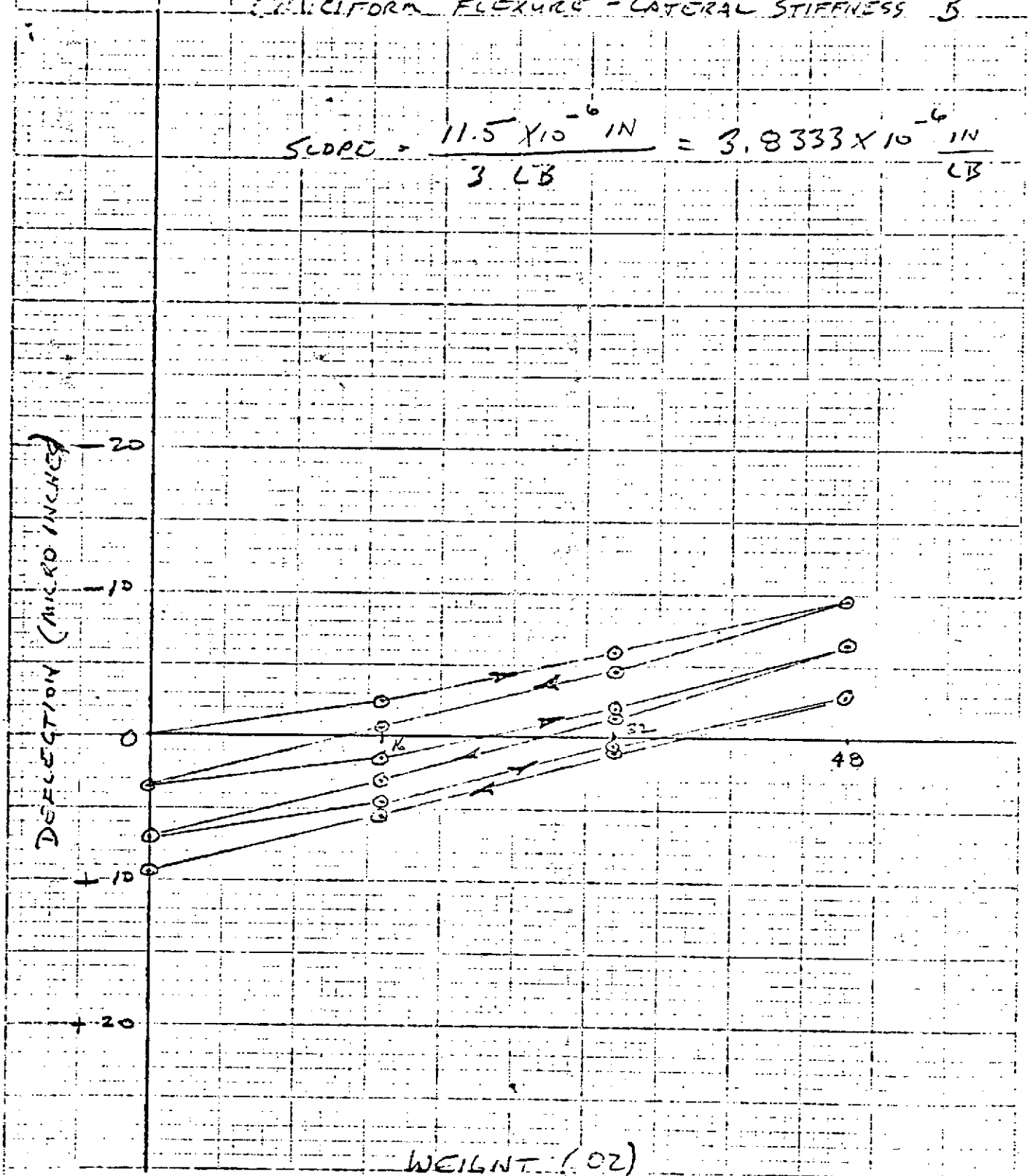

W.E. Kohman 11/7/73

APPENDIX E

TORSIONAL STIFFNESS - CRUCIFORM FLEXURE

Torsional Gradient Experiment

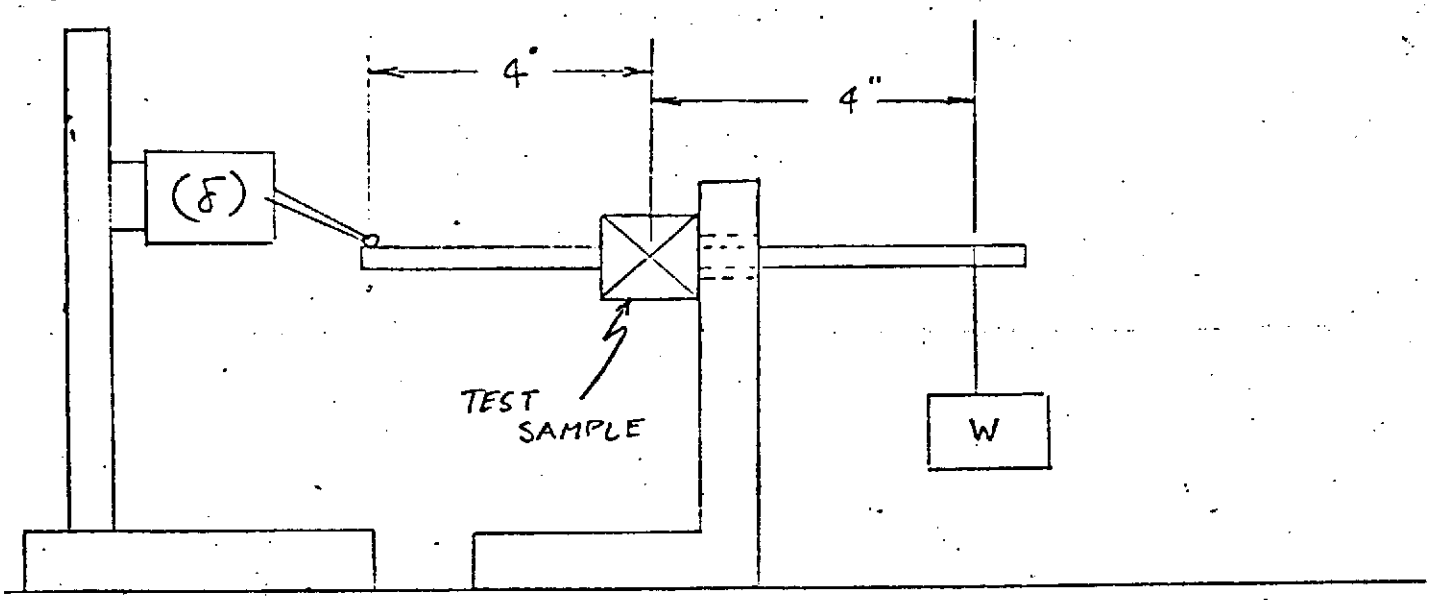

W(gm)	δ(in)
224.5	0.0
546.3	.040
100.0	0.0
420.0	.040

$$k = \frac{T}{\theta} = \frac{4(\Delta\omega)}{(\Delta\delta/4)} = \frac{16\,\Delta W}{\Delta\delta}$$

Test #1 $\quad k = \dfrac{16(546.3 - 224.5)}{.040\,(453.6)} = 283.8 \ \dfrac{in\#}{R}$

Test #2 $\quad k = \dfrac{16(420 - 100)}{.040\,(453.6)} = 282.2 \ \dfrac{in\#}{R}$

$$Avg \simeq 283 \ \frac{in\#}{R}$$

In TITANIUM $\quad k = \left(\frac{17}{10.6}\right) 283 = 454 \ \dfrac{in\#}{rad}$

AK72-1011